

https://dspace.org/

Analysis of cavity PD characteristics' sensitivity to changes in the sinusoidal supply voltage frequency

Venge, Tapiwa

2021

https://hdl.handle.net/10539/33379

Downloaded from a DSpace repository. https://dspace.org/

University of the Witwatersrand, Johannesburg

MASTER'S DISSERTATION



Analysis of Cavity PD Characteristics' Sensitivity to Changes in the Sinusoidal Supply Voltage Frequency

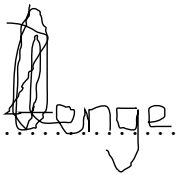
Author: Tapiwa Venge

A dissertation submitted to the Faculty of Engineering and the Built Environment, University of the Witwatersrand, Johannesburg, in fulfilment of the requirements for the degree of Master of Science in Electrical Engineering.

Johannesburg, 2021

Declaration

I declare that this dissertation is my own unaided work. It is being submitted for a Degree of Master of Science in Engineering to the University of the Witwatersrand, Johannesburg. It has not previously been submitted for any degree or examination to any other university.

Signature: .....  .....

Date: ..... 08 October 2021 .....

I dedicate this work to my dad, Thonias Venge who passed away during the final write-up of this dissertation. Thank you for your patience, understanding and dedication in my studies. You were part of the entire journey but could not get to see the finish line. You are greatly missed. May your soul rest in peace.

This is for the Venges: Marshall, Tafadzwa (Rita), Beverley, Ruvimbo, Tariro ...and the future ones.

To my family and friends: May this be a beacon and rudder of hope that through hard work, persistence and consistence greater heights can be reached.

Acknowledgments

The completion of this research was greatly assisted by the support and guidance of a large number of people throughout my academic life thus far.

The author would like to acknowledge with gratitude my supervisor, Prof Cuthbert Nyamupangedengu for his guidance, insightful discussions and the freedom to let me evolve in the world of research and partial discharges. I am also grateful for his financial and fatherly support towards the end of my postgraduate studies.

I would like to sincerely acknowledge with gratitude Hein and Louise Schuld for the unwavering financial support throughout my tertiary studies (my entire undegraduate and most of postgraduate time).

The guidance and assistance of Elizabeth Haikali in kick-starting the simulations in the earliest stages of my research is acknowledged. The long discussions, brainstorming and motivation by my 'best man' Titus Majeza also goes unnoticed. The companionship and advice of my 'partner-in-research' and 'start-together' colleagues Sive Baartman and Sophy Sitole were invaluable. The School of EIE admin staff Jeannine Davids, Mumtaz Adams and Thabiso Motsei are also acknowledged for their priceless support, follow-ups and advice in making the transition to postgraduate and the journey effortless.

The author would like to acknowledge the Bumhira (Godwin and Mary) and Mojapelo (Edward and Grace) families for their prayers, guidance when all seemed blurry and for consistently checking up on my progress when it was needed the most. The Jwili (Maxwell and Tshegofatso) and Mokoena (Pauline and Nonhlanhla) families are also acknowledged for providing a productive 'office and library' space for the write-up.

The author would like to sincerely acknowledge with love and gratitude my mom, Elizabeth Nherera and sister, Tariro Venge for rearranging their lives so that I had everything I needed during the course of my studies.

Last, and mostly, eternal acknowledgment to the Almighty Lord for making everything good and possible in its perfect time.

Abstract

Most high voltage equipment operates at power frequency (50/60 Hz), yet their testing is often done at different supply voltage frequencies for various reasons. Therefore, the study of how partial discharge (PD) phenomena respond to the changes in the supply voltage frequency has continued to draw research interest. Literature has shown that there is a mixture of agreements and inconsistencies on the reported conclusions on how PD characteristics respond to supply voltage frequency variations. However, there has been consensus on the recognition of the mechanisms that influence how and why PD characteristics respond to the changes in the supply voltage frequency. These mechanisms that influence the frequency dependency are; statistical time lag, cavity surface conductivity, and the residual charge effect. The present research work used a PD model implemented in MATLAB® Simulink® to simulate the mechanisms of interest. A 3-capacitor model (ABC) is modified to simulate the extent to which the mechanisms influence PD characteristics and respond to changes in the supply voltage frequency. The PD characteristics studied in the present research are the cavity spark-over voltage, PD repetition rate (PDRR) and the phase-resolved PD patterns (PRPDP). Three configurations of the ABC model are developed to study each phenomenon that influences PD frequency dependency. Simulations are performed on three supply voltage frequencies: 1 Hz, 50 Hz and 200 Hz. The findings are that the phase-resolved partial discharge pattern (PRPDP) and PD repetition rate (PDRR) characteristics are more sensitive to variations in the statistical time lag of the seed electron availability at higher frequencies of the supply voltage. The opposite trend is observed for the cavity surface resistance. At lower resistance of cavity surface, the PRPDP and PDRR characteristics are more sensitive to changes in the supply voltage frequency than at higher resistances. The residual charge effect is more sensitive at higher frequencies of the supply voltage. At higher residual charge, the PRPDP and PDRR are more sensitive to changes in the supply voltage frequencies than at lower residual charge. The trend is in opposition to cavity surface conductivity's response but in compliment to the statistical time lag's response. The study also confirms that incorporating equivalent resistances with the equivalent residual capacitor in the ABC model makes it more authentic than the model comprising of equivalent capacitors and resistances or equivalent capacitors only.

Contents

Declaration i

Acknowledgments iii

Abstract iv

Contents iv

List of Publications viii

List of Figures viii

List of Tables xi

Abbreviations xii

1 Introduction 1
- 1.1 Problem Statement and Motivation . . . 3
- 1.2 Research Question . . . 3
- 1.3 Research Objectives . . . 4

2 Partial Discharges versus Electrical Insulation 6
- 2.1 Electrical Insulation Systems . . . 6
  - 2.1.1 Electrical Insulation Failure Analysis . . . 7
  - 2.1.2 Electrical Insulation Failure Mechanism . . . 8
- 2.2 Partial Discharges and Electrical Insulation Failure . . . 10
  - 2.2.1 PD Measurement and Diagnosis . . . 11
  - 2.2.2 PD Measurement Methods . . . 12

3 Partial Discharge Measurements and the Test Voltages 15
- 3.1 Non-Sinusoidal Test Voltages . . . 16
  - 3.1.1 Harmonics . . . 16
  - 3.1.2 Impulse Voltages (Lightning and Switching) . . . 16
  - 3.1.3 Direct-Current (DC) . . . 17
- 3.2 Sinusoidal Test Voltages . . . 18
  - 3.2.1 Operational or Power Frequency(50/60 Hz) . . . 19
  - 3.2.2 Oscillating Wave Test Set (OWTS/DAC) . . . 20
  - 3.2.3 Very Low Frequency (VLF) . . . 21
  - 3.2.4 Resonant Test System (RTS) . . . 21

4 Partial Discharges at Sinusoidal Supply Voltage Frequency (SVF) 23
4.1 PD and Supply Voltage Frequencies; A Literature Review . . . 23
4.2 Factors Responsible for Frequency Dependence of PD Mechanisms . . . 28
4.2.1 Statistical Time Lag . . . 28
4.2.2 Surface Conductivity . . . 29
4.2.3 Residual Charge . . . 30

5 Modeling Approaches to Studying Partial Discharge Phenomena 31
5.1 Overview of Techniques Used in PD Studies . . . 31
5.1.1 The Usefulness of PD Modeling . . . 32
5.2 PD Models Overview . . . 32
5.3 The 3-Capacitor (ABC) PD Model Review . . . 33

6 Experimental Design and Development of the ABC PD Model in MATLAB® Simulink® 39
6.1 Partial Discharge Measurements: IEC60270 . . . 39
6.1.1 General Scope . . . 39
6.1.2 Test and Measuring Circuits . . . 40
6.2 Mechanisms Responsible for PD Dependence on SVF . . . 42
6.2.1 The Statistical Time Lag . . . 42
6.2.2 Cavity Surface Conductivity . . . 43
6.2.3 PD Residual Charge Effect . . . 44
6.3 Equivalent Electrical Circuits in the Model . . . 45
6.4 Determination of the PD Equivalent Circuit Components Values . . . 48
6.4.1 Cavity Spark-Over Voltage, PDIV and PDEV . . . 48
6.4.2 Cavity Surface Conductivity Values . . . 51
6.4.3 Capacitances Values in the Model . . . 52
6.5 Implementation of the Model in MATLAB® Simulink® . . . 53

7 Simulation Results, Analysis and Discussion 57
7.1 The Statistical Time Lag's Influence on PD Characteristics' Response to SVF Variations . . . 59
7.1.1 Influence of Statistical Time Lag Variations on PD Behavior at SVF of 1 Hz . . . 59
7.1.2 Influence of Statistical Time Lag Variations on PD Behavior at SVF of 50 Hz . . . 60
7.1.3 Influence of Statistical Time Lag Variations on PD Behavior at SVF of 200 Hz . . . 61
7.2 The Cavity Surface Conductivity's Influence on PD Characteristics' Response to SVF Variations . . . 63
7.2.1 PD Characteristics as a Function of Cavity Surface Resistance at SVF of 1 Hz . . . 63
7.2.2 PD Characteristics as a Function of Cavity Surface Resistance at SVF of 50 Hz . . . 64
7.2.3 PD Characteristics as a Function of Cavity Surface Resistance at SVF of 200 Hz . . . 65
7.3 The Residual Charge Effects on PD Characteristics' Response to SVF Variations . . . 66

7.3.1 The Residual Charge Effect on PD Characteristics' Response at SVF of 1 Hz . . . 69
7.3.2 The Residual Charge Effect on PD Characteristics' Response at SVF of 50 Hz . . . 70
7.3.3 The Residual Charge Effect on PD Characteristics' Response at SVF of 200 Hz . . . 71
7.4 Summary of Simulation Results on the Extent to which Factors Responsible for Frequency Dependence of PD Mechanisms Influence PD Characteristics' Response at Different Supply Voltage Frequencies . . . 73
7.5 Comparison of the Three Modified ABC Model Configurations; Simulation Results versus Experimentally Measured Results Obtained from the Literature . . . 77

8 Conclusions and Recommendations 79

A SAUPEC 2019 Conference Paper 94

B SAUPEC 2020 Conference Paper 101

C MDPI 2021 Energies Journal Article 108

D AFRICON 2021 Conference Paper 126

List of Publications

1. T. Venge and C. Nyamupangedengu, "Influence of Variable Frequency of the Applied Voltage on Cavity Partial Discharge Parameters: A Critical Review," *2019 Southern African Universities Power Engineering Conference/Robotics and Mechatronics/Pattern Recognition Association of South Africa (SAUPEC/RobMech/PRASA)*, 2019, pp. 582-587

2. T. Venge and C. Nyamupangedengu, "Influence of Supply Voltage Frequency on Cavity Partial Discharge Parameters: Simulation Results," *2020 Southern African Universities Power Engineering Conference/Robotics and Mechatronics/Pattern Recognition Association of South Africa (International SAUPEC/RobMech/PRASA)*, 2020, pp. 1-6

3. Venge, T.; Nyamupangedengu, C. "Analysis of Cavity PD Characteristics' Sensitivity to Changes in the Supply Voltage Frequency." **Energies** 2021, 14, 478

4. T. Venge and C. Nyamupangedengu, "A Review of Test Voltages Used in Partial Discharge Measurements," *2021 IEEE Africon, Tanzania*, 2021, pp. 1-6

List of Figures

1.1 'Setting up the scene'; The context of the present research work 2

5.1 3-capacitor equivalent circuit (**a**) with cavity illustrated inside the insulation and (**b**) with aggregated equivalent circuit parameters 33
5.2 Modified 3-capacitor PD model with resistors in parallel with capacitors used for simulating cavity surface conductivity 34
5.3 Modified 3-capacitor PD model with an additional capacitor used for simulating residual charge effect 36
5.4 Modified 3-capacitor PD model with an array of capacitors used for simulating PD activity in closely-coupled multiple voids 38

6.1 IEC60270 PD test circuit with coupling device in series with the coupling capacitor 41
6.2 Equivalent circuit of the PD detection system with 'capacitors only' ABC model implemented in MATLAB® Simulink® 46
6.3 Equivalent circuit of the PD detection system with 'capacitors and resistors' ABC model implemented in MATLAB® Simulink® 47
6.4 Equivalent circuit of the PD detection system with 'capacitors and resistors with a residual capacitor' ABC model implemented in MATLAB® Simulink® 48
6.5 Relationship between cavity spark-over voltage and PDIV 49
6.6 Paschen curve for an air-filled void marked for a 1.5 mm depth cavity [98] 50
6.7 Flowchart logic of implementing PDIV and PDEV into the model 50
6.8 Surface conductivity and resistivity of polyethylene and epoxy resin insulation media [81] 51
6.9 Surface conductivity values from un-aged to aged states [99] 52
6.10 Flowchart representing PD mechanisms implemented in ABC model demonstrating the dependence of PD behavior on supply voltage frequency . . . 55
6.11 MATLAB® Simulink® equivalent circuit implemented as ABC model for simulating statistical time lag effect on PD behavior at different SVF . . . 56
6.12 MATLAB® Simulink® equivalent circuit implemented as ABC model for simulating cavity surface conductivity effect on PD behavior at different SVF 56
6.13 MATLAB® Simulink® equivalent circuit implemented as ABC model for simulating residual charge effect on PD behavior at different SVF 56

7.1 Over-voltage scenario due to delayed or scarce seed electron availability [48] 58

7.2 Cavity voltage waveforms at SVF of 1 Hz for seed electron availability at: (**a**) Scarcity and (**b**) Abundancy 59
7.3 PRPDP (PD pulses per phase angle) at SVF of 1 Hz for seed electron availability at: (**a**) Scarcity and (**b**) Abundancy 60
7.4 Cavity voltage waveforms at SVF of 50 Hz for seed electron availability at: (**a**) Scarcity and (**b**) Abundancy 61
7.5 PRPDP (PD pulses per phase angle) at SVF of 50 Hz for seed electron availability at: (**a**) Scarcity and (**b**) Abundancy 61
7.6 Cavity voltage waveforms at SVF of 200 Hz for seed electron availability at: (**a**) Scarcity and (**b**) Abundancy 62
7.7 PRPDP (PD pulses per phase angle) at 200 Hz for seed electron availability at: (**a**) Scarcity and (**b**) Abundancy 62
7.8 Cavity voltage waveforms at SVF of 1 Hz for surface resistance value: (**a**) R_{min} and (**b**) R_{max} 63
7.9 PRPDP (PD pulses per phase angle) at SVF of 1 Hz for cavity surface resistance value: (**a**) R_{min} and (**b**) R_{max} 64
7.10 Cavity voltage waveforms at SVF of 50 Hz for surface resistance value: (**a**) R_{min} and (**b**) R_{max} 65
7.11 PRPDP (PD pulses per phase angle) at SVF of 50 Hz for cavity surface resistance value: (**a**) R_{min} and (**b**) R_{max} 65
7.12 Cavity voltage waveforms at SVF of 200 Hz for surface resistance value: (**a**) R_{min} and (**b**) R_{max} 66
7.13 PRPDP (PD pulses per phase angle) at SVF of 200 Hz for cavity surface resistance value: (**a**) R_{min} and (**b**) R_{max} 66
7.14 Illustration of residual charge contribution to PD event occurrence [48] . . 67
7.15 Cavity voltage waveforms at SVF of 1 Hz for residual charge capacitor value: (**a**) C_{min} and (**b**) C_{max} 70
7.16 PRPDP (PD pulses per phase angle) at SVF of 1 Hz for residual charge capacitor value: (**a**) C_{min} and (**b**) C_{max} 70
7.17 Cavity voltage waveforms at SVF of 50 Hz for residual charge capacitor value: (**a**) C_{min} and (**b**) C_{max} 71
7.18 PRPDP (PD pulses per phase angle) at SVF of 50 Hz for residual charge capacitor value: (**a**) C_{min} and (**b**) C_{max} 71
7.19 Cavity voltage waveforms at SVF of 200 Hz for residual charge capacitor value: (**a**) C_{min} and (**b**) C_{max} 72
7.20 PRPDP (PD pulses per phase angle) at SVF of 200 Hz for residual charge capacitor value: (**a**) C_{min} and (**b**) C_{max} 72
7.21 ABC Model configurations' results comparison of supply voltage frequency sweep plotted together with experimental-based data obtained from the literature (*** : measured values as reported by Cavallini et al [9]). 77

List of Tables

2.1 Electrical failure-initiating and contributing causes in power transformers [13] . . . 8
2.2 Advantages and Disadvantages of On-line and Off-line PD Testing . . . 14

4.1 Key findings obtained in the literature on the effect of supply voltage frequency on cavity PD characteristics . . . 24

5.1 List and description of symbols used in the ABC PD model equivalent electrical circuits in this Chapter (Figure 5.1 - 5.4) . . . 34

6.1 Basic components of a PD test and measuring system . . . 41
6.2 Comparison of basic components of the implemented equivalent PD test circuit with the IEC60270 one . . . 45
6.3 Parameter definition and typical values used for the ABC models simulated in MATLAB® Simulink® . . . 53

7.1 Statistical time lag variations (from scarce to abundant) influence on PD characteristics at different supply voltage frequencies . . . 74
7.2 Cavity surface resistance variations (from R_{min} to R_{max}) influence on PD characteristics at different supply voltage frequencies . . . 75
7.3 Residual charge effect variations (from C_{min} to C_{max}) influence on PD characteristics at different supply voltage frequencies . . . 76

Abbreviations

AC	**A**lternating **C**urrent
DAC	**D**amped **A**lternating **C**urrent
DC	**D**irect **C**urrent
EI	**E**lectrical **C**urrent
HV	**H**igh **V**oltage
HVAC	**H**igh **V**oltage **A**lternating **C**urrent
HVDC	**H**igh **V**oltage **D**irect **C**urrent
IEC	**I**nternational **E**lectrotechnical **C**ommission
OWTS	**O**scillating **W**ave **T**est **S**et
PD	**P**artial **D**ischarge
PDEV	**P**artial **D**ischarge **E**xtinction **V**oltage
PDIV	**P**artial **D**ischarge **I**nception **V**oltage
PDRR	**P**artial **D**ischarge **R**epetition **R**ate
PRPDP	**P**hase-**R**esolved **P**artial **D**ischarge **P**attern
RLC	**R**esistor **L**(Inductor) **C**apacitor
RTS	**R**esonant **T**est **S**et
SVF	**S**upply **V**oltage **F**requency
VLF	**V**ery **L**ow **F**requency
XLPE	Cross-**L**inked **P**oly**E**thylene

Chapter 1

Introduction

High voltage (HV) power equipment and the components are important parts of electrical power systems i.e generation, distribution, transmission systems. Such equipment includes transformers, generators and motors, switchgear, solid dielectric cables and castings [1–4]. A major part of HV equipment is electrical insulation which is often regarded as the weakest link in the whole network [5]. Hence, studying and understanding how to effectively assess electrical insulation (EI) becomes paramount. The presence of partial discharges (PD) is one of the main indicators used to assess electrical insulation system quality. Hence, understanding PD phenomena enables corrective measures to be planned and implemented prior to further insulation degradation which in turn leads to saving costs by averting the risk of equipment failure [6]. Within the past decades there has been more interest in the research on further understanding PD phenomena. Insulation health assessment, diagnosis and monitoring is crucial in determining whether there is a need to reject, replace or repair the degraded equipment. Therefore, PD measurement becomes an important diagnostic tool in forecasting, assessing and improving HV insulation systems reliability. It is used in design tests, quality assurance and diagnostic assessments of electrical equipment [7]. PD diagnosis is applied in detection and monitoring of gradual deterioration of EI in HV equipment such as power cables. Moreover, it is used to check and test the quality and performance of new equipment insulation so that their reliability and integrity is known [1, 8]. The present work is therefore in the context of expanding knowledge on PD phenomena for improved efficacy of PD diagnosis. Figure 1.1 presents the road map and directions taken in the work under investigation.

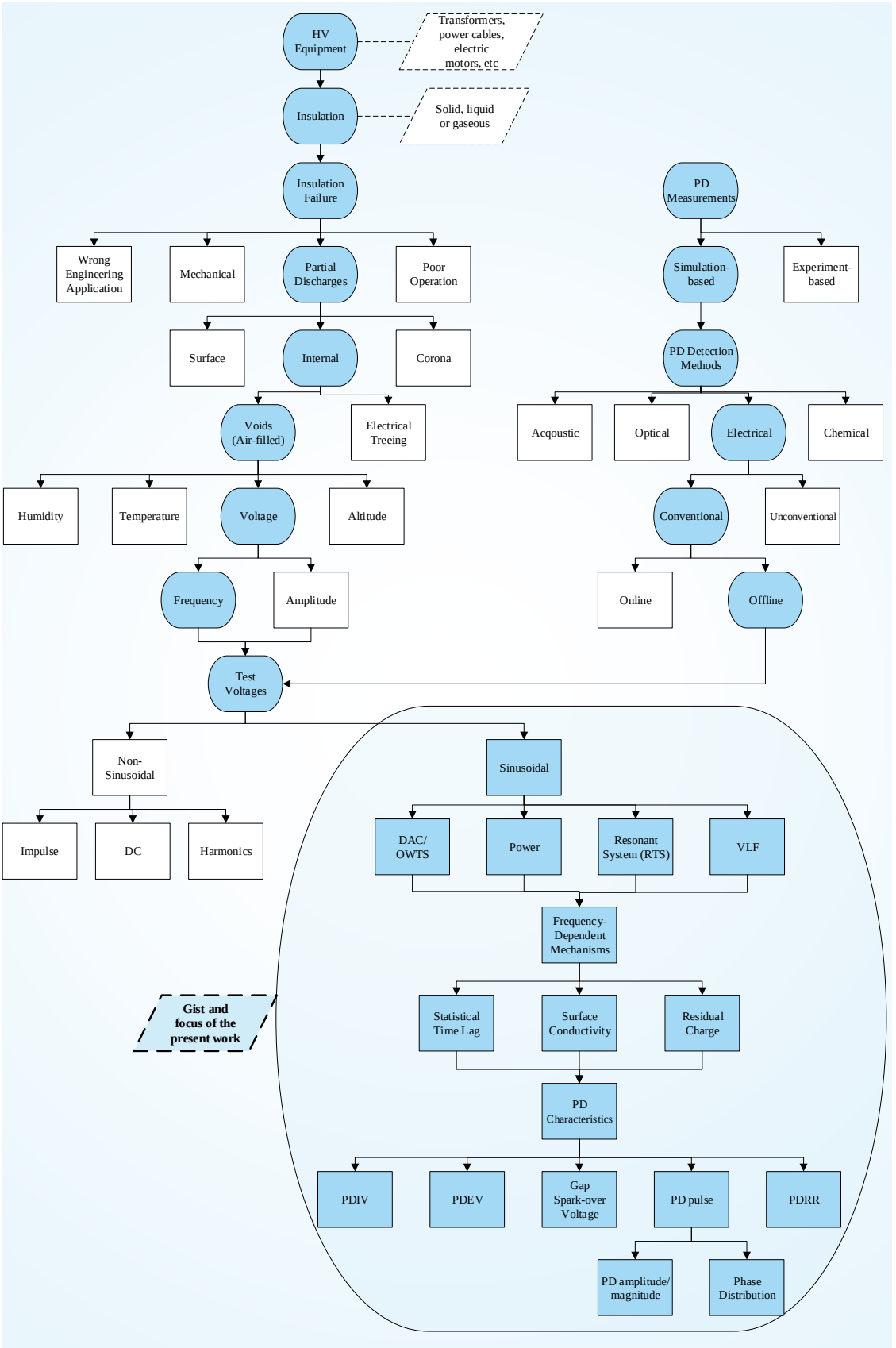


FIGURE 1.1: 'Setting up the scene'; The context of the present research work

PD activity is influenced by many factors and conditions. These factors include humidity, temperature, altitude, equipment type, and types of supply voltage. Extensive research has been done on most of these factors and researchers have agreed on how each respective factor influences PD activity. However, there is no consensus yet concerning the relationship between supply voltage frequency (SVF) and PD mechanisms. In practice, a wide range of test voltage and frequencies is used for different applications depending on the equipment being measured or tested. Most HV equipment operates at power frequency (50/60 Hz), but they are often tested at different frequencies. The use of very low frequency for capacitive equipment reduces power, cost and weight of the test voltage source [9]. It is not technically and/or economically feasible to test some of the equipment such as long cables at power frequency. As a result, low frequency test voltages are used for capacitive components like power cables and rotating machines (0.1 Hz), and higher frequencies are used for inductive equipment like transformers (150 - 400 Hz) [9–11]. Hence, the main study focus of the present work is to understand the behavior of PD activity under different supply voltage frequencies.

1.1 Problem Statement and Motivation

In PD diagnosis of electrical equipment, misdiagnosis often occurs and could be attributable to insufficient knowledge in interpreting PD signals. An area of insufficient knowledge is how PD relates to the frequency of the test voltage. The review of the available knowledge in literature has shown that more work needs to be done in understanding the influence of variable supply voltage frequency on PD phenomena, based on the lack of consensus, especially with regard to the frequency dependence of the mechanisms. Hence, how partial discharges relate to frequency variations of the test voltage has been an area of insufficient knowledge and is the focus of the present research work.

1.2 Research Question

In relation to the problem statement and motivation, it is established that there is more work that needs to be done in understanding the influence of frequency-dependent mechanisms on PD activity. The present work seeks to address the following question:

"To what extent do cavity PD mechanisms respond to changes in the sinusoidal supply voltage frequency?"

The study approach in the present research work is that of a simulation-based investigation. In order to answer and address the research question, simulation results are to be validated through comparison with experimentally-obtained results obtained from the literature on similar experimental conditions. In addition, the research objectives are outlined in the next section.

1.3 Research Objectives

This research aims at investigating the influence of variable frequency of the applied voltage on cavity PD parameters by attaining the following objectives:

- Identify and critically analyze the literature on the effect of frequency-dependent mechanisms on PD activity.
- Identify the knowledge gaps on the dependence of PD mechanisms on variable supply voltage frequency.
- Discretely analyze the frequency-dependent mechanisms and understand how they respond to the changes in supply voltage frequency.
- Identify a suitable model and develop further to simulate and interpret the extent to which frequency-dependent mechanisms behave to variations of the sinusoidal supply voltage frequency.

The structure of this dissertation is as follows:

- **Chapter 2** gives a literature review on partial discharges and their effect on electrical insulation.
- **Chapter 3** presents a literature review on partial discharges and the different types of test voltages used.
- **Chapter 4** presents a literature review on partial discharges and sinusoidal supply voltage frequencies.

- **Chapter 5** details a review on the techniques used on studying partial discharges with particular focus on PD modeling.
- **Chapter 6** unpacks the simulation design and development on the Matlab® Simulink® implemented model.
- **Chapter 7** presents the simulation results and their discussion and analysis.
- **Chapter 8** concludes the dissertation and presents recommendations for possible future extension of the research work.
- **Appendix A** is a copy of a paper published in the 2019 South African Universities Power Engineering Conference. The paper constitutes a part of **Chapter 4**.
- **Appendix B** is a copy of a paper published in the 2020 South African Universities Power Engineering Conference.
- **Appendix C** is a copy of an article published in the MDPI Energies journal as part of the Special Issue *Partial Discharge Monitoring and Analysis* edition. Part of the findings and analysis in this article constitutes part of **Chapter 7**.
- **Appendix D** is a copy of a paper published in the 2021 AFRICON Conference. The paper constitutes most part of **Chapter 3**.

Chapter 2

Partial Discharges versus Electrical Insulation

Opening Summary

There is a correlation between electrical insulation quality and partial discharges [7]. This chapter presents an analysis on electrical insulation failures and their relationship with partial discharges. Furthermore, the importance of PD measurement and diagnosis as well as electrical methods of PD detection are discussed.

2.1 Electrical Insulation Systems

Electrical insulation's main function is to electrically isolate two points of different voltages/potentials either from each other or from the zero potential (ground/earth) so that current flow and electrical stresses between them is minimal and of acceptable values [12]. Electrical insulation (EI) is used in HV equipment such as power transformers, generators, transmission lines, power cables, motors, switchgear [1, 13]. As such, EI systems are a significant and vital part of HV equipment. The electrical stresses that an EI system has to sustain for normal operation can be caused by applied voltage, varying environmental conditions (temperature, humidity), mechanical stress etc [14]. If these electrical stresses are not of acceptable values, they can be destructive to the insulation

system. Failure of EI to sustain these electrical stresses can reduce equipment lifespan leading to premature failure of the whole equipment. Thus, its quality and health status is crucial in determining the reliability of the whole HV network. The consequences of such failures can include, among others, electrical faults, more downtime on customers, low productivity and loss of profit on companies, damage on other equipment that would have been in good working conditions and frequent unscheduled interruptions [15]. In the context of South Africa, large disturbances such as load shedding (scheduled or not) can be a possible result of direct or indirect insulation failure. Due to the vulnerabilities on such large scale and vital networks, EI is considered as the weakest part of most medium voltage (MV) and high voltage (HV) equipment and their accessories [5].

2.1.1 Electrical Insulation Failure Analysis

Electrical failure is any malfunction on a power system component that results in partial or complete equipment breakdown, below-optimal equipment operation standards or unacceptable performance of users' equipment [13]. Electrical failure occurrences on a national utility supply system like ESKOM (South Africa) may result in forced outages, power interruption or loss of service (load shedding) as well as undesired deviations from normal operating voltage or frequency (50 Hz) [13].

In HV equipment, deterioration especially on electrical insulation is normal and inevitable. Insulation-related failures are commonly known as the main initiating and contributing causes of electrical equipment failures. Table 2.1, according to the IEEE Recommended Practice for the Design of Reliable Industrial and Commercial Power Systems standard [13], presents the typical failure-initiating and failure-contributing causes of electrical faults in power transformers. Direct insulation breakdown contributes about 50% of electrical failure-initiating causes. Transient voltage disturbances and overheating are indirect insulation breakdown failure-initiating causes that contributes about 20% of electrical failures. In addition, it has been reported that insulation-related failures contribute about 30% to motor damage [16]. Other failure-initiating causes that are not insulation related include improper operation and handling procedures, loose connections and terminations, and mechanical damages that may be caused by digging or during transportation. The most common electrical-contributing factor of 33.3% to electrical failure causes are due to a component being delivered with a defect from the

manufacturer. These defects may be from manufacturing imperfections, human errors and/or poor workmanship. Other failure-contributing causes are presented in Table 2.1.

TABLE 2.1: Electrical failure-initiating and contributing causes in power transformers [13]

Failure-Initiating Causes		**Failure-Contributing Causes**	
Cause	***%***	***Cause***	***%***
Winding insulation breakdown	29.1	Manufacturer defective component	33.3
Transient Voltage Disturbance (e.g arcing ground faults)	16.4	Inadequate maintenance	26.0
Insulation bushing breakdown	13.6	Normal deterioration from aging	13.3
Other insulation breakdown	5.5	Contamination, degradation of oil or other cooling medium	10.0
Overheating	2.7	Inadequate installation and testing	6.3

Unless it is mechanically damaged, electrical insulation normally does not fail instantaneously. It can fail with time from normal deterioration, which is commonly known as aging. More details on how normal deterioration and/or electrical insulation failure mechanisms occur and lead to complete insulation breakdown is presented in the next section.

2.1.2 Electrical Insulation Failure Mechanism

Electrical insulation does not normally fail instantaneously, however with progressing operational time, if it is not checked, constant deterioration can lead to its failure. Inadequacy of the EI system to sustain electrical stresses across the insulation medium is called 'dielectric breakdown' [12]. Such dielectric breakdown can be further enhanced by the presence of defects, such as air-filled cavities (voids) and/or other impurities. The process in which voids and/or defects contribute to EI failure mechanisms is described below.

In order to get better insight into how air-filled cavities and/or defects contribute to EI failure mechanism, the relationship between electric field intensity and material permittivity has to be understood. Equations 2.1 and 2.2 are used to illustrate this relationship.

$$E = (\frac{D}{\varepsilon}) \tag{2.1}$$

$$\varepsilon = \varepsilon_r.\varepsilon_o \tag{2.2}$$

where E is the electric field intensity (kV/mm), D is the electric field density (cm/m^2), ε is the absolute permittivity of the material with ε_r as the relative permittivity of the material and ε_o as the permittivity of a vacuum or free space.

Equation 2.1 shows that there is an indirect proportional relationship between electric field intensity and the permittivity of a material. Electric field intensity is dependent on the material/medium's permittivity characteristics [17]. Therefore, a material with a lower permittivity (ε) or relative permittivity (ε_r) experiences a higher electric field intensity. On the same note, a lower electric field intensity is experienced in a material with a higher permittivity. The magnitude and force of the electric field intensity is useful in testing if the material's dielectric strength is able to sustain the electrical stresses. Dielectric strength of a material is the measure of the capability of the respective material to sustain dielectric stress [12]. Failure of the material's dielectric strength to sustain the stress leads to the medium's failure, a phenomenon known as dielectric breakdown.

Air, considered as natural insulation, has relatively lower permittivity and dielectric strength compared to materials used in electrical insulation such as paper, transformer oil, epoxy or cross-linked polyethylene (XLPE) in power cables. Therefore, the presence of an air defect inside insulation media such as transformer oil or XLPE can result in dielectric breakdown occurring at the defect site due to high and concentrated electrical stresses. If this dielectric breakdown does not completely bridge the gap in between the electrodes, it is called a 'partial' breakdown also known as a 'partial discharge'. Consistent and repeated dielectric breakdown at the defect site causes irreversible damage to the insulation and consequently can result in complete insulation breakdown. Partial discharges are the main contributor to insulation deterioration and breakdown in electrical equipment. The following section highlights the graveness of partial discharges, how they contribute to the EI failure of electrical equipment as well as how they are used in determining the health status on the EI system.

2.2 Partial Discharges and Electrical Insulation Failure

According to the IEC 60270 standard [18], a PD is 'a localized electrical discharge that only partially bridges the insulation between conductors and which can or cannot occur adjacent to a conductor'. Other researchers have also termed partial discharges as the 'cancer' of power cables insulation [19] and as the main source of insulation breakdown [17]. Such terms have been used because the presence of a PD reduces lifespan of HV equipment as the insulation gets damaged with time.

Partial discharges can occur in solid, liquid or gaseous dielectrics. The presence of voids or impurities in the dielectrics leads to transitions from one permittivity to another within the same insulation medium. The differences in permittivity values (and dielectric strengths), as mentioned in Section 2.1.2, results in situations whereby the parts of the material with a lower permittivity initiate PDs due to higher localized stress concentrations. Hence, the presence of air-filled cavities or voids inside dielectrics is considered as the most common source of PDs because air has a lower permittivity than the surrounding dielectrics [4]. The voids in insulation can be caused by air leaking and settling into molds during epoxy insulation curing, poor workmanship during manufacturing processes, and bubbles forming through handling during transportation of equipment such as transformers. Fissures (cracks) in insulation due to mechanical stresses also are a form of cavities that may develop in insulation of equipment while in service.

When partial discharges occur in solids, they lead to irreversible physical and chemical deterioration on the dielectric which, if not monitored and mitigated, usually results in total breakdown of the insulation [20]. This 'delayed' total breakdown is commonly known as electrical aging and it leads to the formation of electrical 'trees' and loss in the material's mechanical strength [21]. Dielectric materials are designed to sustain electrical stresses and voltages for normal operations. Hence, loss of mechanical strength compromises the quality and ability of the insulation material to function as intended. In liquid dielectrics, such as transformer oil, PD occurrence can lead to formation of corrosive gases and chemical decomposition in the transformer oil which in turn also compromises the mechanical and chemical properties of the insulation [12]. In order to monitor PD activity in equipment, the PD signals have to be detected and interpreted as explained in the next section.

2.2.1 PD Measurement and Diagnosis

A partial discharge can be regarded as a symptom of an insulation's deteriorating condition. It is an indicator that there is a defect, electrical fault, progressive insulation degradation or weak points in the insulation. EI failure is mostly associated with PD progressive occurrence. The study of PDs becomes important as it is a tool used to assess, quantify, confirm and monitor insulation health status in high voltage equipment. PD diagnosis is then used in deciding whether the insulation requires replacement, maintenance or rejection. Therefore, the ultimate objective of PD diagnosis becomes the ability to predict the remaining lifespan of the equipment [19].

During normal HV tests on new or old equipment (power transformers and cables), such as withstand tests which can be done at twice the rated voltage, insulation might not fail immediately during testing. However, that does not automatically mean that there might not be defects or weak points in the insulation. Therefore, 'special' measurement tests are done in addition to other normal routine tests to check the integrity of the insulation. A PD test is one such 'special' test. PD tests are used in design tests, quality assurance tests and as a diagnostic tool. In design tests, PD tests are specially used to assess the reliability of new insulation system designs. In quality assurance tests, PD measurement is used as an additional test to ascertain that no defects were introduced during manufacturing before transporting the equipment into the field for installation [1]. As a diagnostic tool, PD tests are done on either new or old equipment to assess the possible causes of failure. For example, on a power transformer that would have malfunctioned or failed in the field during operation. Presence of PDs on such an equipment is a sign that the insulation system may have deteriorated due to aging caused by electrical, chemical, environmental stresses or presence of defects that might have occurred during the operational lifetime.

PD measurement and diagnosis is important because it ensures that insulation systems are tested for their quality and reliability enabling prevention of premature failures. If not properly done, PD measurement and interpretation can lead to poor decision making that may lead to unanticipated breakdown of equipment. For example, in design testing, a new insulation system may be approved as reliable because of wrong results interpretation and/or the testing method was not done properly resulting in unreliable insulation being used in the field. Therefore, methods used to measure PDs and interpret

results have to be reliable. Accurate PD signal interpretation is dependent on how the PD phenomena is understood. The present research addresses an aspect of PD phenomena that needs further understanding.

2.2.2 PD Measurement Methods

PD detection and measurement in HV equipment is performed using conventional and/or unconventional methods. In addition, PD tests and monitoring on these methods can be done 'off-line' or 'on-line'. Off-line PD testing is performed when the equipment under test is stand-alone and taken out of operation conditions. On-line PD testing is performed while the equipment under test is in operation. The advantages, disadvantages and relationship between conventional, unconventional, online and offline methods of PD testing are explored in this section.

Conventional, also known as classical, method of PD detection and measurement is mainly based on the IEC60270 standard [18] of High-voltage test techniques - Partial discharge measurements. The standard is specifically targeted at measuring partial discharges for alternating current (AC) voltages of up to 400 Hz and/or direct current (DC) voltages. Important information on PD activity is obtained through the understanding and interpretation of a wide range of PD parameters such as PD pulse, repetition rate, inception and extinction voltage as well as PD phase distributions. Conventional methods are widely used in research and development, design and maintenance tests in universities, testing centers, power utilities and in the manufacturing industry [20]. Under off-line PD testing conditions, the classical method's use of different test voltages is one of its advantages. More details on the advantages of using different test voltages are presented in Chapter 3. PD tests can be done under elevated electrical stresses and over-voltage conditions for improved PD signals such that the classical PD measurement method is commonly used, and adopted in the present research work.

Unconventional method of PD measurement is also known as the high frequency (HF) or ultra-high frequency (UHF) technique. It is also now standardized by the International Electrotechnical Commission (IEC). The PDs are detected using ultra-wide techniques as well as non-electrical methods. One significant advantage over the conventional counterpart is that it is more suitable for online PD testing. However, PDs can be diminished and absent at the instance of observation which may result in the

insulation being falsely deemed healthy. The consequence of this is that equipment's failure may occur prematurely leading to unscheduled interruptions.

On-line and off-line conditions of PD testing can be used in conventional and/or unconventional methods. The advantages and disadvantages of on-line and off-line conditions of PD testing are presented in Table 2.2.

The implementation of online PD testing is difficult under classical methods. Hence, off-line PD tests are mainly associated with the conventional way of PD measurement and the on-line tests with unconventional method. The use and importance of continuous data logging and monitoring of equipment has led to the growing interest in on-line condition of PD measurements. It should be noted that a single technique might not be sufficient to completely analyze and assess the condition of insulation. As such, the use of multiple techniques may be recommended in order to create a complete picture and yield better results.

Closing Summary

The relationship between partial discharges and the electrical insulation system has been established. The presence of partial discharges has been noted to be an indication of the vulnerability of the insulation system and should be properly measured and interpreted. Various techniques used in PD measurement and detection have also been discussed. Use of different types of test voltages is done under off-line conditions and therefore using the classical PD detection method. The rest of this dissertation is on partial discharges detected using classical techniques and with test voltage of different frequencies. The practice of detecting partial discharges at different test voltage frequencies is reviewed in the next chapter including the challenges that become the subject of this dissertation.

TABLE 2.2: Advantages and Disadvantages of On-line and Off-line PD Testing

On-line PD Testing		**Off-line PD Testing**	
Advantages	***Disadvantages***	***Advantages***	***Disadvantages***
There is no downtime i.e equipment under test does not need to be switched off for it to be tested	Advanced earthing measures are required for safety on personnel	It is a proven and commonly used technology (uses the IEC60270 standard [18])	There is downtime i.e equipment under test has to be isolated from the system for it to be tested
Equipment under test is live or loaded when tested which may be useful in providing all information present during failure/PD activity	Data interpretation can prove to be difficult due to the vulnerability of this method to external interference/noise in the system	Measurement equipment or devices can be easily calibrated for better results and interpretation	Equipment under test is not live/ loaded during testing which may omit relevant information present during failure/PD activity
This method can be considered as economical due to the absence of downtime during PD testing	It is difficult to target specific equipment in the system (e.g transformer only) to be tested	Specific equipment can be easily targeted and selected for testing	This method can be costly due to downtime and outage costs when equipment is out of operation
Equipment is easily monitored through continuous data logging	Diminished PD magnitudes at instance of observation is illusive	Different customized test voltages (e.g DAC, VLF) can be used	Equipment to be tested has to be transported to testing facilities
Exact operational environmental conditions are easily monitored and are available for interpretation and analysis of results		This method has limited or no noise/external interference which isolates the PD signal for better interpretation/analysis of results	

Chapter 3

Partial Discharge Measurements and the Test Voltages

Opening Summary

This chapter reviews different types of test voltages that are used when measuring partial discharges. The advantages, disadvantages and rational behind the use of the respective test voltages are described and discussed.

Test voltage or supply voltage is defined as the high voltage that is experienced on an object under test which causes partial discharges [22]. In addition, in the context of this dissertation and partial discharges, it is referred to as the voltage that is experienced in the electrical insulation of high voltage equipment. If the insulation media has the presence of impurities or air-filled cavities, it is the voltage that results in the occurrence of partial discharges. Therefore, any voltage present and responsible for PD activity in the insulation medium may be referred to as test voltage. Test voltage can be experienced intentionally and/or unintentionally depending on the operational or testing conditions of HV equipment.

Intentional test voltage experiences are those done in laboratory tests, design tests and factory acceptance tests. Under these conditions, a test voltage is intentionally applied across the insulation or object under test to check for the presence of partial discharges in the respective objects. Operational pure sinusoidal (power frequency: 50/60 Hz)

test voltage may be considered as intentional test voltage. Unintentional test voltage experiences are those that are undesired. For instance, the voltages across the insulation that are experienced due to harmonics, lightning strikes, switching transients and over-voltages. Intentional or not, these test voltages have an impact on partial discharges hence it is important to understand their importance, relationship and effect on PD activity for better detection and classification of the phenomenon. The relationship between respective test voltages and PD activity is discussed in more detail next.

3.1 Non-Sinusoidal Test Voltages

3.1.1 Harmonics

Harmonics are non-power frequency components riding on the operational power frequencies. The addition of grid-tied inverter-based renewable energy onto the national grid in order to sustain power demand has enhanced the presence of harmonics. The increased intensive use of modern power electronic gadgets also promotes 'noise' disturbances (which can be classified as harmonics) in communication and HV equipment [23]. The challenges associated with the presence of harmonics are common in all PD measurements and still need to be understood. Harmonics and other noise disturbance characteristics produce additional adverse effects on dielectric stress that are non-negligible [24]. Therefore, research on understanding harmonics occurrence and their control in electrical power systems as well as their effect on PD activity has been a sustained area of research. Florkowski [22] investigated the influence of harmonics on PD activity as well as PD pattern interpretation. Experimental results concluded that disturbances caused by harmonics have a significant influence on PD occurrence, affecting parameters such as PD intensity and maximum charge. Understanding the influence that harmonics have on PD activity is therefore important in properly assessing PD signatures in avoiding misinterpretations and assessment of PD severity [25].

3.1.2 Impulse Voltages (Lightning and Switching)

Lightning strikes are one of the main contributors of high voltage impulses in electric power systems [26]. Another contributor is switching transient over-voltages which are

a result of the increased use of power electronics gadgets that make use of pulse width modulation (PWM) characteristics. In addition, higher switching-on start-up currents of devices like induction motors can also present impulse-like signatures to equipment insulation. Impulse and switching over-voltages can have adverse consequences on PD activity, and consequently electrical insulation health. Therefore, the study of impulse voltage's effect on partial discharges is an area of research interest. Sun et al [27] experimentally investigated the influence of lightning impulse on a needle-plane configuration PD source in air. They observed that PD occurrence under impulse and AC voltages are similar. Kiiza et al [26] investigated the influence of HV impulses on PD activity in an artificial cavity embedded in oil-impregnated paper insulation. Their results concluded that HV impulses have an adverse impact PD activity occurrence as they can speed up the insulation degradation process. Investigations of PD activity in mineral oil under impulse voltage conditions have been conducted [28]. Other studies have been done on the combined effect of HV impulse stress superimposed on AC voltages in order to simulate conditions where a lightning strike occurs on an operating transmission line or HV equipment [29, 30]. In laboratory and factory acceptance tests, to simulate lightning conditions, voltage and current impulse voltages are applied on equipment under test. The most commonly used impulse voltage under these tests is the 1.2/50 μs standard lightning voltage waveform.

3.1.3 Direct-Current (DC)

Direct-current (DC) voltage has been an alternative technology to AC technology in HV power transmission. The main advantage of high voltage DC (HVDC) is the better viability in power transmission over very long distances compared to high voltage AC (HVAC). This is because HVDC power transmission has less corona, minimal radio interference, dielectric and power losses due to the absence of the reactive component which in turn removes the need to compensate power system stability as in HVAC [31, 32]. In the South African context, an example of such a scheme is the Cahora–Bassa HVDC line which transmit electricity between Mozambique (Songo Station) and South Africa (Apollo Station) over a distance of 1 420 km. Other applications of HVDC include bulk power transmission of offshore wind parks and oil platforms, long overhead and sea cables as well as linking renewable energy sources such as hydro, geothermal, solar and wind farms to each other and/or the national grid [32, 33]. Geo-politically,

HVDC transmission can be strategically used to transmit power across countries with or without political connections so as to avoid regional power competition. The study of PD activity under DC voltage has been an area of ongoing research.

Partial discharges in HVDC systems are not the main contributing factor to insulation degradation as compared to HVAC voltage systems. This is because PD inception at DC voltage can be three times higher than the one required at AC [32, 34]. However, presence of partial discharges is still a precursor to insulation failure. Major problems in identifying PD activity under DC voltage stress has been the difficulty of distinguishing PD signals from 'noise' and identifying defect types mainly because of the absence of the voltage waveform's phase information [35, 36]. In addressing these difficulties, experimental work and strategies for noise rejection and identification of defect types have been studied [35, 37, 38]. Other research studies have also been done on PD activity under AC and DC voltage combinations [38–40]. This approach uses PD characteristics under AC voltage as a benchmark test to check if a sample will experience PD activity. In addition, combined AC-DC voltage is the recommended test voltage for testing converter transformers' valve winding insulation [39].

3.2 Sinusoidal Test Voltages

Sinusoidal test voltages have the frequency attribute in common. Most HV equipment operate at power frequency (50/60 Hz) however they may be tested at different voltage frequencies. The same principle applies for PD measurements; whereby partial discharges are measured at power frequency for online and some offline (laboratory) test conditions. In most offline tests applied voltage amplitudes similar to those that occur during normal operation are used to initiate PD activity in test objects. Equation 3.1 [41] shows that the power required by the supply voltage source to energize the electrical insulation is determined by the test voltage frequency f, test voltage magnitude U, and capacitance, C of the device under test.

$$P = 2\pi f C U^2 \tag{3.1}$$

PD testing in highly capacitive HV equipment at operational frequency (50/60 Hz) has presented limitations on the economical and realistic practicality of energizing sources [42]. Hence, the concept of using strategically varied supply frequencies has been adopted to solve this limitation. The selection of very low frequencies for highly capacitive test objects such as power cables is a commonly used approach in order to minimize the power rating, size, weight of the test equipment. For instance, with reference to Equation 3.1, using a power source frequency of 0.1 Hz rather than 50 Hz can reduce the testing equipment power demand by a factor of 500 [43]. The concept of using varied supply frequencies has also been used on testing highly inductive equipment. Higher frequencies (150-400 Hz) have been adopted in testing inductive equipment such as power transformers and reactors in order to avoid the transformer's magnetic core saturation [9, 12].

HV equipment operational frequency, normally known as the power frequency (50/60 Hz) can be often different from the testing frequency for reasons outlined above. Therefore, PD activity and parameters may differ due to the use of different operating and testing frequencies. However, despite the differences that might occur, these supply frequencies have to be used. The most commonly used test voltages are the operational/power frequency, damped ac (DAC) or oscillating wave test set (OWTS), very low frequency (VLF) and the resonant test system (RTS) techniques. How partial discharges behave under these different test voltage frequencies needs to be fully known to aid accurate comparative analysis of measurement results. The knowledge in that regard is however still immature. The next sections discuss the common types of PD test voltage frequency techniques.

3.2.1 Operational or Power Frequency(50/60 Hz)

The operational and or power frequency (50/60 Hz) is the most common used operational frequency. Almost all HV equipment operate at this supply frequency. It is also the most commonly used test and supply frequency in laboratory tests during design and diagnostic tests as it brings some of the equipment's 'operating conditions' into the laboratory environment. The main reason for using this technique in PD measurement and testing is that PD effects and occurrence is directly comparable with how they would have been during normal in-service operation [44]. This technique presents a

disadvantage especially for off-line testing of long power cables as it demands more power from the testing equipment. However, shorter cables and cable accessories can be tested without having the need for higher power from the testing equipment. Most of the knowledge on PD has been generated using power frequency voltages. However, due to the increasing use of non-power frequency test voltages, as presented in the next sections, the interest to understand PD behavior under non-power frequency test voltages has increased.

3.2.2 Oscillating Wave Test Set (OWTS/DAC)

Oscillating Wave Test Set (OWTS), also known as Damped AC (DAC) is an alternative technique of measuring partial discharges of highly capacitive test objects at frequencies other than the power frequency. An oscillating wave excitation voltage is achieved by charging the capacitive object (power cable) with a DC voltage and then discharging through an inductor. The DAC method offers temporary excitation to the test objects because it is short-lived i.e only last for milliseconds which can be considered as both an advantage and disadvantage [44]. It has been considered a lesser destructive method compared to the VLF counterpart [41]. Consequently, DAC has been the more preferred testing technique for non-destructive PD detection and diagnosis. Another advantage of using OWTS is that it provides excitation similar to that at operational frequency and therefore PD measurements are comparable to those at 50/60 Hz. In addition, it requires less power in comparison to that required at power frequency and is convenient to transport for onsite PD measurements [45]. Morshuis et al [46] investigated the use of OWTS/DAC to stress and detect PD activity of a service aged power cable. They found their results comparable to those obtained at power frequency, However, for frequencies above 200 Hz, PD amplitudes were slightly lower as compared to those observed at power frequency. The conclusion to this slight difference was the abundant availability of seed electrons after a PD event. Due to some shortfalls in the OWTS/DAC technique of PD detection, other non-power frequency techniques such as the very low frequency (VLF) have been developed.

3.2.3 Very Low Frequency (VLF)

Very Low Frequency (VLF) test voltage method uses supply frequency range between 0.01 and 1 Hz, with the most commonly used frequency being 0.1 Hz [47]. The two mainly used waveforms are the cosine–rectangular and the sinusoidal waveforms. VLF technique was adopted to solve the problem of the lack of polarity of DC voltage testing method as well as minimizing the size of HV supply source in comparison with the one required at 50 Hz. By using a power source frequency of 0.1 Hz rather than 50 Hz the testing equipment power demand can be reduced by a factor of 500 [43, 44]. Hence, it is the most preferred method of measuring PD activity in power cables especially at distribution level. The technology has also been used for PD measurements on generator stator bars, on-site extruded cable testing as well as oil-paper insulation MV cable testing [43]. Other advantages of using VLF include the ability to test longer cables, convenient transportation and installation of the testing equipment. One of the major disadvantages of using VLF is that, in most cases, test objects such as power cables must be taken out of operation or service when they have to be tested offline. Hence, it is mainly used in diagnostic and quality acceptance tests that are done offline in laboratory and factory facilities. Research shows that VLF PD measurements can be slightly different from those that are observed at 50 Hz [48–51], and this is the rational of the present research work.

3.2.4 Resonant Test System (RTS)

Resonant Test System (RTS) technique uses supply frequency range between 20 and 300 Hz, although it is capable of measuring up to 400 Hz which falls under the range of the IEC60270 standard's allowable supply frequency [52]. This method is capable of on-site diagnosis of long power cables using higher frequencies. To further understand the parameters involved when dealing with RTS, Equation 3.2 is used.

$$At\ Resonance = \begin{cases} X_L = X_C \\ j\omega L = \frac{1}{j\omega C} \\ f = \frac{1}{2\pi\sqrt{LC}} \quad (resonant\ frequency) \end{cases} \tag{3.2}$$

where X_L and X_C are inductance and capacitance impedance, respectively. f is the resonant frequency, L is the resonant test set's inductance and C is the test object capacitance. For given C and L, the frequency that gives resonance is the one that becomes the frequency of the test voltage. RTS systems can be implemented by making use of variable inductance and/or variable frequency [53, 54]. Inductance-tuned resonant system allows the usage of a fixed frequency and variable inductance to achieve resonance. The main advantage of this option with regard to PD measurement includes the flexibility that tests are done in laboratories using the grid national frequency (50/60 Hz) since no complex varied frequency is required from the test equipment [45]. Frequency-tuned resonant system uses the option of fixed inductance and variable frequency to achieve resonance. The main advantage of this option is the flexibility to test different types and lengths of cables [44]. In addition, RTS technique uses less power as the one required at power frequency and PD measurements are comparable to those at 50/60 Hz. However, RTS test equipment is heavy and requires large vehicles for transportation. This can present a limitation if testing has to be done in a constrained environments. RTS test techniques are therefore often more economically viable for use in transmission networks. The fact that RTS can test partial discharges at non-power frequency further underlines the need to understand the influence of SVF on PD mechanisms which is the subject of the present work.

Closing Summary

Different types of test voltages used when measuring partial discharges are presented. The present work focuses on the use of the sinusoidal test voltages since they contain the frequency attribute; which is the study of interest. Variable frequencies of test voltages are used for economical and feasibility purposes hence the effect that supply frequency has on test voltages as well as partial discharge activity must be understood. The next chapter is on the state-of-the-art literature review of the relationship between partial discharges and sinusoidal supply voltage frequencies.

Chapter 4

Partial Discharges at Sinusoidal Supply Voltage Frequency (SVF)

Opening Summary

This chapter is on the findings in the research literature on the influence of the applied voltage frequencies on PD activity.

4.1 PD and Supply Voltage Frequencies; A Literature Review

Various research studies have been done to understand the influence of varied SVF on cavity PD mechanisms. The commonly investigated PD characteristics include the PD pulse (magnitude and amplitude), Phase-Resolved Partial Discharge Patterns (PRPDP), PD Repetition Rate (PDRR), PD Inception Voltage (PDIV) and PD Extinction Voltage (PDEV). Table 4.1 summarizes the landscape of the research and key findings in the literature. The second and fifth columns show the frequency ranges and the key findings by different researchers, respectively.

TABLE 4.1: Key findings obtained in the literature on the effect of supply voltage frequency on cavity PD characteristics

Researchers	**Frequency Ranges**	**Defect Types**	**Parameters**	**Key Findings**
Cavallini et al [9, 55, 56]; Hauschild et al [57]	0.1 to 300 Hz	2 mm diameter spherical cavity in epoxy resin	- PRPDP - PDIV - PDRR - PD magnitude (max)	- maximum PD magnitude decreases with increase in SVF. - PDIV slightly increase with increase in SVF. - PRPD patterns closer to zero crossing with increase in SVF. - PDRR both increases and decreases due to increase in SVF.
Forssen & Edin [11, 58, 59]	0.01 to 100 Hz	1.5 - 10 mm diameter disc-shaped cavities in polycarbonate	- PDRR - PD magnitude (max, min, mean) - PD phase - PDIV	- maximum PD magnitude decreases with decrease in SVF. - minimum PD magnitude independent to variations of SVF. - PDRR decreases with decrease in SVF. - phase-resolved PD patterns respond to SVF variations.
Illias et al [60] Chen et al [61]	0.01 to 100 Hz	1 mm diameter spherical cavity in epoxy resin	- PD magnitude (mean and maximum) - PDRR	- PDRR decreases due to increase in SVF. - PD magnitude decreases with increase in SVF.
Gafvert et al [62]	0.01 to 100 Hz	cavity embedded in homogeneous insulation	- PDIV - PD magnitude	- PDIV independent to variations in SVF. - smaller PD magnitudes at lower frequencies than at higher.
Mauseth et al [63]	0.01 to 100 Hz	cavity embedded in XLPE cable	- PDIV - PDEV	- PDIV increases as SVF is increased. - PDEV increases as SVF is increased.
Forssen & Edin [64]	0.02 and 100 Hz	1.5 - 10 mm diameter disc-shaped cavities in polycarbonate	- PD magnitude - PDRR - PRPDP	- PDRR decreases as SVF is increased. - PRPDP responds to variations in SVF. - maximum PD magnitude decreases with increase in SVF.

Table 4.1 :(continued) Key findings obtained in the literature on the effect of SVF on cavity PD characteristics

Researchers	**Frequency Ranges**	**Defect Types**	**Parameters**	**Key Findings**
Forssen [65]	0.01 and 100 Hz	4 mm diameter void	- PDRR - PD magnitude (min, mean, max)	- total PD magnitude increases with increase in SVF. - maximum PD magnitude increases with increase in SVF. - minimum PD magnitude independent of variations in SVF. - PD patterns are wider spread at higher frequencies. - PDRR increases due to increase in SVF.
Seri et al [66]	DC to 60 Hz	disc-shaped cavity embedded in polymeric insulation	- PDRR - PD amplitude	- PDRR increases due to increase in SVF. - PD charge amplitude increases with increase in SVF.
Miller & Black [50, 51]	0.1 to 50 Hz	4 mm diameter cylindrical cavity in epoxy resin	- PDIV - PD magnitude	- PDIV independent to variations in SVF. - smaller PD magnitudes at lower frequencies than at higher.
Illias et al [67–70]	0.5 to 50 Hz; 0.1 and 50 Hz	1 - 2.3 mm diameter spherical cavity in epoxy resin	- PDRR - total apparent charge - PD magnitude	- PDRR increases with increase in SVF. - maximum PD magnitude decreases with decrease in SVF. - total apparent change decreases with decrease in SVF. - mean PD magnitude decreases with increase in SVF.
Senoamadi et al [71]	0.02, 0.1 and 50 Hz	5 mm diameter cylindrical cavity in polyethylene	- PDRR - PD magnitude - PRPDP - PDIV	- PDRR increases with increase in SVF. - PDIV invariant to changes in SVF. - PD magnitude decreases with decrease in SVF. - PRPDP are further from zero-crossing at lower frequencies.

Table 4.1 :(continued) Key findings obtained in the literature on the effect of SVF on cavity PD characteristics

Researchers	**Frequency Ranges**	**Defect Types**	**Parameters**	**Key Findings**
Mosito et al [72]	0.02, 0.1 and 50 Hz	1 mm diameter disc shaped cavity in polyethylene	- PDEV & PDIV - PRPDP - PD magnitude	- PDIV and PDEV increase due to increase in SVF. - PRPDP shifts away from zero crossing as SVF is increased. - PD magnitude increases with increase in SVF.
Fynes-Clinton & Nyamupangedengu [48]	0.1 and 50 Hz	1 - 2 mm v-shaped cavity in XLPE	- PDIV - PD magnitude - PRPDP	- PRPDP independent to variations in SVF. - PD magnitude increases due to increase in SVF. - PDIV increases due to increase in SVF.
Nguyen et al [73–75]	0.1 and 50 Hz	2 mm diameter cylindrical void	- PDRR - PD magnitude (mean and max)	- PDRR increases due to increase in SVF. - mean PD magnitude increases due to increase in SVF. - max PD magnitude increases due to increase in SVF.
Bodega et al [42, 49]; Morshuis et al [46]	0.1 Hz; 50 Hz; DAC(260, 520, 930)	2 - 3 mm diameter spherical cavities in cast polyester resin	- PD magnitude - PRPDP - PDIV	- maximum PD magnitude decreases with increase in SVF (above 200 Hz). - PRPDP shape generally independent of variations in SVF. - minimum PD magnitude independent of variations in SVF.
Negm et al [76, 77]	50 to 1 000 Hz	1.5 mm diameter cavity	- PDRR - PRPDP - PD magnitude	- PDRR decreases due to increase in SVF. - PD magnitude decreases due to increase in SVF. - PRPDP has a wider spread from zero crossing at higher SVF.
Haghjoo et al [78]	50 and 100 Hz	1 mm diameter cavity	- PRPDP - PDRR - PD magnitude	- PDRR decreases due to increase in SVF. - PD magnitude increases due to increase in SVF. - PRPDP has a wider spread from zero crossing at higher SVF.

As evident in Table 4.1, significant knowledge has been accumulated in the literature on the attempt to understand the relationship between SVF and PD phenomena. Although there are some inconsistencies that still need further research, there have been notable agreements in some of the key findings and observations.

A general consensus by researchers that studied the PDIV characteristic is that it is independent and/or slightly increases with increase of SVF. The slight increase may be explained by the influence of the statistical time lag [65]. Plessow et al [79] and Forssen et al [11] have shown that PDIV is mainly dependent on the applied voltage amplitude and the geometry of the cavity. Another general consensus is that the minimal PD magnitude is unchanged from the variations of the supply voltage frequency.

Bodega et al [42] and Morshuis et al [46] concluded that PRPDP are generally unchanged with the variations of the applied voltage frequency. However, Cavallini & Montanari [9] reported that the overall shape of the PRPDP changes and shifts towards the zero crossing of the applied voltage waveform as the SVF is increased. Forssen & Edin [59] reported notable changes in the phase-resolved PD patterns in response to variations of the supply voltage frequency that were opposite to those reported in [9]. The lack of a general consensus in the literature on the relationship between the phase-resolved PD pattern and variable SVF can be attributed to the complex statistical nature and memory effect in PD activity's frequency dependent occurrence.

PD repetition rate and PD amplitude are the other cavity PD characteristics that have been widely investigated for their dependency on the variations of the applied voltage frequency. Similar to the observations reported on PRPDP characteristics, there is generally a balance of consensus and disagreements on how PDRR and magnitude are influenced by variations of the supply voltage frequency.

It can be argued that contributing to some contradictions in research findings in the literature is the fact that the ranges of the sinusoidal SVF as well as defect shapes and sizes investigated widely vary. Some have only investigated two frequency points such as 0.1 Hz and 100 Hz. Generalized conclusions that are drawn up from these frequency choices can be regarded as being too brave to deduce trends from too far apart data points. Some have used frequency range between VLF to 50 Hz, others between VLF to 300 Hz and VLF to 100 Hz, whereas some used frequency ranges above 50 Hz only (e.g 50 to 1 000 Hz). Considering only test voltage frequencies that are above 50 Hz

leaved out PD activity's behavior at very low frequencies and the latter is important since some HV equipment are tested at these low frequencies. Therefore, understanding PD phenomena over a more comprehensive frequency range that incorporate very low frequencies up to frequencies greater than 50 Hz is needed in order to clear up some grey areas in the literature.

Despite the agreements and contradictions on the key findings on the relationship between PD phenomenon and variable SVF, there has been general consensus on the identification of factors responsible for PD activity's frequency dependence. The identified factors, to be discussed in the following section, are: statistical time lag, surface bulk conductivity of the cavity, and the surface and residual charge decay. These factors influence PD activity both independently and dependently to each other, and sometimes synergistic and in some cases in contradiction.

4.2 Factors Responsible for Frequency Dependence of PD Mechanisms

The frequency dependence of PD activity and its signal characteristics and/or trends is a result of the relation between characteristics times/constants and the period time of the applied voltage waveform (T), and therefore the supply voltage frequency due to the relationship between time and frequency. A qualitative discussion of how the relationship contributes to the frequency dependence behavior of PD activity's characteristics is discussed in the following section.

4.2.1 Statistical Time Lag

For a partial discharge to occur, two conditions have to be met; a voltage condition whereby the applied electric field in the cavity should be greater than the minimum field for a PD to occur and the availability of a seed electron. The seed electron comes from either natural ionization of the air in the cavity or de-trapping from the cavity surface. In both cases, the availability is a statistically random event that is dependent on other parameters. Statistical time lag in a PD event is therefore the time it takes

for the two conditions necessary for a PD to occur to be both satisfied. The statistical time lag is represented as τ_{stat}. If τ_{stat} is shorter than the applied voltage period (T), then it does not significantly contribute to the frequency dependence of cavity PD activity. The reverse is true; whereby $\tau_{stat} > T$ indicating a scarcity of seed electrons. As a result there will be a notable time delay for a PD to occur after the critical electric field has been reached or exceeded. Consequently, pulses occur latter in the phase and at higher voltage magnitudes. This phenomenon is known as the statistical effect [11]. The statistical effect results in reduced PDRR with wider spread patterns, and gap over-voltage scenarios resulting in higher PD magnitudes/amplitudes. In addition, the statistical effect becomes insignificant at lower frequencies whereby $\tau_{stat} < T$, and more significant with increased applied frequency whereby the period time is shortened ($\tau_{stat} > T$). Therefore, that is how the statistical time lag characteristic time (τ_{stat}) contributes to PD activity's frequency dependence. Despite the seemingly understandable behavior explained above, a question still arises; to what extent does the statistical time lag respond to variations of the supply voltage frequency? This is the question to be addressed in the present research work.

4.2.2 Surface Conductivity

Cavity surface conductivity, sometimes coupled with bulk conductivity is represented by these characteristic times: void relaxation time (τ_{void}) and the dielectric time ($\tau_{material}$). These characteristic times are dependent on the distribution of the electric field on the surface walls of the cavity [60]. They have a synergistic relationship that leads to how they contribute to the frequency dependence of PD activity. The first relationship is when the void relaxation time is shorter than the dielectric time constant ($\tau_{void} < \tau_{material}$). In this scenario, the surface walls of the cavity are more conducting due to repetitive PD activity and insulation ageing. As a result, the PD repetition rate decreases with decreasing supply voltage frequency due to the screening effect that is intensified at very low frequencies [62]. The second relationship is when the void relaxation time takes longer or is greater than the dielectric time constant ($\tau_{void} > \tau_{material}$). As a result, the PD repetition rate may be increased at low frequencies due to the slow incremental rate of change of the applied voltage. How these parameters influence cavity PD characteristics' response to variations of SVF over a wide range is a question that needs to be addressed.

4.2.3 Residual Charge

Residual charge, which sometimes is referred as 'memory effect', is represented by the times: decay time (τ_{decay}) and trap time (τ_{trap}). These characteristic times account for charge transport processes in void and the surrounding insulation material. Residual charge effects are significant after subsequent partial discharges have occurred. After a PD occurs, the residual charge that is trapped on the cavity walls establishes an opposing electric field to the background one. The trapped residual charge is responsible for some PD pulses to occur at zero crossing of the applied waveform resulting in PDs occurring earlier in the circle. The resulting PRPDP signature becomes wider. Consequently, the PD repetition rate is increased. If the residual charge characteristic times decay faster than the rate of change of applied voltage ($\tau_{decay/trap} < T$), then it does not significantly contribute to the frequency dependence of cavity PD activity. However, if the residual charge decays slower than the period time of the applied voltage ($\tau_{decay/trap} \geq T$), its frequency dependence is significant. Therefore, the present research work investigates further to what extent residual charge affects PD characteristics

---

Closing Summary

A literature review on the influence that the variable sinusoidal supply voltage frequency has on PD activity and parameters has been presented. The review has shown that there are shortcomings on the findings reported in the literature. Despite these shortcomings, there has been general consensus on the identification of factors responsible for PD activity's frequency dependence occurrence. The identified factors have been noted to be the statistical time lag, surface conductivity of the cavity, and the residual charge decay. These factors influence PD activity sometimes in synergistic and in some cases in opposition. The presence of such shortcomings has motivated the present study. The next chapter presents the techniques used on studying partial discharges in further understanding and providing more information to the phenomenon. The choice of the PD study technique used in the present work is then presented.

Chapter 5

Modeling Approaches to Studying Partial Discharge Phenomena

Opening Summary

This chapter presents the techniques used on studying PD phenomena. Among the various techniques is the simulations approach which is the PD study technique used in the present work. The various common PD models used in PD simulations are discussed leading to the choice of the ABC model used in the present research.

5.1 Overview of Techniques Used in PD Studies

Various techniques have been used in the literature on the studying of PD activity. These techniques include laboratory-based experimental work, field measurement-based investigations, numerical and electrical modeling (simulations), and/or combinations thereof. Under experimental work, the object under test is either service-aged equipment or artificially-created defects. Artificial defects/cavities have an advantage of being controllable. However, this can also be a disadvantage especially because operational conditions are not always easy to identify or control. Lastly, numerical modeling results can be used to verify and validate measurements. The study technique in the present research work is that of simulations.

5.1.1 The Usefulness of PD Modeling

PD activity is a complex process as it is influenced by many mechanisms and parameters. Many of these parameters are critical in influencing how PD activity occurs and behaves under a wide range of conditions and stresses. More insight in understanding how each condition, mechanism and parameter contributes to the phenomenon can be attained through modeling. PD modeling can be used to confirm theories as well as verify and validate measurements. Modeling of PD is a vital tool in facilitating a better understanding and contribution to the knowledge body on the complexity of PD activity. The main objectives of PD modeling can be summarized as follows [6, 80];

- To increase the understanding of PD phenomena and behavior.
- To identify critical parameters and physical mechanisms influencing PD events, such as electron generation, surface conductivity and residual charge effects. Some of these parameters may be difficult to measure and control in a physical PD measurement experiment.
- To derive relations of defect characteristics, insulation design parameters, and test conditions.

5.2 PD Models Overview

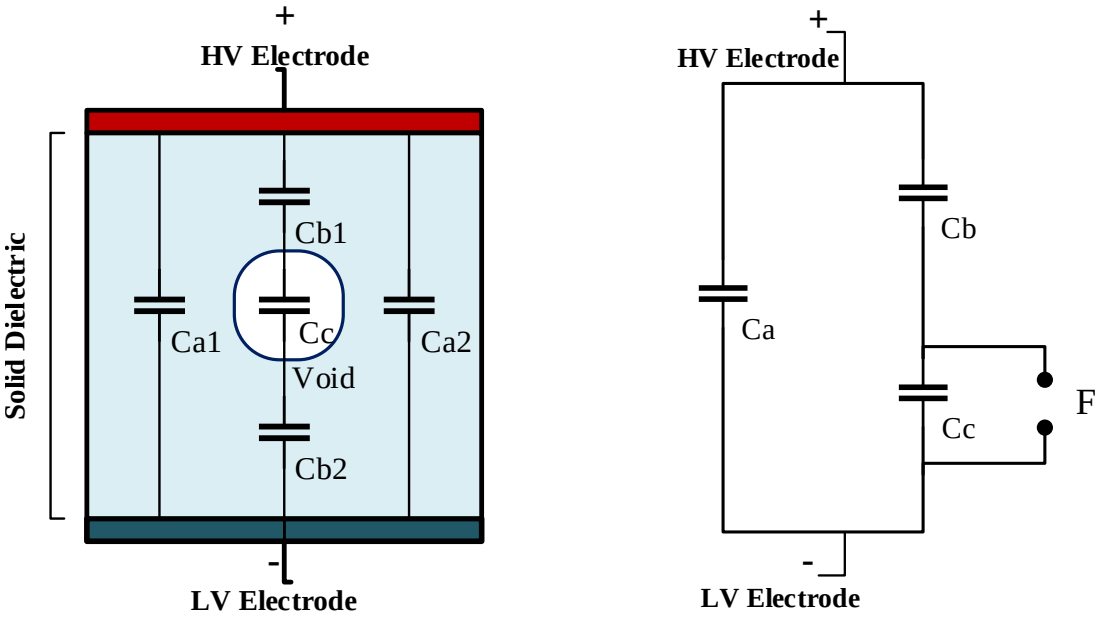
PD models can be classified into three broad categories, namely; the 3-capacitor (ABC), induced charge concept and Finite Element (FEMM) Analysis model. Modeling has enabled more insights into PD activity and has validated experimental-based measurements. A detailed insightful critical review of PD modeling was presented by Pan et al [81]. The significant takeaway from the latter is that each PD modeling selection has its strengths and weaknesses depending on the context of its application.

PD modeling has been useful in verifying and validating the general understanding of PD phenomena. In the context of the present work, PD modeling is used to investigate various aspects responsible for PD activity's frequency-dependence mechanisms under variable SVF. The 3-capacitor model has been the most preferred technique for this study because, as compared to other PD models as it requires less computing power.

Furthermore, the various parameters of interest in studying PDs under variable SVF can be controlled discretely. The model can be easily modified to incorporate other aspects of PD mechanisms such as seed-electron availability, electrical aging and memory effects. In the next section, the ABC PD model is introduced followed by a more detailed literature review on some of the modifications that have been applied to the ABC PD model.

5.3 The 3-Capacitor (ABC) PD Model Review

Many researchers have shown that the 3-capacitor (ABC) model is a valid and powerful tool for studying and interpreting PD phenomena. The ABC PD model can be described as representing the PD specimen as an assemble of three equivalent capacitors; the A, B, C capacitors. The ABC model reduces the cavity and surrounding dielectric material to a combination of equivalent capacitors as shown in Figure 5.1. Table 5.1 shows the description of the symbols that are used in the ABC models. A PD event is then characterized by the event of charging and discharging of the capacitor that represents the cavity. In 1952, Whitehead [78] incorporated a statistically controlled switch across the discharging capacitor in the ABC model to represent the statistical nature of PD activity.



(A) (B)

FIGURE 5.1: 3-capacitor equivalent circuit (**a**) with cavity illustrated inside the insulation and (**b**) with aggregated equivalent circuit parameters

TABLE 5.1: List and description of symbols used in the ABC PD model equivalent electrical circuits in this Chapter (Figure 5.1 - 5.4)

Symbol	**Parameter Description**
C_a	Capacitance of the health part of the insulation
C_b	Capacitance of the health part of the insulation in series with the void
C_{b1-4}	Capacitances of solid dielectrics above and under the cavities
C_c	Capacitance of the void/cavity
$C_{c1\&2}$	Capacitance of the two cavities (in multiple voids)
C_1 or C_{res}	Residual charge capacitance of the space charges within the void
C_12	Capacitance of the solid dielectrics between two cavities
F	Spark gap of the cavity
$F_{1\&2}$	Spark gaps of the two cavities (in multiple voids)
R_a	Resistance of the remaining health part of the dielectric insulation
R_b	Resistance of the solid dielectric above and under the cavity
R_c	Resistance through and around the cavity

Paoletti and Golubev [3, 16, 82] modified the classical ABC model by representing the insulation and cavity with combinations of equivalent capacitors and resistors in parallel with each other. The equivalent resistor in parallel to the cavity's equivalent capacitor represents the resistance of the cavity walls. This is illustrated in Figure 5.2. The same approach is also used by Takahashi et al [83] to investigate the dissipation that is associated with PD occurrence since such effect cannot be ignored in real phenomena. This modification of adding the resistor-in-parallel is of interest in the present work where variations of cavity surface conductivity (resistance) under SVF are investigated.

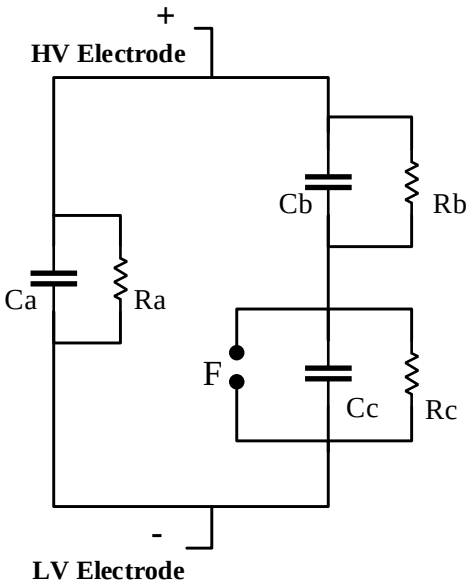


FIGURE 5.2: Modified 3-capacitor PD model with resistors in parallel with capacitors used for simulating cavity surface conductivity

Achillides et al [15] modified the classical ABC model by representing ideal switch operations of an air-filled cavity using a voltage-controlled triggering device. The ideal switch operations (ON and OFF) are dependent on the cavity's geometry and location. Gowda and Anandraj [84] also implemented the same approach but instead used a comparator to control the ON and OFF states. The switch's ON state is achieved when the voltage in the cavity reaches or exceeds the minimum level for PD inception whereas the OFF state is achieved when the voltage across the cavity is below the calculated voltage level for a PD to extinct. The present work utilizes the concept of using voltage-controlled switching against preset voltages to represent PD activity inception and extinction.

Haghjoo et al [78] implemented a comprehensive 3-capacitor PD model in artificially manufactured voids in MV power cable insulation. They mathematically modeled, among others, the statistical time lag of the seed electrons, residual voltage in the cavity and a statistically controlled switch function to determine when a PD gets initiated or halted. Van Jaarsveldt & Gouws [17] used the same approach and implemented it in MATLAB® Simulink®. The same technique of hosting the PD model in MATLAB® Simulink® is adopted in the present work but adjusted to be that of insulation between parallel plates.

Negm et al [76] developed a modified frequency-dependent ABC PD model to investigate the extent to which statistical time lag and trap time constant influence PD magnitude and phase distribution under variable SVF. The model uses equivalent resistors in parallel with equivalent capacitors to represent the conductivity in series and parallel to the cavity surface walls. The work by Negm et al [76] is of particular interest to the present work as it investigates frequency dependence of PD phenomena. Although the work was focused on the statistical time lag effect, in the present work it is extended to also investigate the other frequency-dependent mechanisms: cavity surface conductivity and residual charge.

Chen et al [85] presented a modified ABC PD model for PD activity occurring in transformer oil bubbles. The modified conditions included: (i) representation of seed electron availability using controlled switches to manipulate the discharge time, (ii) representation of the role of space charge using controlled current sources, (iii) representation of the role of residual voltage using controlled voltage sources, and (iv) adding a detection impedance in series with cavity for simulating the IEC60270 standard of PD

magnitude/amplitude measurements. With the residual charge effect being another frequency dependent variable of interest in the present work, some of these modifications have been critically adapted to a cavity that is embedded in solid dielectric insulation.

Subsequently, on the aspect of residual charge, Patsch et al [86–88] presented a modified version to the 3-capacitor model. They included an additional fourth capacitor to represent residual charge effect as illustrated in Figure 5.3. The fourth capacitor, C_1 produces a voltage drop in the cavity that represents the opposing electric field that is generated by the residual/space charge after a PD event. In addition, equivalent resistors in parallel to the residual charge capacitor and the spark gap are used to model the decay of residual charge with time and any local space charge that might have occurred externally, respectively.

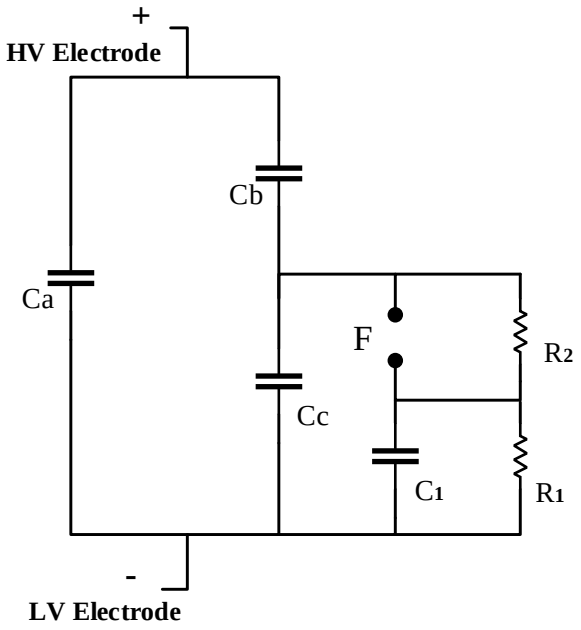


FIGURE 5.3: Modified 3-capacitor PD model with an additional capacitor used for simulating residual charge effect

Patsch and co-workers [86–88] investigated the role of residual charge using experimental-based measurements on a test transformer, stator of a small motor as well as its effect on surface discharges and influence on electrical treeing. The presence of residual charge plays a significant role in the nature of PD activity. Although, their reported results do not show the simulation-based results but just the presentation of the PD model that would address the role of residual charge, the modifications applied are adopted in the present work. The various parameters mentioned are further discretely controlled, in the present work, to understand further their full contribution to PD activity occurrence.

Various other modifications have been implemented on the 3-capacitor model to investigate various aspects and parameters of PD phenomena. It has been used to describe PD occurrence in solid dielectrics [89], investigate apparent charge and PD energy characteristics [2], and in investigations on the effect of applied voltage amplitude [90]. In addition, the model has been used to investigate the influence of temperature on PD activity [78, 91] as well as the effect of void geometry parameters (size, shape, location) [58, 76, 78]. Pan et al [81] gave a critical review of numerical modeling comprising of circuit structures, characteristics and explanations on how each of the capacitance models can be modified to address different applications [81]. In the review, the ABC model circuit structures and representations for multiple cavities modeling, residual charge effects, insulation and cavity's surface conductivity, as well as the discharge channel resistance are presented. The circuit structures provides directions on how the various combination of equivalent resistors and capacitors can be implemented and placed on the ABC model. The wide ranging possibilities on how the ABC model can be modified and discretely controlled to meet required needs further confirms its attractiveness in using it to investigate PD activity's variety of parameters.

Danikas et al [92] compared simulations and experiment-based results from artificially manufactured cylindrical voids embedded in polyethylene sheets. The simulated results compared well to the experimental-based results thus further confirming the usefulness of the ABC model in PD activity analysis.

The ABC model has also been used to investigate the interaction of PDs in two closely-coupled cavities [93–95]. The PD occurrence in the lumped capacitances, as illustrated in Figure 5.4, is modeled as voltage-controlled switches that are governed by breakdown voltage conditions in the respective multiple voids. When dealing with multiple voids, a combination of equivalent capacitors can be strategically placed to further analyze the precise nature of PD activity within each void and/or in relation to the other surrounding voids. The study of closely-coupled voids is important as in practice voids and defects do occur in multiples. Use of the ABC model in studying double cavities is a possible future extension to the present research work.

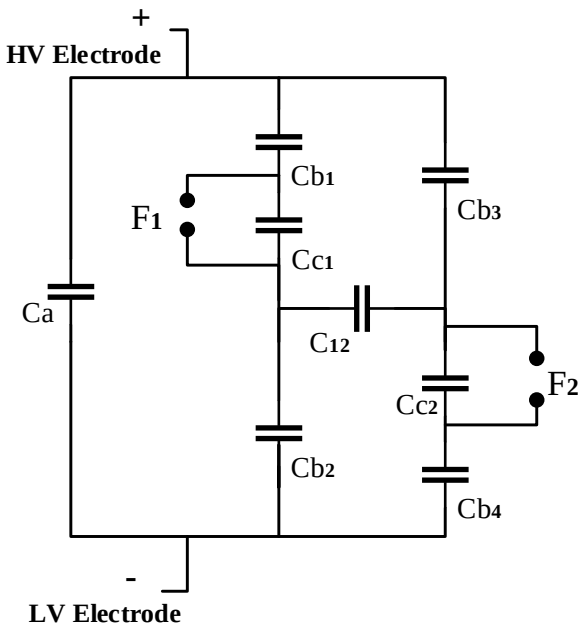


FIGURE 5.4: Modified 3-capacitor PD model with an array of capacitors used for simulating PD activity in closely-coupled multiple voids

In order to study the supply voltage frequency-dependent PD mechanisms (the area of focus in this research work), some of the aspects, modifications and circuit architectures reviewed in this section have to be fused. The frequency-dependent PD mechanisms being focused on are; (i) the statistical time lag, (ii) surface resistance of the cavity walls and, (iii) the residual charge effect.

Closing Summary

PD modeling has been found to be a powerful tool for use in understanding the PD phenomena and dependence on various factors. The 3-capacitor (ABC) PD model has been selected in the present work to be used in investigating frequency dependence mechanisms of PD activity. The next chapter details, among other approaches, how the chosen 3-capacitor model is modified to simulate the three factors; statistical time lag, cavity surface conductivity and the residual charge effect.

Chapter 6

Experimental Design and Development of the ABC PD Model in MATLAB® Simulink®

Opening Summary

This chapter outlines the processes and procedures taken in designing and developing the simulation model that is implemented in MATLAB® Simulink®. It uses the information that has been presented in the literature reviews in the previous chapters. The steps and decisions taken are also informed by the reviewed literature. The IEC60270 standard forms the basis of the model's design and implementation.

6.1 Partial Discharge Measurements: IEC60270

6.1.1 General Scope

The IEC60270:2000 (High-voltage test techniques - Partial discharge measurements) [18] is a standard that is designed for offline PD measurements in electrical apparatus and/or systems like power transformers, cables and insulation. It is applicable on PD measurement techniques that use alternating (AC) voltages of up to 400 Hz as well as

DC. This frequency range flexibility is most suitable to the research work at hand of studying the effect of different supply voltage frequencies on partial discharge activity. The range of SVF selected for the present work of study is for test voltage frequencies up to 200 Hz which falls under the IEC60270 standard's scope of work. In addition, the standard can also be applicable to measure partial discharges under direct (DC) voltage which is useful if the present work is extended to PD measurements under DC voltages i.e 0 Hz.

The IEC60270 standard, among other important information and in conjunction with the IEC60060-1 (High-voltage test techniques – Part 1: General definitions and test requirements) [96] standard; (i) defines the terms used in relation to PD measurements, (ii) defines the PD quantities that are to be measured, (iii) describes the test and measuring tests that may be used when doing PD measurements, and (iv) gives guidance on the procedures that are supposed to be taken when doing PD tests. The aforementioned are relevant to the present of work and will be referenced and used throughout the rest of this dissertation. Partial discharges are noted to be the effect of local electrical stress build-ups in the insulation. Other respective definitions and PD quantities that are related to partial discharge measurements in the context of the present research work are presented into more detail in Chapter 7. The next section gives details on the chosen test circuit for the present research work.

6.1.2 Test and Measuring Circuits

The IEC60270 standard presents four general circuit variations that can be used when performing PD testing and measuring. Other circuit derivatives that are adopted in PD measurements to specific testing requirements can then be derived from the mentioned four generic variations presented in the standard. Despite having different configurations and the flexibility of more circuit derivatives in order to suit user specifications, all the circuits involved in PD testing and measurement have common elements which are presented in Figure 6.1 and Table 6.1 [18]. The circuitry shown in Figure 6.1 is the one selected as the option of choice based on the advantages that it provides such as better sensitivity for test circuits with low capacitance components as the one in the present research work.

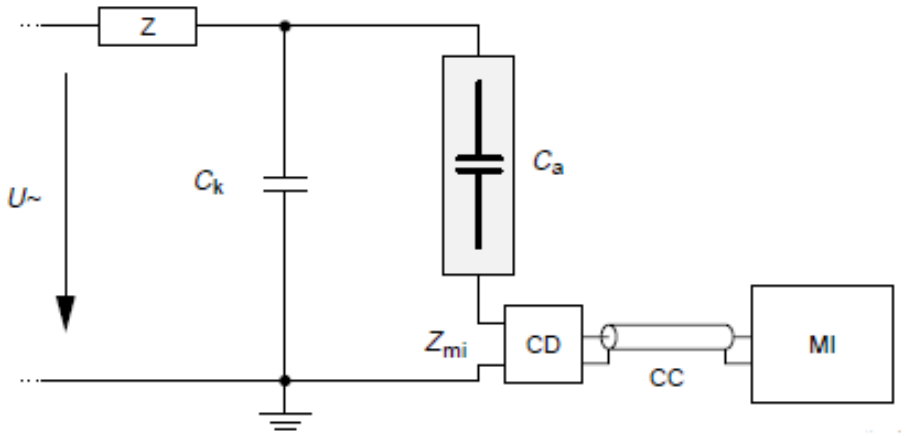


FIGURE 6.1: IEC60270 PD test circuit with coupling device in series with the coupling capacitor

TABLE 6.1: Basic components of a PD test and measuring system

Symbol	Description
U∼	High voltage (HV) supply
Z	Filter
C_k	Coupling capacitor
C_a	Test object
Z_{mi}	Input impedance of measuring system
CD	Coupling device
CC	Coupling cable
MI	Measuring instrument

In addition to the test and measuring circuit shown in Figure 6.1 and Table 6.1, more details are addressed on the components of the system. The test object or the device-under-test, C_a is usually regarded as a capacitor and in the context of the present work it is the cavity PD ABC model which satisfies the condition of being an ideal test object i.e a capacitor. The coupling capacitor, C_k is preferred to be of low inductance and PD-free when test voltage is applied for the allowance of PD quantities measurements. The minimal PD quantities' magnitudes under PD testing are limited by disturbances that arise from internal noise on the measuring instruments, and test circuit's layout, physical dimensions and used parameter's values [18]. The capacitance ratio of the test object and the coupling capacitor, (C_a/C_k) contributes as another limitation of minimal PD measurements. The ideal condition to achieve highest PD measurement sensitivity is when C_k is much greater than C_a $(C_k >> C_a)$ which is difficult to satisfy as the value of C_k is limited in actual or experiment-based tests. However, most of these limitations

are assumed to be negligible in the present research work as it focuses on simulation-based tests. Low levels of background noise are crucial in order to achieve reliable PD measurements hence the high voltage supply and connections (cables) should be as short as possible and dimensioned to minimize inductance therefore reduce picking up electromagnetic interference. A filter or an impedance is generally introduced at the high voltage side of the test circuit in order to reduce and/or eliminate noise levels that may be generated by the high voltage supply and also reduce fault currents in the case of failure of the test object.

How the information gathered from the IEC60270 and presented in this section is used in designing and developing the equivalent circuits used in the present research work is presented in Section 6.3. But firstly, how the frequency-dependent mechanisms are designed and incorporated into the simulations are addressed in the next section.

6.2 Mechanisms Responsible for PD Dependence on SVF

It has been presented in the earlier Chapters that the three main mechanisms responsible for PD activity's frequency dependence are; statistical time lag, surface conductivity and the residual charge effect. These factors are the focus area of the present research work. The mechanisms are implemented in Matlab® Simulink®. More information on this follows in Section 6.5.

6.2.1 The Statistical Time Lag

The two conditions that have to be both met for a partial discharge to occur are; a sufficient electric field strength in the cavity that results in breaking down a cavity's electric field strength and the availability of a 'seed' electron that will initiate an electron avalanche process. In this section, the second condition of the initiating electron is discussed. It is the latter condition that is mainly responsible for the random and stochastic nature in PD activity occurrence. Thus, the availability of a seed electron condition is implemented in two stages. The first stage is selecting and setting a 'probability' value between 0 and 1 ([0, 1]) that is a representation of the probability that a seed electron will be available. The second stage, which represents the stochastic nature behavior, makes use of random numbers generator function in Matlab® Simulink® that

generates an array of random numbers. The two stages are combined to control the probability of seed electron availability. For instance, for randomly generated numbers between 0 and 1, selection of probability values 0.25, 0.5 and 1, respectively represent a 25%, 50% and 100% probability of the seed electron being available to initiate an electron avalanche process.

It should be noted that when investigating the statistical time lag effect on SVF dependence, two co-dependent parameters are varied; seed electron availability and the applied voltage frequency. Any other parameters, factors and mechanisms of the PD model are kept constant. Figure 6.10 (Section 6.5) shows how the statistical time lag component is linked to the rest of the other parameters and mechanisms.

A 25 % probability (0.25 value) is chosen to simulate the scarce seed electron availability condition. Under the scarce electron condition, the applied voltage frequency is swept from 1 Hz to 200 Hz and the extent to which the cavity PD characteristics' respond are noted. The simulation of scarce seed electron availability is representative of situations where cavity defects are unvented and unaged. The same procedure is repeated to simulate abundancy (100 % probability). The abundancy condition signifies that seed electron(s) are readily available. Abundancy seed electron availability is representative of situations where cavity defects have severely aged.

6.2.2 Cavity Surface Conductivity

The cavity walls of an air-filled void become conductive when a partial discharge or a breakdown occurs. Hence, the surface conductivity of the cavity walls is another frequency dependent mechanism being investigated in the present research work. The resistor, R_c in parallel with the cavity capacitor, C_c as shown in Figure 6.3 and 6.4 represents the surface resistance of the cavity walls. It is assumed that the conductivity of the air in the cavity is negligible. In order to investigate the influence of surface conductivity on PD characteristics, the cavity surface resistor, R_c is varied from a minimum selected value, R_{min} to a maximum selected value, R_{max}. The values to be used in the range R_{min}:R_{max} are presented in Section 6.4 below. Whilst varying R_c, all the other parameters, factors and mechanisms of the PD model are kept constant. Figure 6.10 (Section 6.5) shows how the surface conductivity component is linked to the rest of the other parameters and mechanisms. Keeping all the other parameters and mechanisms

constant enables monitoring of the extent to which surface conductivity influences PD characteristics as a function of the SVF.

At each surface resistance, R_c value between R_{min} to R_{max}, the applied voltage frequency is swept from 1 Hz to 200 Hz. Whilst varying the supply voltage frequency, the resultant cavity PD characteristics are then observed and monitored at each surface resistance value. The process of varying the cavity walls' conductivity and/or the applied voltage frequency therefore partly address the answering of the research question to the extent the surface conductivity of the cavity walls respond to changes in the supply voltage frequency.

6.2.3 PD Residual Charge Effect

A partial discharge event deposits space/residual charge on the surfaces of the discharge area. The space charge deposited on the cavity surfaces after every PD event can also influence subsequent PD characteristics. In the present case of an air-filled cavity, the space charges are deposited on the opposite sides of the cavity. The resultant potential difference due to the space charge, also termed residual charge, influences the next PD event. The component of interest representing the influence of residual charge on PD activity is the 'residual' capacitor, C_{res}. The 'residual' capacitor is introduced inside cavity capacitor, C_c to represent the processes that occurs when space charge is deposited on the surface of the discharge area. Figure 6.4 is presented for investigating the residual charge effect and illustrates how this phenomenon is to be implemented into the model.

In order to investigate the residual charge effect on PD characteristics, the 'residual capacitor, C_{res} is varied from a minimum selected value, C_{min} to a maximum selected value, C_{max}. The values to be used in the range C_{min}:C_{max} are presented in Section 6.4. Whilst varying C_{res}, all the other parameters, factors and mechanisms of the PD model are kept constant. Figure 6.10 (Section 6.5) shows how the residual charge effect component is linked to the rest of the other parameters and mechanisms. Keeping all the other parameters and mechanisms constant enable monitoring of the extent to which PD characteristics respond to the residual charge effect as a function of SVF.

At each 'residual' capacitor, C_{res} value between C_{min} to C_{max}, the applied voltage frequency is swept from 1 Hz to 200 Hz. Whilst varying the supply frequency of the

applied voltage, the resultant cavity PD characteristics are then observed and monitored at each capacitor C_{res} value. The process of varying the residual charge effect and/or the applied voltage frequency therefore partly addresses the answering of the research question on the extent the residual charge affect PD characteristics' dependence on changes in the supply voltage frequency.

The next section details the electrical equivalent circuits that are used in addressing each of frequency dependent mechanisms described in this section in relation to the IEC60270 [18] guidelines.

6.3 Equivalent Electrical Circuits in the Model

This section continues from the previous sections in showing the equivalent electrical circuit used to simulate the effect of the frequency dependent mechanisms according to the prescribed partial discharge measurements standard IEC60270 [18].

Table 6.2 shows the compare and contrast of the IEC60270 elements against the ones chosen for the equivalent electrical circuits. It is a necessary comparison to show that the integrity of the prescribed test and measuring system specifications are maintained. The high voltage supply, coupling capacitor and measuring system input impedance are maintained. The filter for the test circuit has been replaced with a current limiting resistor. The measuring instrument used in the simulations is an oscilloscope. The minor adjustments and derivations made on the IEC60270 test and measuring system are assumed not to compromise the integrity of the PD system and its measurements.

TABLE 6.2: Comparison of basic components of the implemented equivalent PD test circuit with the IEC60270 one

IEC60270	**Description**	**Equivalent Circuits**
U∼	High voltage (HV) supply	✓
Z	Filter	Supply resistance
C_k	Coupling capacitor	✓
C_a	Test object	3-capacitor model
Z_{mi}	Measuring system input impedance	✓ RLC impedance
CD	Coupling device	Detector (RLC) circuit
CC	Coupling cable	Negligible impedance
MI	Measuring instrument	Oscilloscope

Figures 6.2 to 6.4 show the equivalent electrical circuits designed and developed to simulate the PD measurements of the present work. The common components are essential and required in all the equivalent circuits in order to maintain the consistency of the simulated PD measurements. The statistical time controller is responsible for checking if the conditions necessary for a PD to occur have been met or not. The controller is a voltage-controlled switch that uses set inception and extinction voltages as well as seed electron availability to open or close the switch for PD activity to be observed and measured. Figures 6.7 and 6.10 show more information on the functionality of the controller. The detector circuit, that produces a voltage and/or current pulse at its output according to the IEC60270 standard, is introduced in the test circuit to measure the voltage and/or current pulse that results from PD activity within the device under test [18]. In this case, the device under test is the cavity PD ABC model. The IEC60270's device under test, C_a is replaced and is now representative of the ABC model i.e C_a, C_b, C_c and all its other components. Thus the mention of C_a in the rest of the research work, unless specified, refers to the C_a of the ABC PD model.

Figure 6.2 shows the equivalent electrical circuit developed and designated for the simulation of the statistical time lag effect. This equivalent circuit does not have many components or parameters that would have contributed to the overall PD activity in the model. Thus, the general resultant PD measurements are mainly due to the extent statistical time lag respond to its and applied voltage frequency variations.

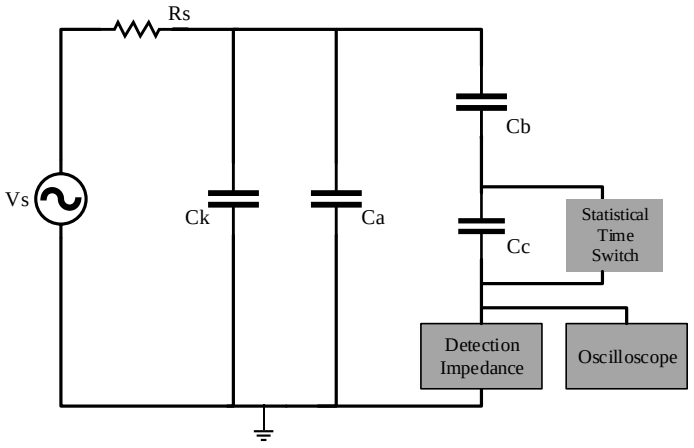


FIGURE 6.2: Equivalent circuit of the PD detection system with 'capacitors only' ABC model implemented in MATLAB® Simulink®

Figure 6.3 shows the equivalent electrical circuit developed for the simulation of the surface conductivity of the cavity walls. Equivalent resistors in series with the equivalent ABC capacitors are introduced to represent the resistance of the cavity, as well as the resistance of the health insulation in parallel side and in series below and above the cavity. The parameter of focus in Figure 6.3 is the surface resistance of the cavity's walls, R_c.

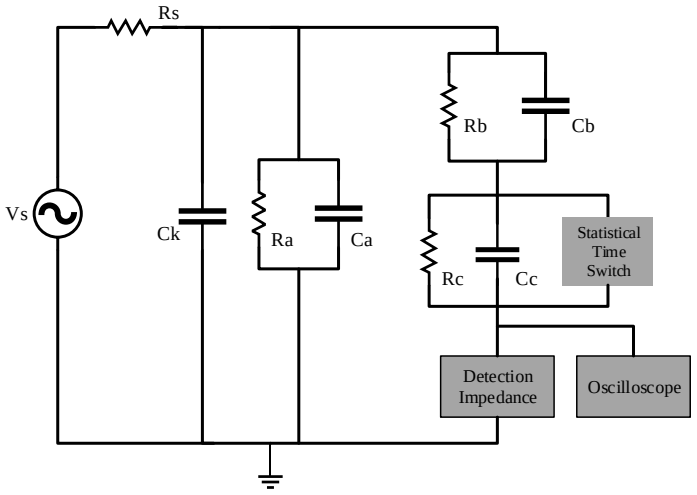


FIGURE 6.3: Equivalent circuit of the PD detection system with 'capacitors and resistors' ABC model implemented in MATLAB® Simulink®

Figure 6.4 shows the equivalent electrical circuit developed for the simulation of the residual charge on the surfaces of the discharge area. Few improvements have been added to this equivalent circuit in comparison to the ones presented in the literature (Figure 5.3). Equivalent resistors in series with the equivalent ABC capacitors are introduced to represent the conductivity of the cavity, as well as the resistance of the health insulation in parallel side and in series below and above the cavity. These additions represent the actual insulation more accurately. C_{res} represents the potential difference, V_{res} that is due to the space charge build-up. The resultant voltage across the cavity (gap spark-over voltage) is then a function of the residual charge voltage and is represented by Equation 6.1.

$$V_g = \vec{V_c} + \vec{V_{res}} \tag{6.1}$$

where V_g is the resultant voltage across the cavity, V_c is the total voltage across the cavity and V_{res} is the residual voltage that is deployed on cavity walls after a PD event. The varying of C_{res} (consequently, V_{res}) whilst all the parameters are kept constant varies the space charge potential difference. Subsequently, how PD characteristics respond

to residual charge and/or applied voltage frequency variations is then monitored and measured.

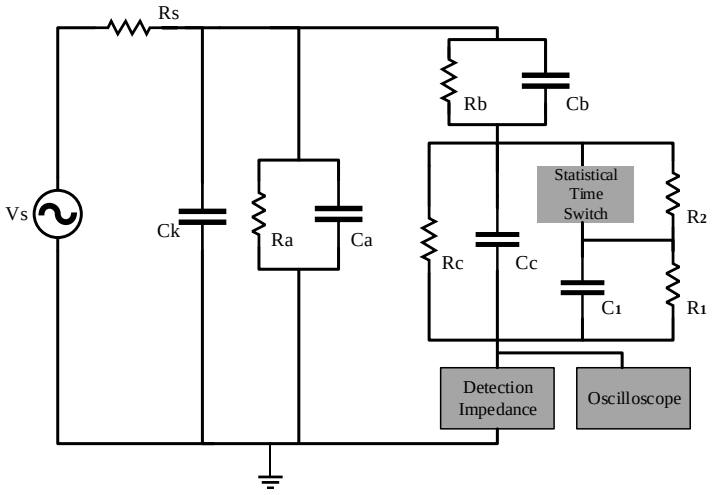


FIGURE 6.4: Equivalent circuit of the PD detection system with 'capacitors and resistors with a residual capacitor' ABC model implemented in MATLAB® Simulink®

With the equivalent electrical circuits presented in this section, the next section details how some of the parameters and PD characteristics are implemented in MATLAB® Simulink®.

6.4 Determination of the PD Equivalent Circuit Components Values

6.4.1 Cavity Spark-Over Voltage, PDIV and PDEV

PDIV is defined as the applied voltage at which repetitive partial discharges are first observed in the device under test, when the voltage applied to the device is gradually increased from a lower value at which no partial discharge activity is observed till it initiates [18]. In other words, it is the voltage across the electrodes at which the cavity breakdown strength is exceeded and PD activity is initiated. The corresponding voltage across the cavity at which the cavity breakdown strength is exceeded is the cavity spark-over voltage (V_{so}). Figure 6.5 illustrates the relationship between cavity spark-over voltage and the PD inception voltage.

The origins and limitations of the physical concepts used in PD activity modeling have been highlighted by Callender & Lewin [97]. Their discussion was restricted to cavity PD

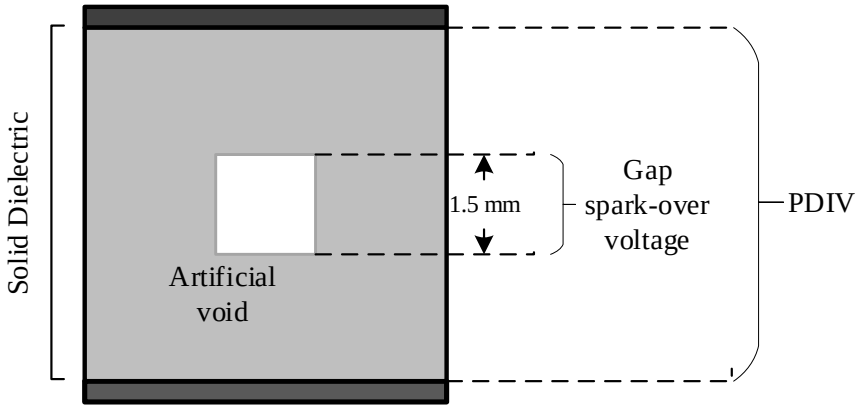


FIGURE 6.5: Relationship between cavity spark-over voltage and PDIV

occurrence under alternating voltage which is relevant to the present research work. A critique of the applicability of PD modeling concepts such as the PD inception electric field are of particular interest especially in the context of the present research. The critical field intensity that initiates self-propagating electron avalanches in a PD event is represented the mathematical expression given by Equation 6.2 [97].

$$E_{cr} = Ap[1 + \frac{B}{(pL)^{\frac{1}{2}}}] \tag{6.2}$$

where E_{cr} (Vm^{-1}) is the initiating critical electric field, A is 24.2 $VPa^{-1}m^{-1}$ and B is 8.6 $Pa^{\frac{1}{2}}m^{\frac{1}{2}}$, p is the gas pressure in a cavity (Pa), and L is the cavity length (m) in the direction of the electric field.

The main area of critique was that the inception field equation was empirically determined from a system with bigger discharge gaps (in cm range) which differs from the PD system of smaller gaps (in mm range). Hence, the direct application and extrapolation of Equation 6.2 to smaller gaps such as the one in the present dissertation of 1.5 mm should be carefully analyzed. Alternatively, the discharge cavity spark-over voltage can be determined using the Paschen curve. The Paschen curve approach is adopted in the present research in choosing the cavity spark-over mainly because the curve caters for discharges in smaller gaps. As shown in Figure 6.6, using the Paschen curve, for a 1.5 mm cylindrical void, a breakdown voltage (V_b) of $\approx$ 8 kV (see the red line extrapolation) is determined and selected for use in the simulation development and modeling.

After determining the cavity spark-over voltage from the Paschen curve, the PDIV is then systematically determined by increasing the supply voltage across the electrodes

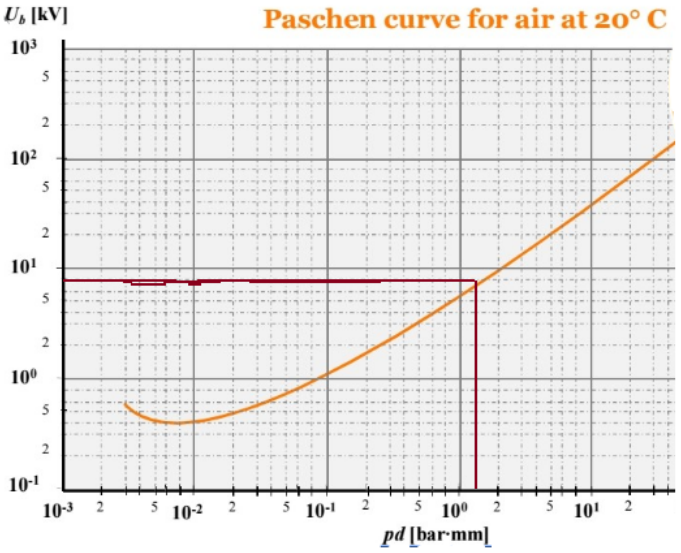


FIGURE 6.6: Paschen curve for an air-filled void marked for a 1.5 mm depth cavity [98]

till PD activity is observed. The minimum voltage at which repetitive PD occurrence is observed is recorded as the PD inception voltage. Figure 6.7 shows a flowchart of how the PD inception and extinction voltage are determined in the model.

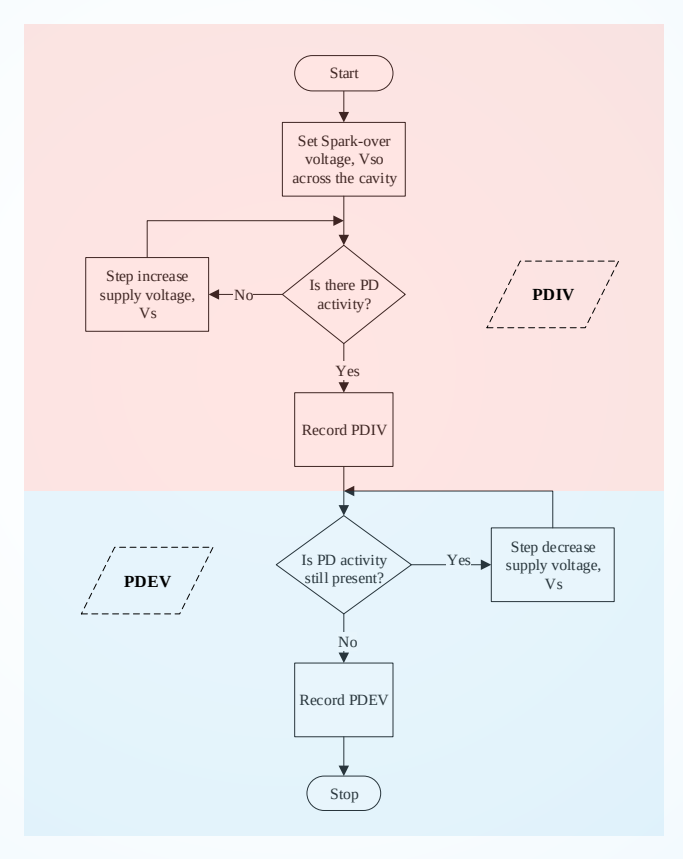


FIGURE 6.7: Flowchart logic of implementing PDIV and PDEV into the model

PDEV is defined as the applied voltage at which repetitive partial discharges cease to occur in the device under test, when the voltage applied to the device is gradually decreased from a higher value at which partial discharge activity was observed till it is 'extinct' [18]. In the present work, the extinction voltage across the gap has been set as 20 % lower than the cavity spark-over voltage.

6.4.2 Cavity Surface Conductivity Values

Typical values of surface conductivity are obtained from the literature [76, 99, 100]. Hudon et al [99] performed surface conductivity measurements and observed that 'virgin' or un-aged polymers are characterized by very low surface conductivity $\approx 10^{-16}$S. Aged and PD activity-exposed specimen have surface conductivity $\approx 10^{-9}$S. Figures 6.8 and 6.9 show the typical surface conductivity and resistivity measurements [81, 99]. From 'virgin' to severe exposure the conductivity values increase by seven orders and tend towards an asymptotic saturation behavior. Un-aged and aged polymers have a typical surface conductivity value range of $10^{-16} : 10^{-12}$ S and $10^{-11} : 10^{-7}$ S, respectively.

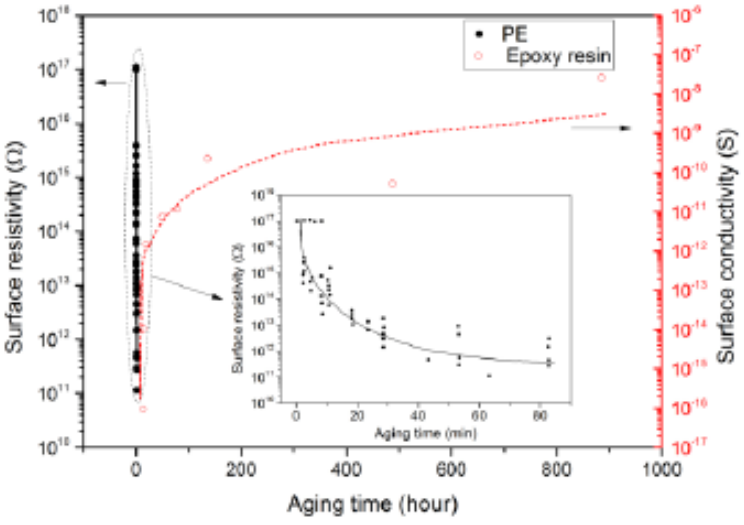


FIGURE 6.8: Surface conductivity and resistivity of polyethylene and epoxy resin insulation media [81]

The present research work uses these ranges in the simulation development especially where the surface conductivity mechanism is concerned. Additionally, all resistor values that are representative of surface conductivity in the present cavity PD model are taken from empirical measurements in the literature.

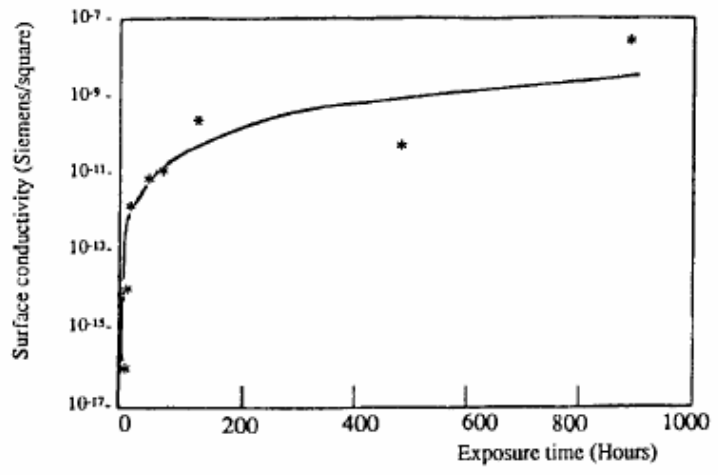


FIGURE 6.9: Surface conductivity values from un-aged to aged states [99]

6.4.3 Capacitances Values in the Model

The calculation of capacitance i.e equivalent capacitor value in a parallel plate configuration is determined by Equation 6.3. The device under test in the research work is that of a parallel plate configuration whereby a void is artificially created in between parallel plate (refer to Figure 6.5). The typical equivalent capacitor values of the health insulation, insulation in series with the void, and the cavity itself are calculated using Equations 6.3 to 6.5.

$$C_a = \frac{\varepsilon_o \varepsilon_r A}{d} \tag{6.3}$$

$$C_b = \frac{\varepsilon_o \varepsilon_r A}{d - h} \tag{6.4}$$

$$C_c = \frac{\varepsilon_o A}{h} \tag{6.5}$$

where ε_o is the permittivity of air in the cavity, ε_r is the relative permittivity of the insulation material (polyethylene sheets), A is the total surface area of the cavity, d is the distance between the electrodes and h the height of the cylindrical cavity.

The above equations (Equations 6.3-6.5) are valid if the following criteria is true; $C_a >> C_b >> C_c$. If this condition is satisfied, the total sum capacitance of the three ABC

capacitors ($C_a + C_b + C_c$) must be less than the coupling capacitor, C_k [18]. Therefore, the condition $C_k >> C_a >> C_b >> C_c$ is implemented in the simulation design. In the literature there are typical equivalent capacitance values used [62, 84, 85, 90, 101]. The capacitor values range between 10^{-14} and 10^{-12} F. The above guideline equations in conjunction with the values from the literature are used in implementing the equivalent capacitances in the present research.

The next section amalgamates all the design and development approaches presented in this section and previous sections in the implementation phase of the model in the MATLAB® Simulink® platform.

6.5 Implementation of the Model in MATLAB® Simulink®

This section presents the implementation phase of the cavity PD ABC models in MATLAB® Simulink®. Figure 6.10 presents the flowchart of the sequence and logical steps taken in implementing and executing a PD event and related processes in MATLAB® Simulink®. Statistical time lag, surface conductivity and residual charge effects are highlighted in Figure 6.10. In addition, how the frequency-dependent mechanisms influence their manifestation in PD characteristics is also presented.

Table 6.3 shows the typical values used on the implemented PD models' components and parameters that remain unchanged for most parts of the simulations.

TABLE 6.3: Parameter definition and typical values used for the ABC models simulated in MATLAB® Simulink®

Parameter	Definition	Value
R_s	Supply source current limiting resistor	5.0×10^{2} Ω
C_k	Coupling capacitor	1.0×10^{-9} F
R_a	Equivalent resistance of the healthy part of the dielectric	2.0×10^{15} Ω
C_a	Capacitance of the healthy part of the dielectric	1.5×10^{-10} F
R_b	Equivalent resistance of the dielectric in series below and above the cavity	3.0×10^{14} Ω
C_b	Capacitance of the dielectric in series below and above the cavity	1.0×10^{-12} F
R_c	Equivalent resistance of cavity surface	6.0×10^{12} Ω
C_c	Capacitance of the cavity	3.0×10^{-13} F
V_{so}	Cavity spark-over voltage	8 kV
V_{ext}	Cavity extinction voltage	6 kV

The models of the ABC equivalent electrical circuits implemented in MATLAB® Simulink® are as presented. The RLC impedance detector circuit, according to IEC60270 [18] is responsible for detecting the PD pulse as a voltage signal.

Closing Summary

This chapter presents the design, development and implementation of the ABC PD model in MATLAB® Simulink®. The implemented ABC model simulates the frequency-dependent mechanisms (statistical time lag, cavity surface conductivity and residual charge effect) as a function of variations of the supply voltage frequency. The next chapter presents the simulation results.

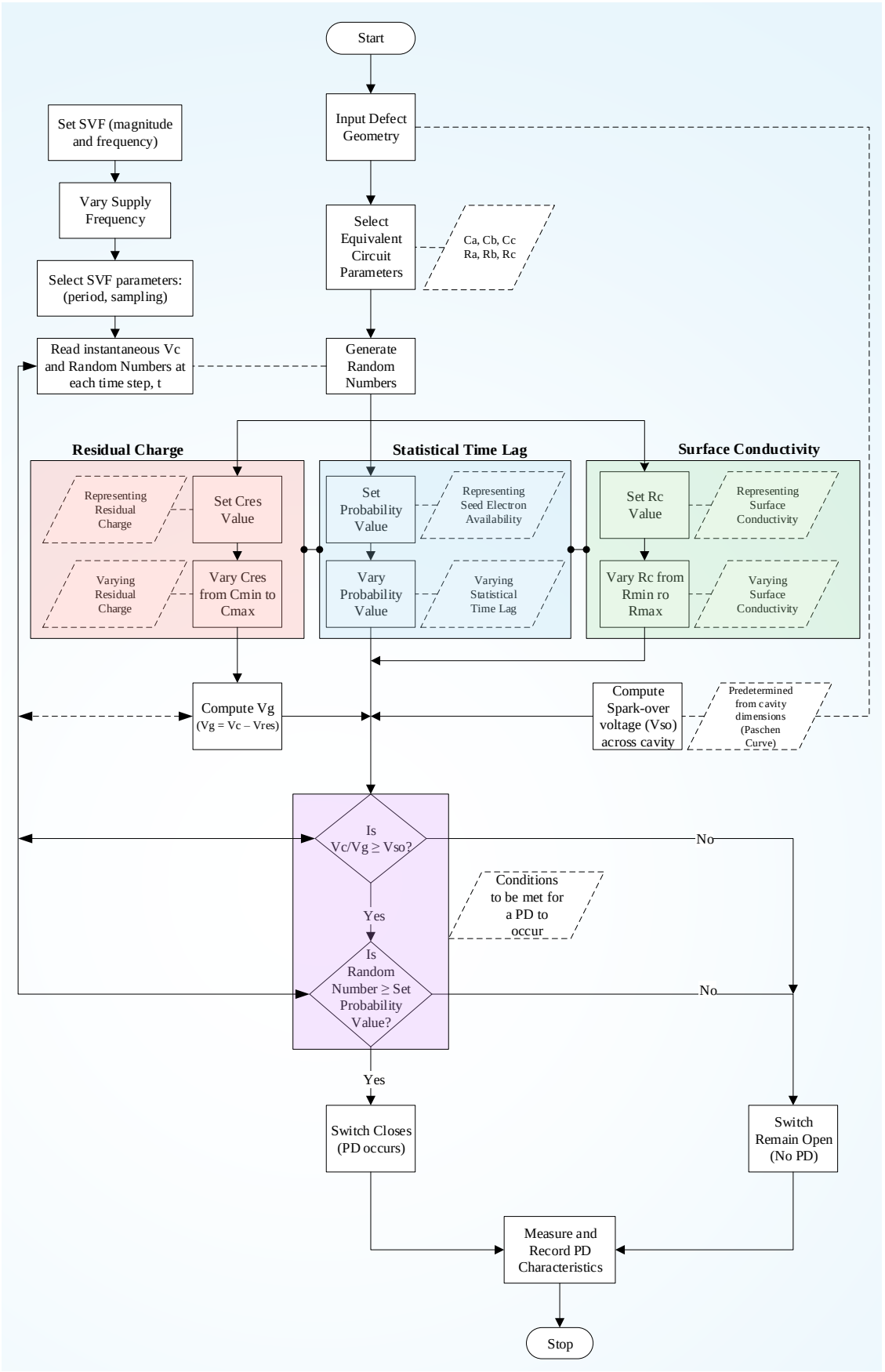


FIGURE 6.10: Flowchart representing PD mechanisms implemented in ABC model demonstrating the dependence of PD behavior on supply voltage frequency

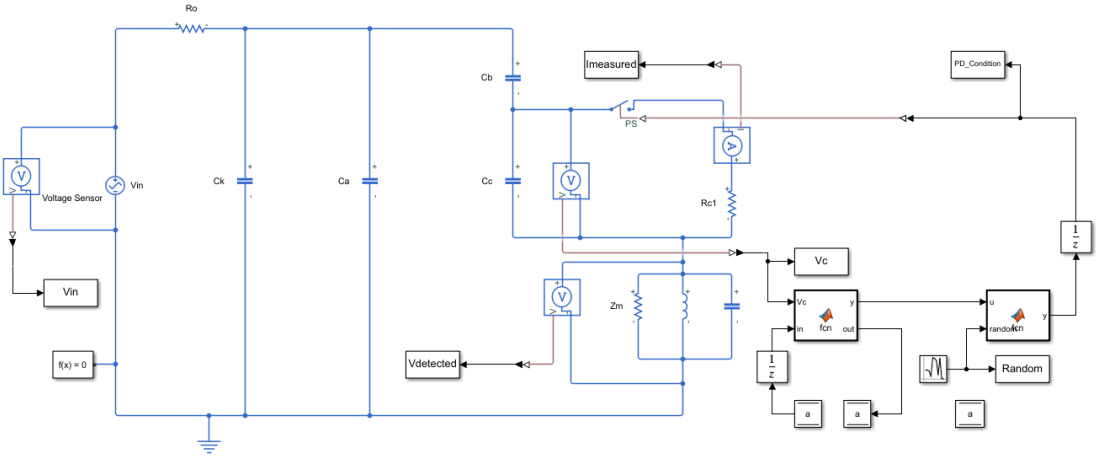


FIGURE 6.11: MATLAB® Simulink® equivalent circuit implemented as ABC model for simulating statistical time lag effect on PD behavior at different SVF

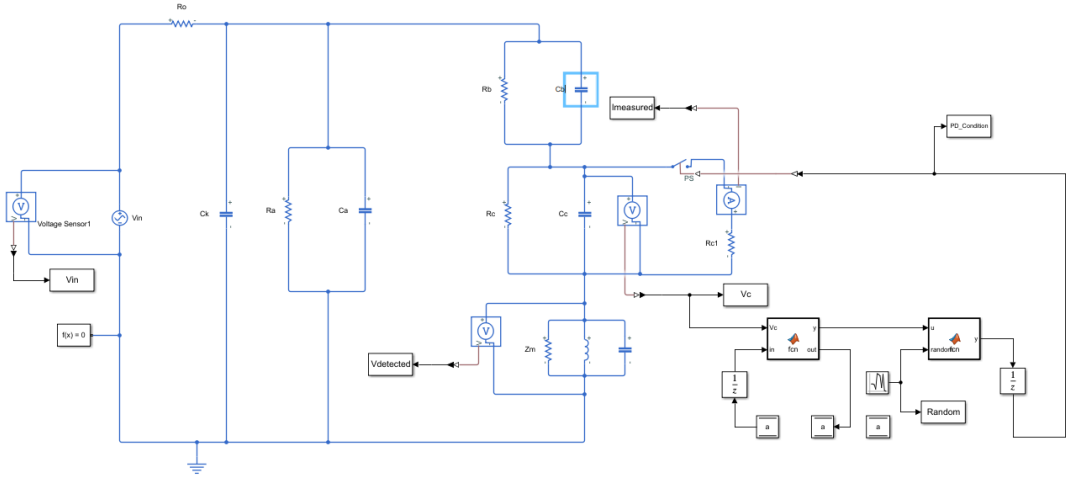


FIGURE 6.12: MATLAB® Simulink® equivalent circuit implemented as ABC model for simulating cavity surface conductivity effect on PD behavior at different SVF

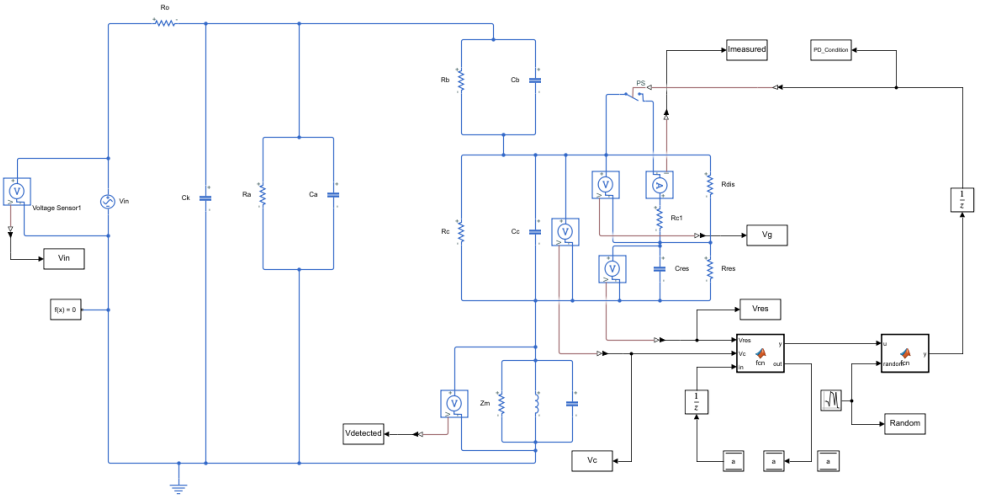


FIGURE 6.13: MATLAB® Simulink® equivalent circuit implemented as ABC model for simulating residual charge effect on PD behavior at different SVF

Chapter 7

Simulation Results, Analysis and Discussion

Opening Summary

This chapter presents the simulated results obtained using the modified ABC PD model implemented in Matlab® Simulink® platform. All the simulations were conducted using an artificial cavity with a depth of 1.5 mm in polyethylene dielectric. Supply voltage frequencies of 1 Hz, 50 Hz and 200 Hz are implemented to cover a wider frequency range from VLF to beyond 50 Hz. VLF has a frequency range of 0.01 Hz to 1 Hz [18]. General trends of PD characteristics are presented and discussed. The PD characteristics studied are the cavity spark-over and extinction voltage, PDIV, PDEV, PDRR and PRPDP (PD pulse shape and amplitude). A brief discussion of the cavity over-voltage phenomenon is presented next as it is the basis for interpreting the effect of PD behavior dependence over supply voltage frequency variations.

The Gap Over-Voltage Phenomenon

For a PD to occur, two conditions have to be met; (i) electric field (voltage) criterion whereby the electric field strength in the cavity has to be sufficiently high enough to cause the cavity to spark-over and (ii) the availability of a seed electron that will initiate

an electron avalanche process for the spark-over to occur. If the seed electron does not become available even though the electric field in the cavity is sufficiently high, the background electric field, E_0 keeps on increasing at a rate proportional to the rate of change of the applied voltage [48]. The time delay till the seed electron becomes available results in the cavity's total electric field, E_{total} having exceeded the critical electric field necessary to initiate an electron avalanche, E_{inc} by a gap over-stress, ΔE_0. Therefore, the resultant PD event in the cavity occurs at a higher electric field ($E_{inc} + \Delta E_0$) or at a voltage across the cavity that is greater than the cavity spark-over voltage if the seed electron had appeared earlier hence the term 'over-voltage'. Figure 7.1 illustrates the cavity over-voltage phenomenon. Another 'over-voltage' scenario occurs when a seed electron does not become available. In this scenario, the voltage across the cavity exceeds the sufficient value to initiate a PD event yet there will be no PD activity occurring because of sustained absence of the seed electron.

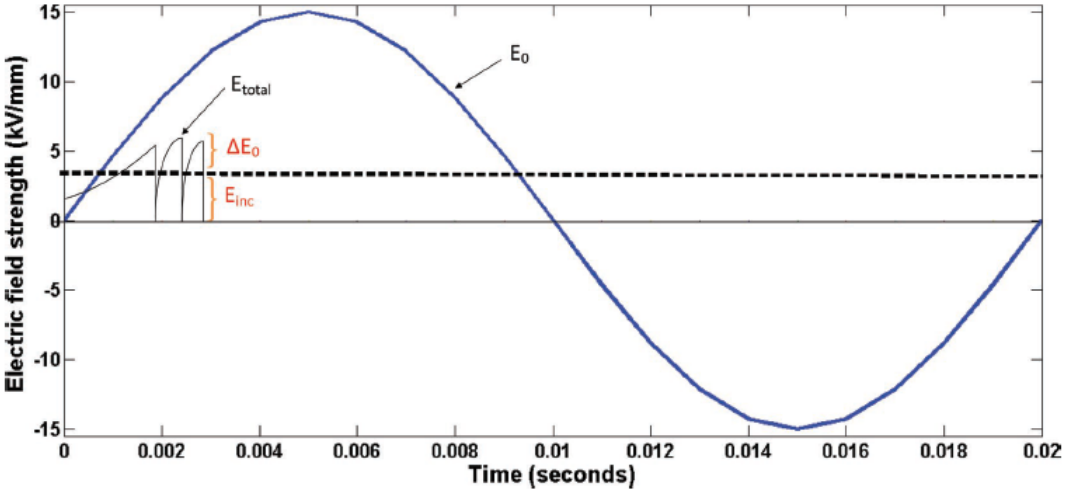


FIGURE 7.1: Over-voltage scenario due to delayed or scarce seed electron availability [48]

The rate of voltage rise which is a function of the supply voltage frequency, together with the probability of seed electron availability therefore determine the cavity over-voltage magnitude which in turn influences PD characteristics' behavior. In the next section, the statistical time lag's influence on PD characteristics' response to SVF is presented.

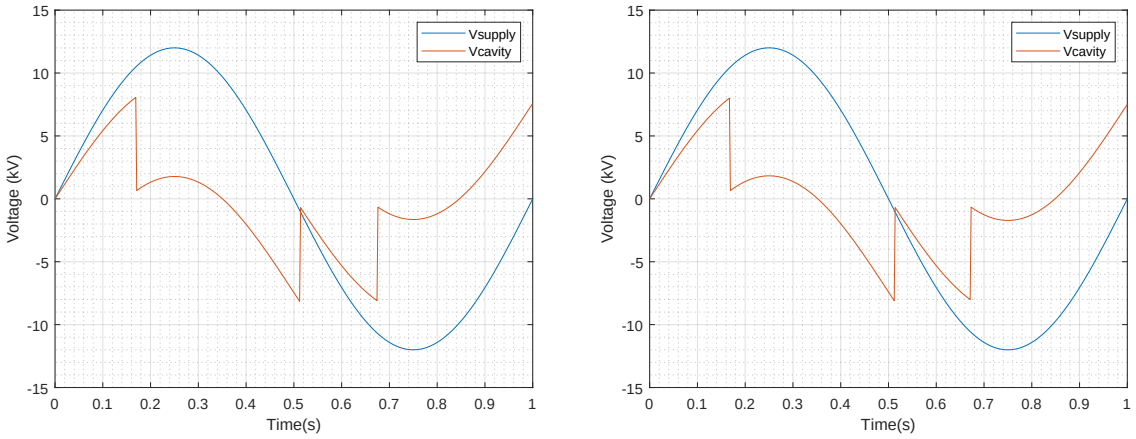
In all the Figures in this dissertation; V_{supply} represents the supply voltage waveform, V_{cavity} is the voltage waveform across the cavity, and $V_{detected}$ represents the PD pulses as detected across the detection impedance circuit with references to Figures 6.11 to 6.13.

7.1 The Statistical Time Lag's Influence on PD Characteristics' Response to SVF Variations

In order to study the statistical time lag's influence on PD characteristics' response to supply voltage frequency variations, the seed electron probability is set to 25% and 100% representing scarce and abundant seed electron situations, respectively. In this section, the resultant PDPRP, PDRR, cavity spark-over and extinction voltages are presented for the supply voltage frequencies: 1 Hz, 50 Hz and 200 Hz.

7.1.1 Influence of Statistical Time Lag Variations on PD Behavior at SVF of 1 Hz

Figure 7.2 presents the cavity voltage waveform showing the PD pulses at scarce and at abundant seed electron availability at SVF of 1 Hz. It can be seen that the cavity spark-over voltage and the PDRR of 3 (pulses per cycle) are not affected by the changes in seed electron availability (statistical time lag) at VLF of 1 Hz.

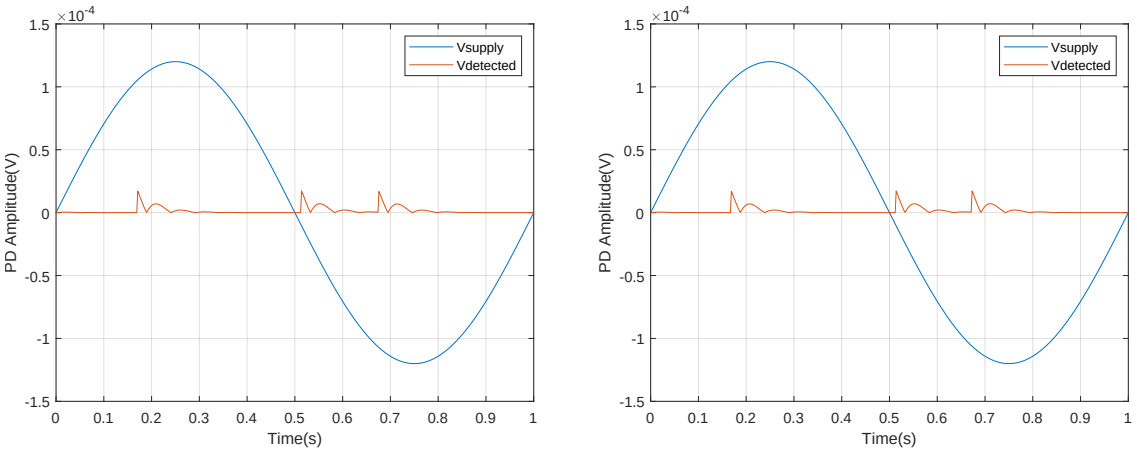


(A) (B)

FIGURE 7.2: Cavity voltage waveforms at SVF of 1 Hz for seed electron availability at: (**a**) Scarcity and (**b**) Abundancy. NB: The sudden drop of the cavity voltage represents a PD event.

Figure 7.3 also shows that at 1 Hz the PRPDP is not affected by statistical time lag variations. The independence of the PD characteristics from seed electron availability variations at VLF is attributable to the relatively slow rise and fall of the applied voltage. At such VLF, the supply voltage rises slowly such that even at scarce seed electron

availability, there is enough time for the seed electron to be available before an over-voltage scenario due to a delayed seed electron occurs.



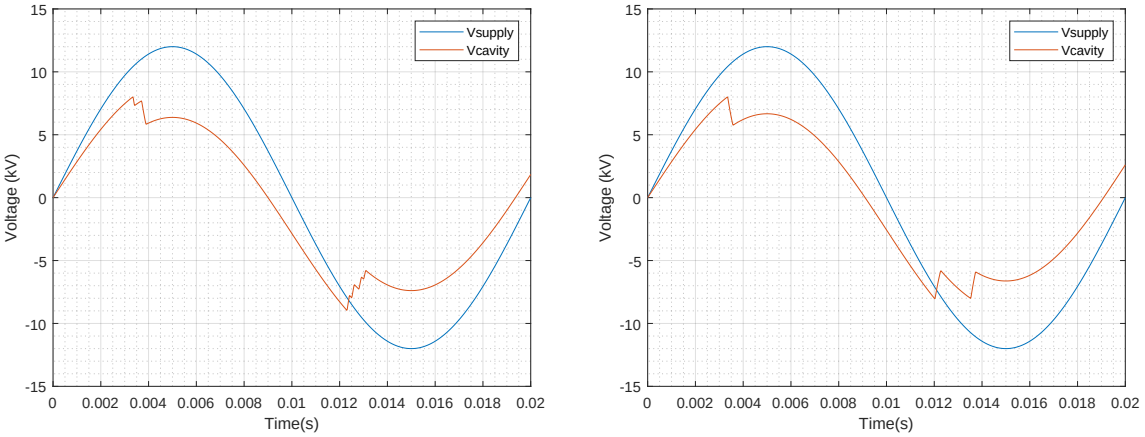
(A) (B)

FIGURE 7.3: PRPDP (PD pulses per phase angle) at SVF of 1 Hz for seed electron availability at: (**a**) Scarcity and (**b**) Abundancy

7.1.2 Influence of Statistical Time Lag Variations on PD Behavior at SVF of 50 Hz

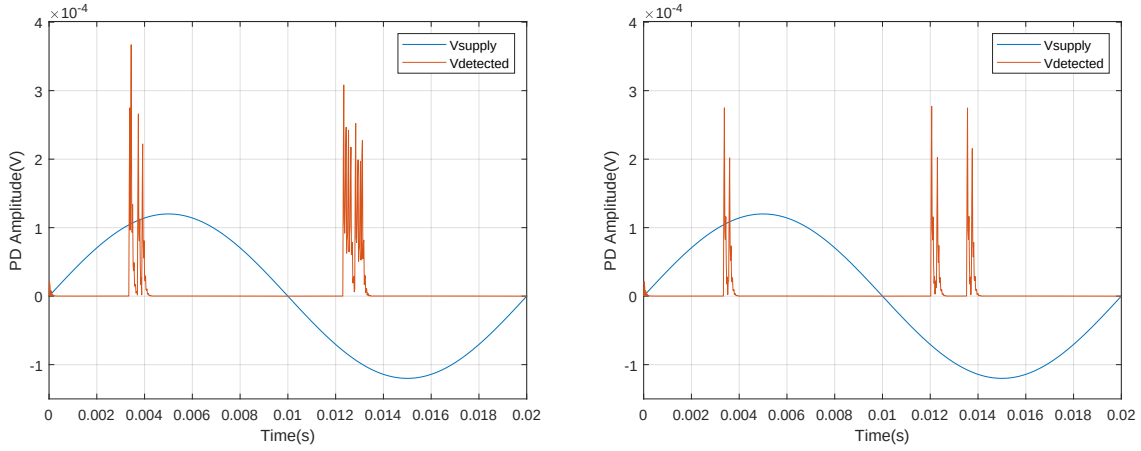
Figures 7.4 and 7.5 present the cavity voltage waveform and PD pulses at scarce and abundant seed electron availability at SVF of 50 Hz. The PDRR slightly increases in the negative half cycle at abundant seed electron availability (Figure 7.4b) as compared to the scarcity condition. This can be explained by the readily availability of the seed electron. At electron scarcity (Figure 7.4a), there is a cavity over-voltage situation where a cavity spark-over voltage of 9 kV is observed in the negative half cycle. However, the cavity extinction voltage remains invariant.

Figure 7.5 shows that the PRPDP has also changed with change in statistical time lag. The PD pulses occur slightly earlier in the phase and the PD amplitude is decreased at abundant seed electron as compared to scarcity. The higher PD amplitude at scarce seed electron than at abundant seed electron availability can be attributed to the gap over-voltage effect. PD amplitudes at 50 Hz have increased in comparison to that at 1 Hz which can be a result of a faster riser time at power frequency than at VLF.



(A) (B)

FIGURE 7.4: Cavity voltage waveforms at SVF of 50 Hz for seed electron availability at: (**a**) Scarcity and (**b**) Abundancy

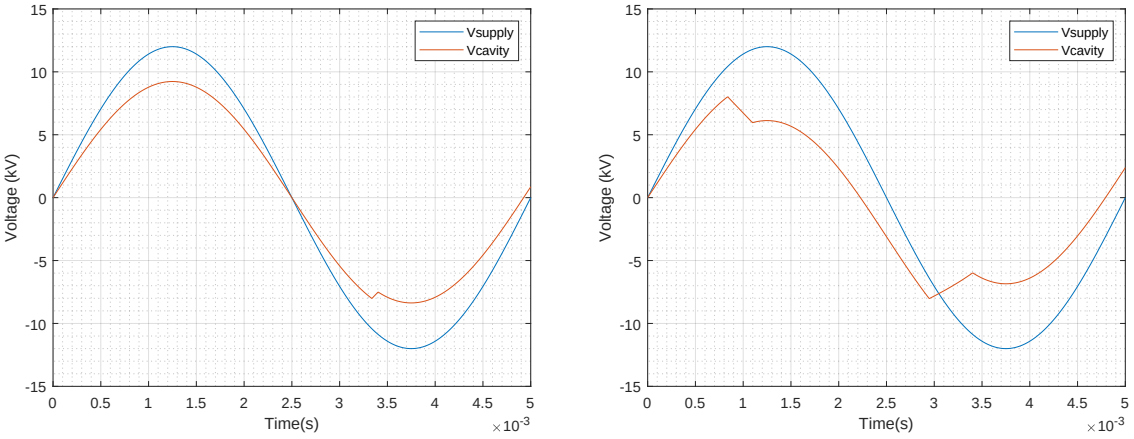


(A) (B)

FIGURE 7.5: PRPDP (PD pulses per phase angle) at SVF of 50 Hz for seed electron availability at: (**a**) Scarcity and (**b**) Abundancy

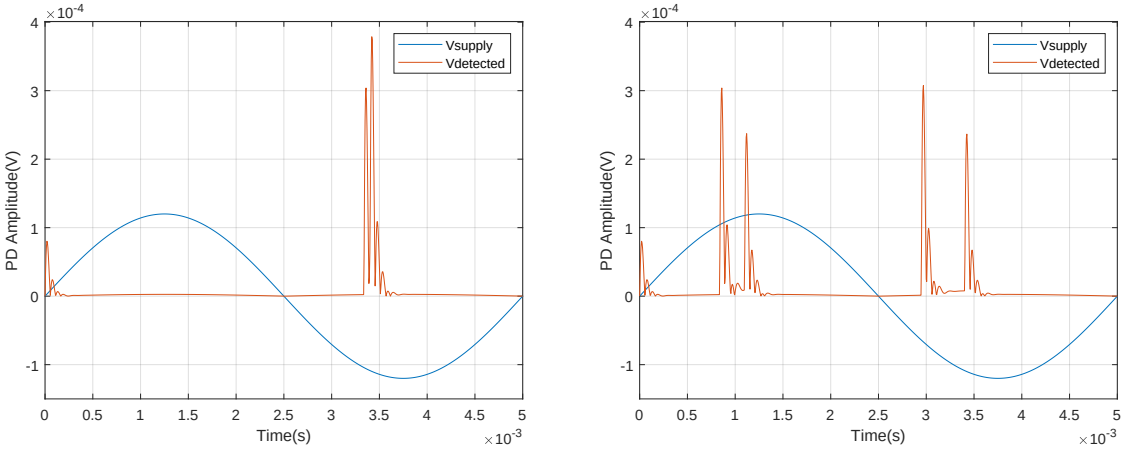
7.1.3 Influence of Statistical Time Lag Variations on PD Behavior at SVF of 200 Hz

Figures 7.6 and 7.7 present the cavity voltage waveform and the subsequent PRPDP at SVF of 200 Hz. It is shown that the PDRR, cavity spark-over voltage as well as the resultant PRPDP are all affected by changes in the statistical time lag. At scarce seed electron, there are no or fewer pulses per cycle than at abundant seed electron availability. For instance, there is no PD occurrence in the negative half cycle regardless of the voltage across the cavity exceeding the expected cavity spark-over voltage for initiating PD activity. A possible explanation is the gap over-voltage scenario.



(A) (B)

FIGURE 7.6: Cavity voltage waveforms at SVF of 200 Hz for seed electron availability at: (**a**) Scarcity and (**b**) Abundancy



(A) (B)

FIGURE 7.7: PRPDP (PD pulses per phase angle) at 200 Hz for seed electron availability at: (**a**) Scarcity and (**b**) Abundancy

In addition, at 200 Hz, the rate of change of the applied voltage can be faster such that a half cycle is completed before the second condition for a PD to occur is met. However, regardless of the fast rising rate of the supply voltage frequency, PDs still occur at abundant seed electron condition.

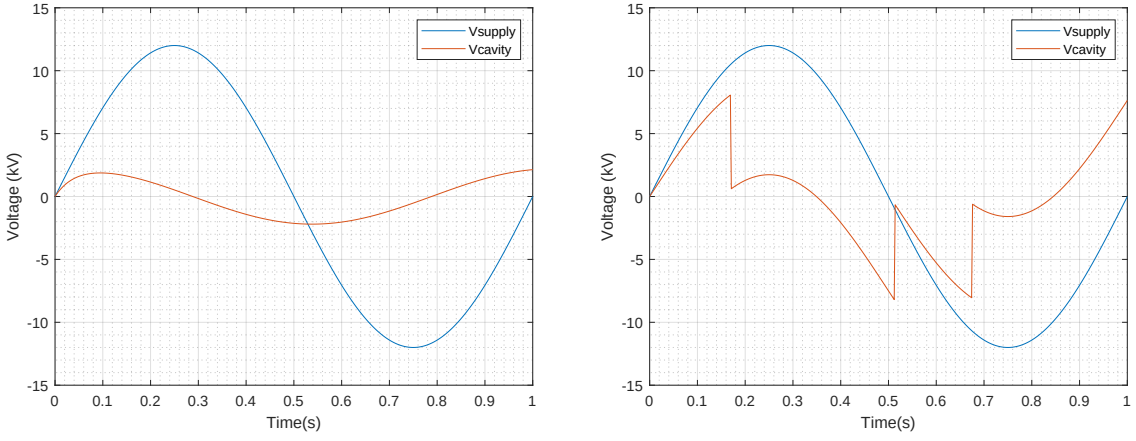
The general trend is that PD characteristics are invariant at VLF. At higher frequencies (50 Hz and 200 Hz), effect of the changes in statistical time lag depend on supply voltage frequency. For instance, PD pulse amplitude increases as supply frequency is increased which is not the case at lower frequencies.

7.2 The Cavity Surface Conductivity's Influence on PD Characteristics' Response to SVF Variations

In order to study the influence of the cavity surface conductivity on PD characteristics' response to supply voltage frequency variations, the cavity surface resistance, R_c is varied from selected minimum R_{min} to the maximum R_{max} value. The term 'surface conductivity' is commonly used in the literature but for the purpose of the present research work's simulations 'surface resistance' is used. In all simulation cases, the seed electron availability variable is fixed by setting an abundant (100%) availability of the seed electron. The resultant PD characteristics are presented in this section. The procedure is repeated for a range of supply voltage frequencies represented by: 1 Hz, 50 Hz and 200 Hz.

7.2.1 PD Characteristics as a Function of Cavity Surface Resistance at SVF of 1 Hz

Figures 7.8 and 7.9 present the cavity voltage waveforms and PD pulses per cycle for R_{min} and R_{max} cavity surface resistances at SVF of1 Hz. It can be seen that there are no observable pulses per cycle at the minimum cavity surface resistance than at maximum cavity surface resistance. The minimum cavity surface resistance represents an increased cavity surface conductivity. The more conductive cavity surface walls reduce the resultant voltage across the cavity.



(A) (B)

FIGURE 7.8: Cavity voltage waveforms at SVF of 1 Hz for surface resistance value: (**a**) R_{min} and (**b**) R_{max}

Figure 7.9 presents the effect of cavity surface resistance on PRPDP at SVF of 1 Hz. There is a significant change in PD pulse amplitude and shape as the cavity surface resistance is varied between the minimum and maximum set boundaries. At minimum surface resistance, R_{min} there is no observable PD activity whereas it there are PD pulses at R_{max}.

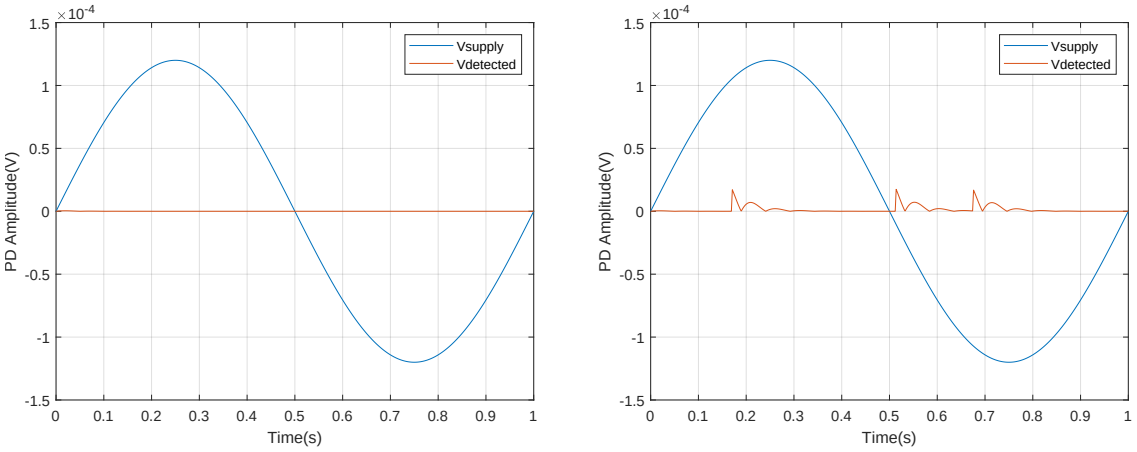
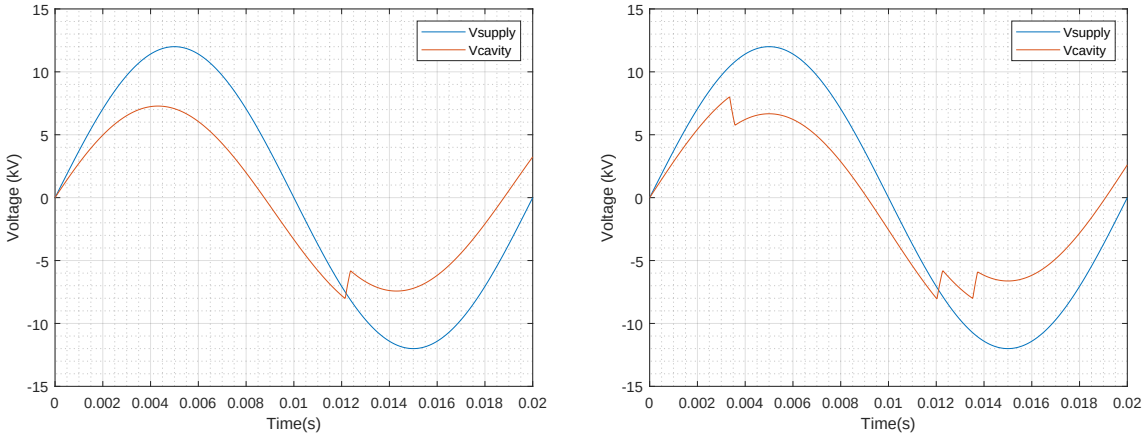


FIGURE 7.9: PRPDP (PD pulses per phase angle) at SVF of 1 Hz for cavity surface resistance value: (**a**) R_{min} and (**b**) R_{max}

7.2.2 PD Characteristics as a Function of Cavity Surface Resistance at SVF of 50 Hz

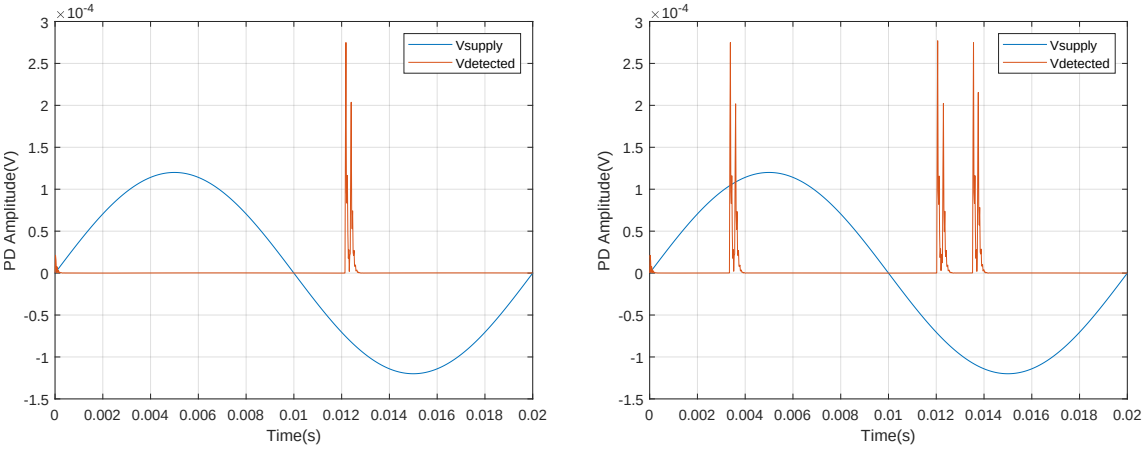
Figures 7.10 and 7.11 present the cavity voltage waveforms and the PD repetition rate for R_{min} and R_{max} cavity surface resistances at SVF of 50 Hz. The waveforms are generally larger than those at VLF.

Figure 7.11 presents the effect of cavity surface resistance variations on PRPDP at SVF of 50 Hz. There is a no change in PD pulse amplitude and shape as the cavity surface resistance is varied between the minimum and maximum. Despite PD pulse amplitude being invariant to cavity surface resistance changes, there is an increase in the PD pulse amplitude. There is an additional PD pulse on both cycles at R_{max} than at R_{min}. The results show that PRPDP changes with surface resistance variations at SVF of 50 Hz, with more activity observed at a higher cavity surface resistance.



(A) (B)

FIGURE 7.10: Cavity voltage waveforms at SVF of 50 Hz for surface resistance value: (**a**) R_{min} and (**b**) R_{max}

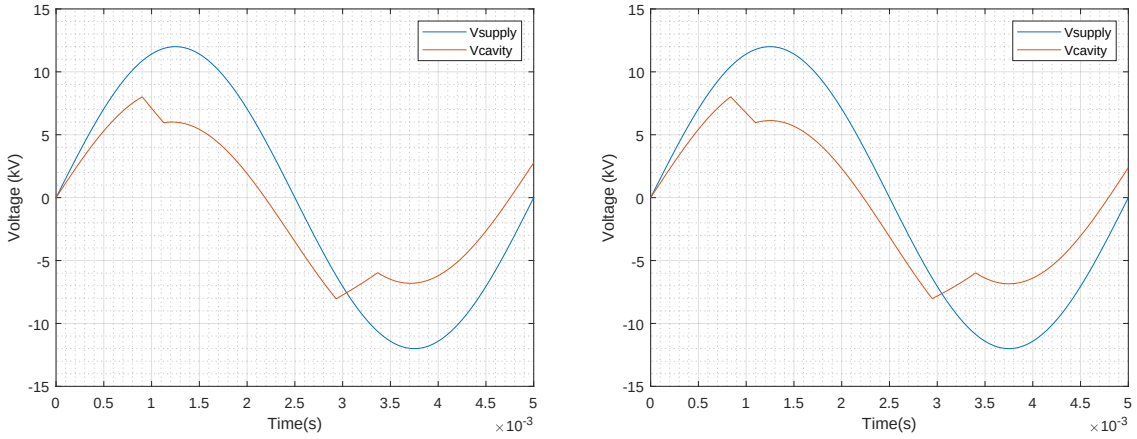


(A) (B)

FIGURE 7.11: PRPDP (PD pulses per phase angle) at SVF of 50 Hz for cavity surface resistance value: (**a**) R_{min} and (**b**) R_{max}. The pulses increase in number with increase in cavity surface resistance.

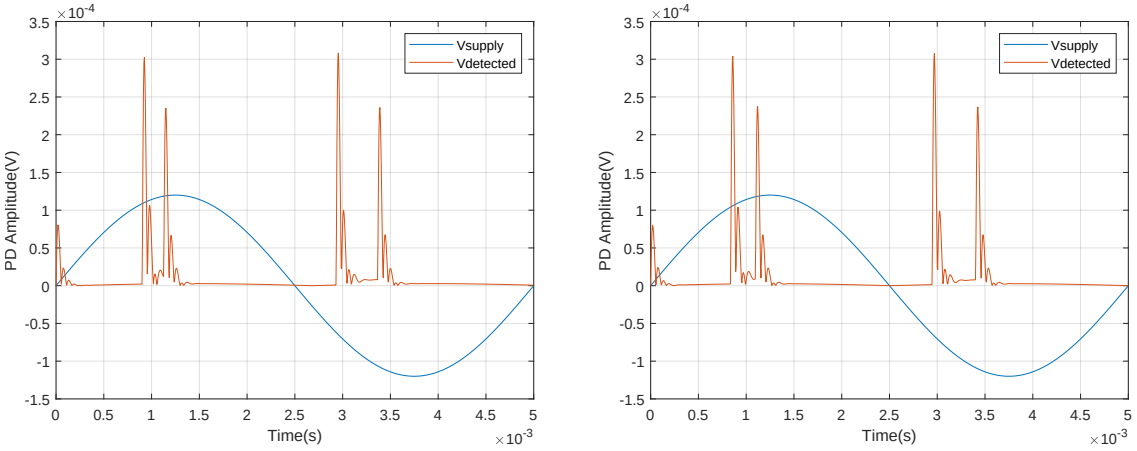
7.2.3 PD Characteristics as a Function of Cavity Surface Resistance at SVF of 200 Hz

Figures 7.12 and 7.13 present the cavity voltage waveforms and the corresponding PRPDP at SVF of 200 Hz. It is observed that at 200 Hz, PD characteristics are invariant to cavity surface resistance changes of R_{min} and R_{max}. A possible explanation to this behavior is the high rate of change of the applied voltage at higher frequencies such that the conductivity of the cavity surface walls become insignificant. However, the responsible mechanisms will be a subject of future research.



(A) (B)

FIGURE 7.12: Cavity voltage waveforms at SVF of 200 Hz for surface resistance value: (**a**) R_{min} and (**b**) R_{max}



(A) (B)

FIGURE 7.13: PRPDP (PD pulses per phase angle) at SVF of 200 Hz for cavity surface resistance value: (**a**) R_{min} and (**b**) R_{max}. There is no significant difference as the cavity surface resistance is varied between minimum and maximum values.

The general trend is that PD characteristics such as the PDRR and PRPDP are more sensitive to cavity surface resistance at VLF (1 Hz) than at higher supply frequencies of the applied voltage.

7.3 The Residual Charge Effects on PD Characteristics' Response to SVF Variations

In order to study the residual charge effects on PD characteristics' response to supply voltage frequency variations, the equivalent residual capacitor, C_{res} in Figures 6.4 and

6.13 is varied from C_{min} to C_{max} values. In all simulation cases, cavity surface resistance, R_c is kept constant and the seed electron probability is set at 100% (abundant) availability. The procedure is applied to the supply voltage frequencies: 1 Hz, 50 Hz and 200 Hz.

A partial discharge, illustrated in the next section, deposits space charge on the cavity surface walls. The deposited space charge that occurs after every PD event can also influence subsequent PD characteristics. A brief illustration of how the deposition of space charge on the cavity surface walls affects PD characteristics is presented next. The resultant simulated results of PD characteristics are presented after the residual charge phenomenon illustration which follows next.

The Phenomena of Residual Charge in a Cavity PD Event

A PD event deposits electrons on opposite ends of the cavity surface walls during a discharge event. The charge is referred to as 'residual or space charge'. The residual charge creates an electric field, E_{res}, that gets superimposed on the background electric field, E_0. If the residual charge is from the negative half cycle, the symbol $E_{res(N)}$ is used. The same is true for the residual charge effect from a positive half cycle, $E_{res(P)}$. Figure 7.14 illustrates the interaction and contribution of respective electric fields in the cavity [48].

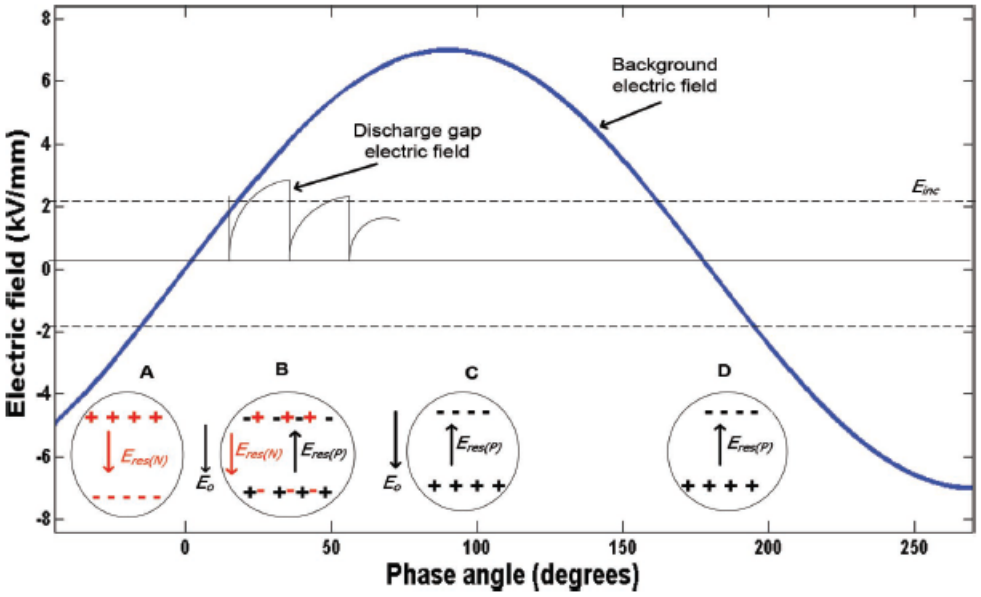


FIGURE 7.14: Illustration of residual charge contribution to PD event occurrence [48]

The chronological description and explanation of Figure 7.14 is outlined. The total resultant electric field, E_{total} in the cavity is a vector sum of the applied background electric field, E_0 and the cavity's residual charge electric field, E_{res} as shown in Equation 7.1.

$$\vec{E_{total}} = \vec{E_0} + \vec{E_{res}} \tag{7.1}$$

At position A, the zero-crossing point from the negative to the positive half cycle of the applied voltage, the background electric field, E_0 of Equation 7.1 is zero hence the total electric field in the cavity is mainly due to the residual charge from the negative half cycle, $E_{res(N)}$ hence $E_{total} = E_{res(N)}$. This condition may not lead to a PD occurring if there has not been previous PD activity. However, if there has been previous PD activity that has sufficient negative residual charge electric field to breakdown the cavity's electric field strength, $E_{total} \geq E_{inc}$ and a seed electron is available, then a PD may occur. This results in PDs occurring at this zero-crossing and earlier in the phase.

At position B, the early rising edge of the positive half cycle of the applied voltage, the total electric field in the cavity, E_{total} of Equation 7.1 is a superimposition of residual charge from the negative half cycle $E_{res(N)}$, the applied background electric field E_0 and residual charge due to consecutive PD events in this positive half cycle $E_{res(P)}$ hence $E_{total} = E_{res(N)} + E_0 - E_{res(P)}$. The same directional superimposition of $E_{res(N)}$ and E_0 enhances the resultant electric field in the cavity. The opposite is true for the positive residual charge, $E_{res(P)}$ which decreases the resultant electric field in the cavity. If $E_{total} \geq E_{inc}$ and a seed electron is available, then a PD may occur. In a case where there is a delayed seed electron availability, the resultant PD magnitudes are relatively larger compared to earlier ones (over-voltage scenario). It is this process at position B that gives rise to the 'ear' part of the 'rabbit' shaped PRPDP [48]. The conditions in this part of the half cycle can lead to over-voltage scenario with higher and forward shifted PD pulse amplitudes and shapes, respectively as well as scenarios whereby cavity extinction voltages (a function of PDEV) occur at lower than expected values and increased PD repetition rates.

At position C, the late falling edge of the positive half cycle of the applied voltage, the total electric field in the cavity, E_{total} of Equation 7.1 is mainly a function of the applied

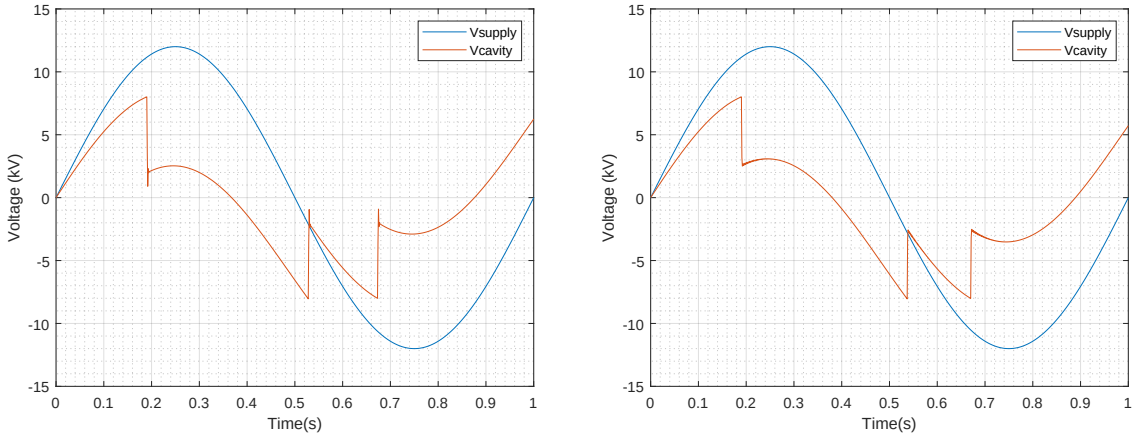
background electric field E_0 and the positive residual charge electric field, $E_{res(P)}$ hence $E_{total} = E_0 - E_{res(P)}$. In this part of the half cycle, the negative half cycle electric field, $E_{res(N)}$ would have fully dissipated. Subsequently with a declining applied electric field, the total resultant field, E_{total} is also reduced leading to PDs of lower PD magnitudes if $E_{total} \geq E_{inc}$ and seed electron availability conditions are met. It is this process at position C that gives rise to the 'body' part of the 'rabbit' shaped PRPDP [48].

At position D, the zero-crossing point from the positive to the negative half cycle of the applied voltage, the background electric field, E_0 of Equation 7.1 is zero hence the total electric field in the cavity is mainly due to the residual charge from the positive half cycle, $E_{res(P)}$ hence $E_{total} = E_{res(P)}$. This condition may not lead to a PD occurring if there has not been previous PD activity. However, if there has been previous PD activity that has sufficient positive residual charge electric field to breakdown the cavity's electric field strength, $E_{total} \geq E_{inc}$ and a seed electron is available, then a PD may occur. This results in PDs occurring at this zero-crossing and earlier in the phase.

With the residual charge effect explanation and description presented in this section, the following sections present the simulation results on how residual charge magnitude influence the changes in PD characteristics as the supply voltage frequency is varied.

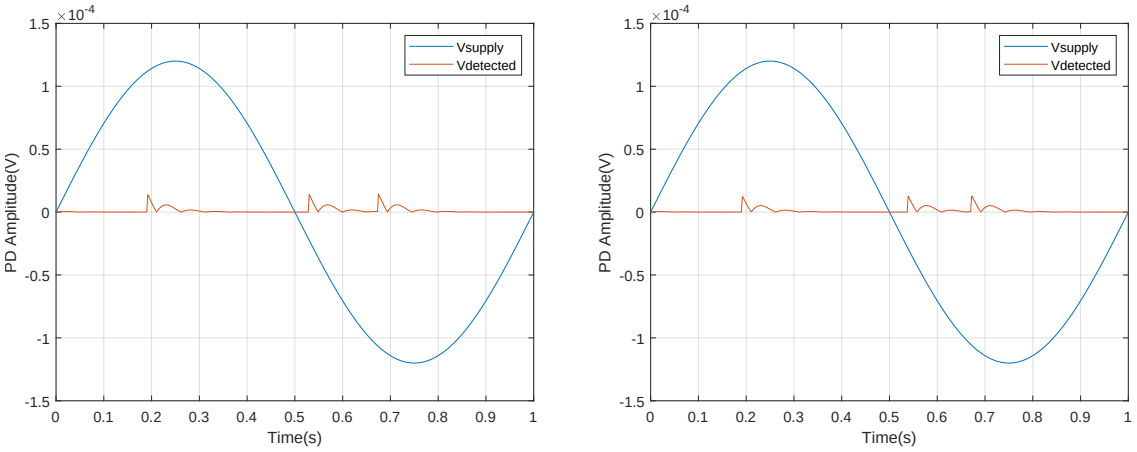
7.3.1 The Residual Charge Effect on PD Characteristics' Response at SVF of 1 Hz

With reference to Figures 6.4 and 6.13, the residual charge is represented by C_{res}. Figure 7.15 presents the cavity voltage waveforms and PD pulses at C_{min} and C_{max} equivalent residual capacitances at SVF of 1 Hz. Figure 7.16 presents the effect of space charge on PRPDP at SVF of 1 Hz. It can be seen that the cavity voltage waveform, PD pulse pattern shape, phase position and amplitude are invariant to residual charge variations. This can be explained by the concept that the rate of voltage increase (at VLF) is much slower than the discharge rate of the residual capacitor, C_{res} which represents the residual charge dissipation rate.



(A) (B)

FIGURE 7.15: Cavity voltage waveforms at SVF of 1 Hz for residual charge capacitor value: (**a**) C_{min} and (**b**) C_{max}. The PD characteristics at 1 Hz do not change as the residual charge magnitude is varied.



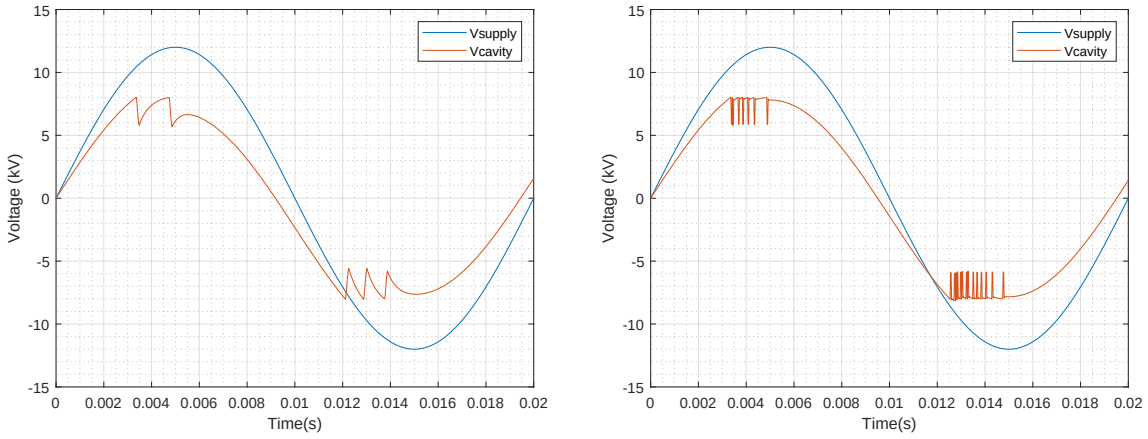
(A) (B)

FIGURE 7.16: PRPDP (PD pulses per phase angle) at SVF of 1 Hz for residual charge capacitor value: (**a**) C_{min} and (**b**) C_{max}

7.3.2 The Residual Charge Effect on PD Characteristics' Response at SVF of 50 Hz

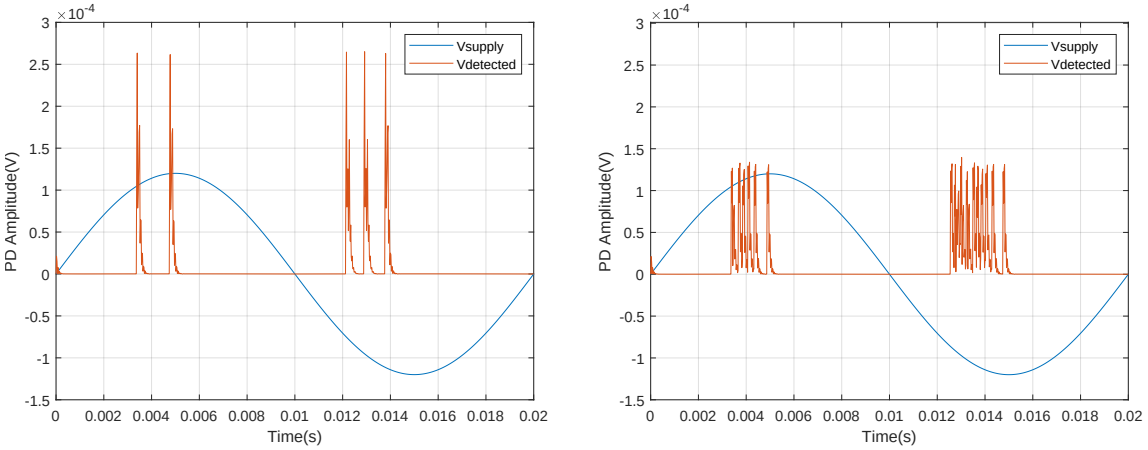
Figure 7.17 presents the cavity voltage waveforms and PD pulses at C_{min} and C_{max} equivalent residual capacitances at SVF of 50 Hz. Figure 7.18 presents the effect of space charge on PRPDP at SVF of 50 Hz. PD characteristics are sensitive to changes in residual charge variations at SVF of 50 Hz. The cavity spark-over and PDRR increase with the increase in residual charge. This is as a result of enhanced resultant electric field, E_{total} due to the contribution of E_{res} to the applied electric field, E_0. The cavity extinction voltage and PD amplitude decrease but with closely packed consecutive PD

pulses as residual charge capacitor value is increased due to the residual field, E_{res} that opposes the applied background electric field E_0 such that PD events are occurring at lower PD magnitudes as illustrated before.



(A) (B)

FIGURE 7.17: Cavity voltage waveforms at SVF of 50 Hz for residual charge capacitor value: (**a**) C_{min} and (**b**) C_{max}



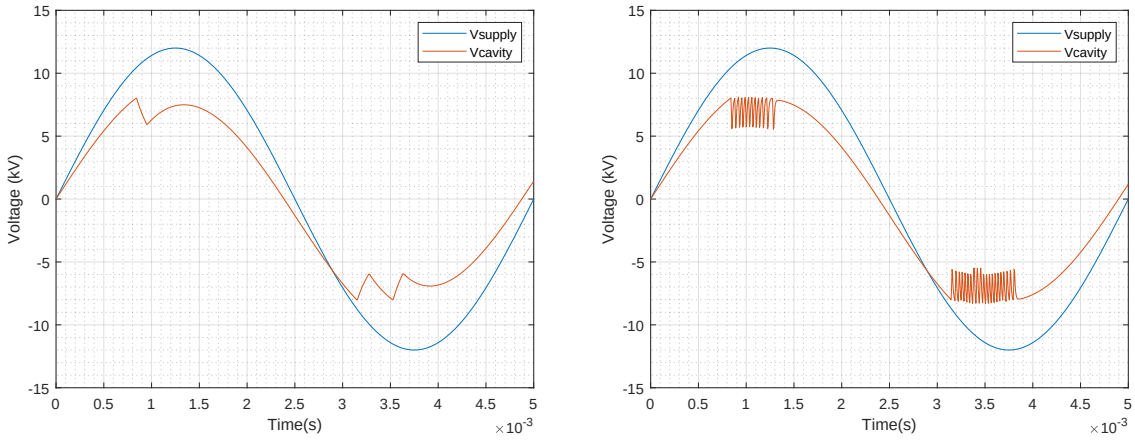
(A) (B)

FIGURE 7.18: PRPDP (PD pulses per phase angle) at SVF of 50 Hz for residual charge capacitor value: (**a**) C_{min} and (**b**) C_{max}

7.3.3 The Residual Charge Effect on PD Characteristics' Response at SVF of 200 Hz

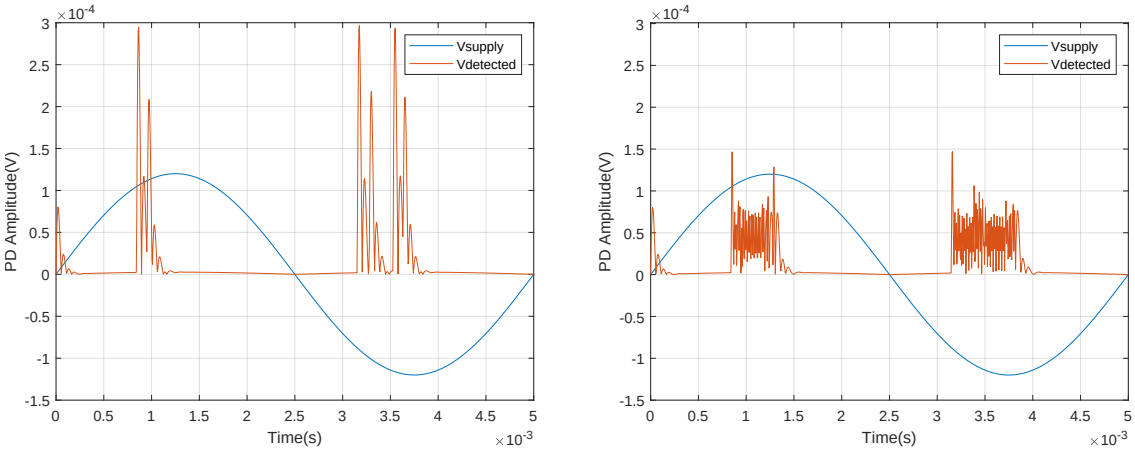
Figure 7.19 presents the cavity voltage waveforms and PD pulses at C_{min} and C_{max} equivalent residual capacitances at SVF of 200 Hz. Figure 7.20 presents the effect of space charge on PRPDP at SVF of 200 Hz. PD characteristics are sensitive to changes in residual charge variations at SVF of 200 Hz. The cavity spark-over and PDRR increase

with the increase in residual charge. This is as a result of enhanced resultant electric field, E_{total} due to the contribution of E_{res} to the applied electric field, E_0. The cavity extinction voltage and PD amplitude decrease but with more dense and closely packed consecutive PD pulses as residual charge capacitor value is increased due to the residual field, E_{res} that opposes the applied background electric field E_0 such that PD events are occurring at lower PD magnitudes as illustrated before. This behavior is the same as the one observed at 50 Hz.



(A) (B)

FIGURE 7.19: Cavity voltage waveforms at SVF of 200 Hz for residual charge capacitor value: (**a**) C_{min} and (**b**) C_{max}



(A) (B)

FIGURE 7.20: PRPDP (PD pulses per phase angle) at SVF of 200 Hz for residual charge capacitor value: (**a**) C_{min} and (**b**) C_{max}. PD pulse amplitudes and phase positions change with variations of residual charge at high SVF of 200 Hz.

The general trend is that PD characteristics are invariant to residual charge variations at VLF. However, at higher frequencies (50 Hz and 200 Hz), PD amplitude decreases as residual charge is increased and is also increased as supply voltage frequency is increased. The PD pulse increases at C_{max} when supply frequency is increased from 1 Hz to 200 Hz. Most of the changes are attributed to the relationship between the rate of rise or falling time of the applied background electric field and the rate of discharge time of the residual charge capacitor.

This section presented simulated results on maximum and minimum boundary points of statistical time lag (scarce and abundant seed electron availability), cavity surface conductivity (R_{min} and R_{max}) and residual charge effect (C_{min} and C_{max}). The next section presents a concise summary of the simulation results.

7.4 Summary of Simulation Results on the Extent to which Factors Responsible for Frequency Dependence of PD Mechanisms Influence PD Characteristics' Response at Different Supply Voltage Frequencies

This sections presents in tabular form a summary on how the statistical time lag, cavity surface resistance and residual charge effect influence PD characteristics' response to supply voltage frequency variations. Table 7.1 presents how the changes in statistical time lag using scarce and abundant seed electron availability influence PD characteristics' response at different supply voltage frequencies. Table 7.2 presents how varying the cavity surface resistance from minimum to maximum values influences the behavior of PD characteristics at different supply voltage frequencies. Table 7.3 presents how the changes in the residual charge magnitude from minimum to maximum values influences the response of PD characteristics at different supply voltage frequencies.

TABLE 7.1: Statistical time lag variations (from scarce to abundant) influence on PD characteristics at different supply voltage frequencies

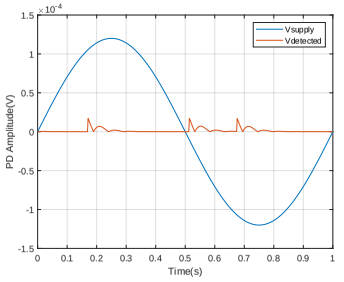
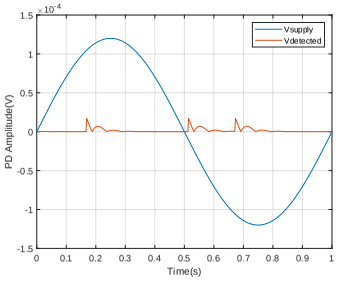
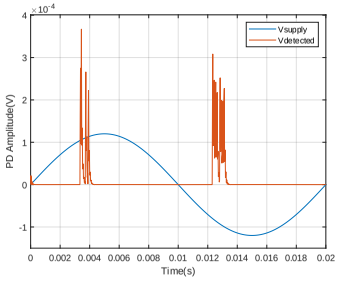
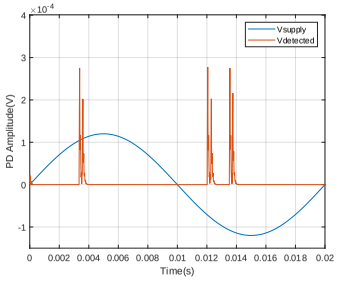
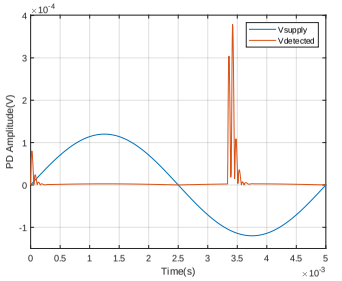
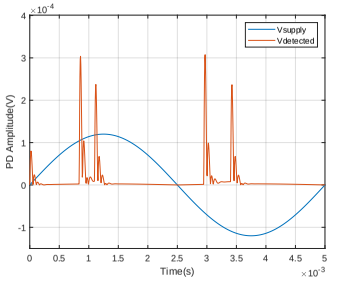
Frequency	Comments	Scarce	Abundant
1 Hz	PD characteristics are not affected by statistical time lag variations from scarce to abundant seed electron availability.		
50 Hz	PD pulses slightly increase and PD amplitude slightly decrease at abundant than at scarce electron condition due to the readily availability of seed electrons. However, the PD amplitude has increased as compared to that at 1 Hz due to a faster rise time of the applied voltage which enhances an over-voltage situation.		
200 Hz	PD amplitude slightly decrease at abundant than at scarce electron condition due to the readily availability of seed electrons. PD pulses are lesser at scarce condition due to lack of seed electrons. No observable PD pulses in the half cycle because of a faster rising rate of change of the applied voltage such that a half cycle is completed before a seed electron is available.		

TABLE 7.2: Cavity surface resistance variations (from R_{min} to R_{max}) influence on PD characteristics at different supply voltage frequencies

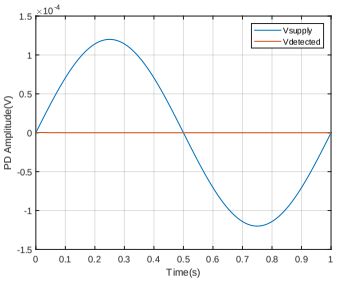
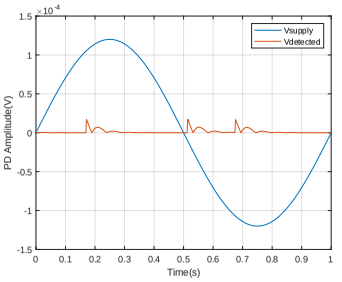
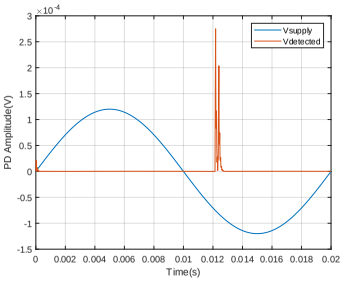
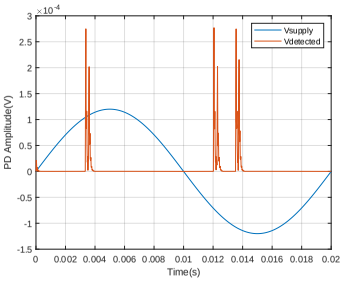
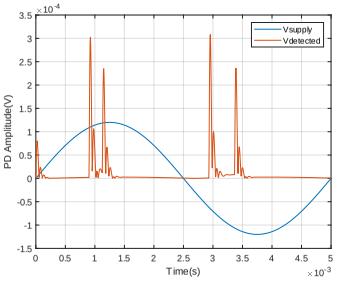
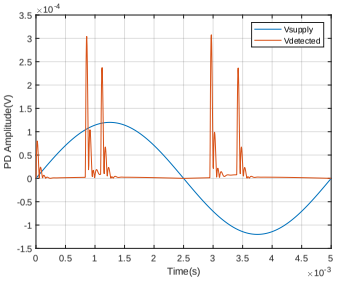
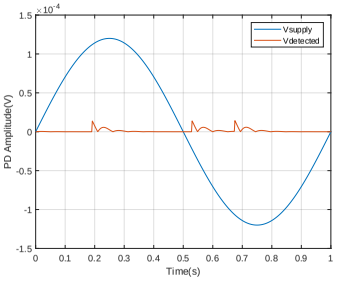
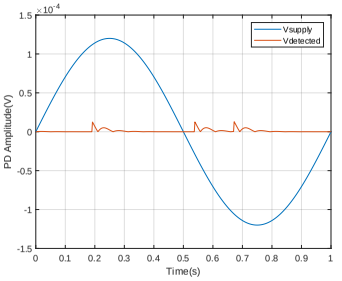
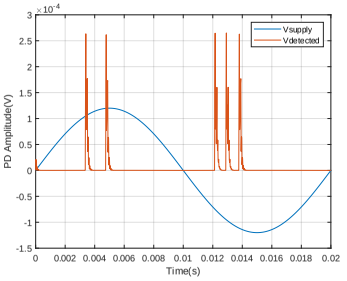
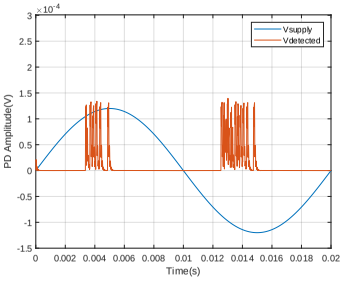
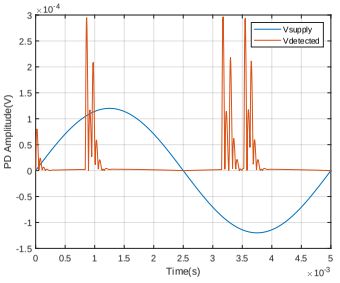
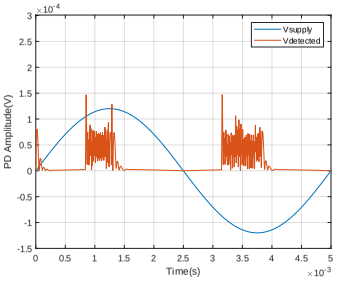
Frequency	**Comments**	**R_{min}**	**R_{max}**
1 Hz	No PD pulses are observed at the minimum selected surface resistance value, R_{min}. However, as the resistance R_c is varied to the maximum, R_{max} PD pulses become detectable.		
50 Hz	At R_{min}, there are no PD pulses in the positive half cycle but are observed in the negative half. As R_c is changed to R_{max} there is an increase in PD pulses observed in both half cycles. The increase in surface resistance at 50 Hz has an effect on PD characteristics.		
200 Hz	There is a slight change on the observed PD patterns as the surface resistance, R_c is changed from R_{min} to R_{max}. Therefore, at 200 Hz (representing higher frequencies) surface resistance of the cavity has a minor influence.		

TABLE 7.3: Residual charge effect variations (from C_{min} to C_{max}) influence on PD characteristics at different supply voltage frequencies

Frequency	**Comments**	**C_{min}**	**C_{max}**
1 Hz	Changes in the residual charge magnitude does not affect PD characteristics at low frequency. The rate of voltage increase at 1H z is much slower than the residual charge, C_{res} dissipation rate.		
50 Hz	PD characteristics are affected by changes in the residual charge at SVF of 50 Hz. At higher residual charge, C_{max} the PD pulses are closely packed to each other than at C_{min}. PD magnitudes are higher than those observed at SVF of 1 Hz, attributed to a faster rise time at 50 Hz.		
200 Hz	PD characteristics are affected by changes in the residual charge at SVF of 200 Hz. At C_{max}, the PD pulses are closely packed to each other and have reduced amplitudes than at C_{min} which is similar response observed at 50 Hz.		

7.5 Comparison of the Three Modified ABC Model Configurations; Simulation Results versus Experimentally Measured Results Obtained from the Literature

This section is on evaluating the efficacy of the three different ABC model versions. The model configurations are ABC models with (i) capacitors only, (ii) capacitors with resistors, and (iii) capacitors with resistors and additional 'residual' capacitor. The ABC model version that gives results closer to the ones practically obtained in the literature is regarded as being more accurate. The simulated results of the different model configurations are compared to the experimental-based measurements obtained from similar studies in the literature [9]. The configuration that gives results that are closer to the experimental-based measurements obtained in the literature is regarded as being more accurate. The experimental-based measurements in the literature that is compared and contrasted with the simulated results presented a frequency range that did not include supply voltage frequencies between 50 Hz and 300 Hz. The present study therefore included more data points in the stated frequency range. The added frequency points in the simulated results are 100 Hz and 200 Hz. Figure 7.21 presents the extent to which PDRR respond to the supply voltage frequency sweep from VLF of 1 Hz to 300 Hz using the three versions of the PD ABC model.

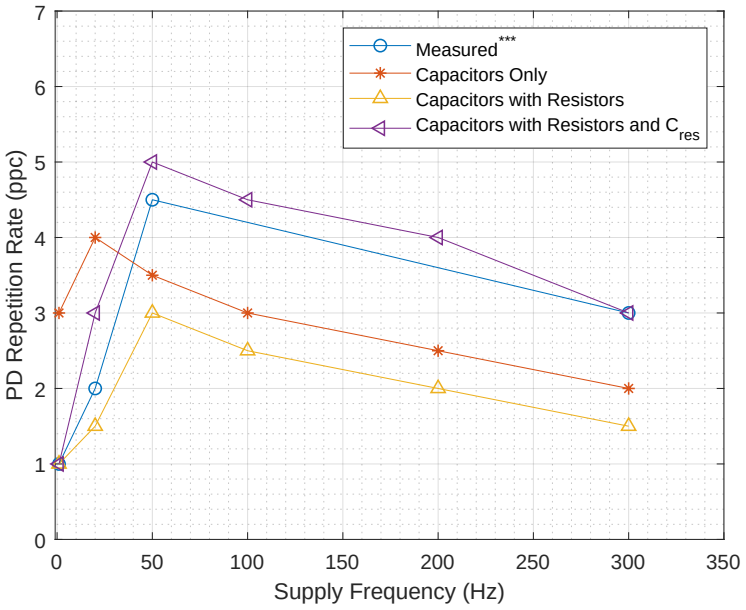


FIGURE 7.21: ABC Model configurations' results comparison of supply voltage frequency sweep plotted together with experimental-based data obtained from the literature (*** : measured values as reported by Cavallini et al [9]).

The overall trend obtained from the simulations is similar to the one presented in the experimental-based measurements from the literature. The fact that PD repetition rate trend as a function of SVF has a peak around 50 Hz needs more research to understand the responsible mechanisms. The PD repetition rate in the present research work increases as the frequency of the applied voltage is increased from 1 Hz to 50 Hz. This trend is in agreement with the research studies in the literature that reported the frequency range between VLF up to 50 Hz [11, 59, 67, 69, 70, 73]. However, beyond 50 Hz, the opposite trend is true; the PD repetition rate decreases as the supply voltage frequency is increased. This trend is also in agreement with the research studies in the literature that reported results of the frequency ranges that are beyond 50 Hz. However, literature review showed that the body of knowledge on studies that reported supply voltage frequencies beyond 50 Hz have been relatively limited. Some studies have presented results with supply voltage frequencies of up to 100 Hz [60, 64, 78]. Other studies have taken two supply frequency points that are sometimes far apart to draw out their conclusions. Others have frequency ranges that deals with frequencies beyond 50 Hz only which misses the behavior of PD activity below the 50 Hz point. For instance, Negm et al [76] who reported results of 50 Hz to 600 Hz frequency range concluded that the PDRR decreases with an increase in the supply voltage frequency. This trend is also in agreement with the simulation results presented in the present research work. Therefore, the addition of the frequency points in the present research work as shown in Figure 7.21, helps in presenting a more complete picture. The ABC model version with the capacitors and resistors with an additional'residual' capacitor is regarded to be more accurate than the others because its simulated results are the closest to the experimental-based measurements obtained from similar studies in the literature.

The next chapter concludes the dissertation and also suggests possible further future extension of the research work.

Chapter 8

Conclusions and Recommendations

Simulation results have been presented in this research based on improved ABC PD model implemented in MATLAB® Simulink®. The main focus was investigation of the factors that influence the frequency dependence of PD mechanisms at different supply voltage frequencies. The factors responsible for the PD frequency dependence are the statistical time lag, cavity surface conductivity and the residual charge effect. The ABC model is modified and extended into three configurations that are developed and implemented to cater for each of the factors responsible for the frequency dependence of PD mechanisms. The extents to which each factor affect the frequency dependence of PD mechanisms at different supply voltage frequencies were evaluated. Simulation results are validated using empirical experimental-based measurement results from similar studies published in the literature. The summary of the findings is as follows:

- At lower supply voltage frequencies, changes in statistical time lag does not affect PD characteristics whereas at higher supply voltage frequencies, the PDRR slightly increases and PD pulse amplitude decreases as seed electron availability is varied from scarce to abundant conditions.
- At lower supply voltage frequencies, PD characteristics respond to the changes in the cavity surface resistance; PD pulses are observed as the cavity surface resistance is increased from minimum to maximum values. However, at higher supply voltage

frequencies, changes in the cavity surface resistance has minor influence on PD characteristics.

- At lower supply voltage frequencies, changes in the residual charge magnitude does not affect PD characteristics whereas at higher supply voltage frequencies, PD pulses are closely packed next to each other however with reduced PD amplitudes and the PD repetition rate increases as residual charge changes from minimum to maximum values.

The possible future extension of the research work include repeating the same studies on double and/or multiple cavities as well as conducting PD activity investigation under DC (0 Hz) test voltage.

References

[1] G. C. Stone. Partial discharge diagnostics and electrical equipment insulation condition assessment. *IEEE Transactions on Dielectrics and Electrical Insulation*, 12(5):891–904, Oct 2005. ISSN 1070-9878. doi: 10.1109/TDEI.2005.1522184.

[2] M. Toader and D. Mariana. Electrical insulation study using partial discharge model. In *2000 10th Mediterranean Electrotechnical Conference. Information Technology and Electrotechnology for the Mediterranean Countries. Proceedings. MeleCon 2000 (Cat. No.00CH37099)*, volume 3, pages 1060–1063 vol.3, May 2000. doi: 10.1109/MELCON.2000.879717.

[3] G. J. Paoletti and A. Golubev. Partial discharge theory and technologies related to medium-voltage electrical equipment. *IEEE Transactions on Industry Applications*, 37(1):90–103, Jan 2001. ISSN 0093-9994. doi: 10.1109/28.903131.

[4] S. A. Boggs. Partial discharge: overview and signal generation. *IEEE Electrical Insulation Magazine*, 6(4):33–39, July 1990. ISSN 0883-7554. doi: 10.1109/57.63057.

[5] G. C. Montanari. Envisaging links between fundamental research in electrical insulation and electrical asset management. *IEEE Electrical Insulation Magazine*, 24(6):7–21, 2008. doi: 10.1109/MEI.2008.4665346.

[6] L. Niemeyer. A generalized approach to partial discharge modeling. *IEEE Transactions on Dielectrics and Electrical Insulation*, 2(4):510–528, Aug 1995. ISSN 1070-9878. doi: 10.1109/94.407017.

[7] Wong Jee Keen Raymond, Hazlee Azil Illias, Ab Halim Abu Bakar, and Hazlie Mokhlis. Partial discharge classifications: Review of recent progress. *Measurement*,

68:164 – 181, 2015. ISSN 0263-2241. doi: https://doi.org/10.1016/j.measurement.2015.02.032.

[8] G. Callender, P. Rapisarda, and P. L. Lewin. Improving models of partial discharge activity using simulation. In *2017 IEEE Electrical Insulation Conference (EIC)*, pages 392–395, June 2017. doi: 10.1109/EIC.2017.8004653.

[9] A. Cavallini and G. C. Montanari. Effect of supply voltage frequency on testing of insulation system. *IEEE Transactions on Dielectrics and Electrical Insulation*, 13(1):111–121, Feb 2006. ISSN 1070-9878. doi: 10.1109/TDEI.2006.1593409.

[10] J. Giddens, H. Edin, and U. Gafvert. Measuring system for phase-resolved partial discharge detection at low frequencies. In *1999 Eleventh International Symposium on High Voltage Engineering*, volume 5, pages 228–231 vol.5, 1999. doi: 10.1049/cp:19990927.

[11] C. Forssen and H. Edin. Partial discharges in a cavity at variable applied frequency part 1: measurements. *IEEE Transactions on Dielectrics and Electrical Insulation*, 15(6):1601–1609, December 2008. ISSN 1070-9878. doi: 10.1109/TDEI.2008.4712663.

[12] Ieee guide for failure investigation, documentation, analysis, and reporting for power transformers and shunt reactors. *IEEE Std C57.125-2015 (Revision of IEEE Std C57.125-1991)*, pages 1–84, 2015.

[13] Ieee recommended practice for the design of reliable industrial and commercial power systems (gold book). *IEEE Std 493-1997 [IEEE Gold Book]*, pages 1–464, 1998. doi: 10.1109/IEEESTD.1998.89291.

[14] H. Edin. *Partial Discharges Studied with Variable Frequency of the Applied Voltage*. PhD thesis, Kungl Tekniska Hogskolan (KTH), Stockholm (Sweden), September 2001.

[15] Z. Achillides, E. Kyriakides, and G. E. Georghiou. Partial discharge modeling: an improved capacitive model and associated transients along medium voltage distribution cables. *IEEE Transactions on Dielectrics and Electrical Insulation*, 20(3):770–781, June 2013. ISSN 1070-9878. doi: 10.1109/TDEI.2013.6518947.

[16] G. Paoletti and A. Golubev. Partial discharge theory and applications to electrical systems. In *Conference Record of 1999 Annual Pulp and Paper Industry Technical Conference (Cat. No.99CH36338)*, pages 124–138, June 1999. doi: 10.1109/PAPCON.1999.779355.

[17] J. H. van Jaarsveldt. Non-intrusive condition monitoring of power cables within the industrial sector. Master's thesis, North-West University, Potchefstroom (South africa), May 2015.

[18] High-voltage test techniques - partial discharge measurements. *SANS 60270:2000 (IEC 60270:2000)*, pages 1–53, 2007.

[19] E. Haikali and C. Nyamupangedengu. Partial discharge simulations used for the design of a non-intrusive cable condition monitoring technique. *ESI Africa's Power Journal*, Issue 4:16–21, 2016.

[20] C. Nyamupangedengu. *PD-Type-Dependent Spectral Bandwidth In Solid Polymer Dielectrics*. PhD thesis, University of the Witwatersrand Johannesburg, Johannesburg (South africa), 2011.

[21] R. S. Nema and V. Prabhashanker. Partial discharges - a brief review and a bibliography. *Department of High Voltage Engineering, Indian Institute of Science, Bangalore*, pages 443–480, 1974.

[22] M. Florkowski. Influence of high voltage harmonics on partial discharge patterns. In *Proceedings of 5th International Conference on Properties and Applications of Dielectric Materials*, volume 1, pages 303–306 vol.1, May 1997. doi: 10.1109/ICPADM.1997.617588.

[23] R. Candela, I. Romano, and P. Romano. Influence on pd parameters due to distorted voltage. In *2003 Annual Report Conference on Electrical Insulation and Dielectric Phenomena*, pages 593–596, Oct 2003. doi: 10.1109/CEIDP.2003.1254924.

[24] P. Romano. Influence on pd parameters due to voltage conducted disturbances. *IEEE Transactions on Dielectrics and Electrical Insulation*, 11(1):160–165, Feb 2004. ISSN 1070-9878. doi: 10.1109/TDEI.2004.1266331.

[25] M. Florkowski, B. Florkowska, J. Furgał, and P. Zydron. Impact of high voltage harmonics on interpretation of partial discharge patterns. *IEEE Transactions on Dielectrics and Electrical Insulation*, 20(6):2009–2016, 2013. doi: 10.1109/TDEI.2013.6678848.

[26] R. C. Kiiza, R. Nikjoo, M. G. Niasar, X. Wang, and H. Edin. Effect of high voltage impulses on partial discharge activity in a cavity embedded in paper insulation. In *2012 Annual Report Conference on Electrical Insulation and Dielectric Phenomena*, pages 133–136, 2012. doi: 10.1109/CEIDP.2012.6378739.

[27] Z. Sun, X. Zhao, J. Li, and Y. Li. Experiment investigation of partial discharges under impulse voltage. In *2009 IEEE 9th International Conference on the Properties and Applications of Dielectric Materials*, pages 525–529, 2009. doi: 10.1109/ICPADM.2009.5252374.

[28] Suwarno and Aulia. Effect of lightning impulse voltage to the pd activity and breakdown voltage of liquid insulation. In *The 2nd IEEE Conference on Power Engineering and Renewable Energy (ICPERE) 2014*, pages 171–174, 2014. doi: 10.1109/ICPERE.2014.7067202.

[29] R. J. Densley. Partial discharges in electrical insulation under combined alternating and impulse stresses. *IEEE Transactions on Electrical Insulation*, EI-5(4): 96–103, 1970. doi: 10.1109/TEI.1970.299117.

[30] J. Wu, P. V. M. van Nes, A. Rodrigo Mor, and J. J. Smit. Partial discharges in xlpe insulated cable under superimposed transient voltages. In *2019 IEEE Electrical Insulation Conference (EIC)*, pages 221–225, 2019. doi: 10.1109/EIC43217.2019.9046529.

[31] M. R. Rahimi, R. Javadinezhad, and M. Vakilian. Dc partial discharge characteristics for corona, surface and void discharges. In *2015 IEEE 11th International Conference on the Properties and Applications of Dielectric Materials (ICPADM)*, pages 260–263, 2015. doi: 10.1109/ICPADM.2015.7295258.

[32] M. H. Okba, M. H. Saied, M. Z. Mostafa, and T. M. Abdel- Moneim. High voltage direct current transmission - a review, part i. In *2012 IEEE Energytech*, pages 1–7, 2012. doi: 10.1109/EnergyTech.2012.6304650.

[33] P. K. Olsen, F. Mauseth, and E. Ildstad. The effect of dc superimposed ac voltage on partial discharges in dielectric bounded cavities. In *2014 ICHVE International Conference on High Voltage Engineering and Application*, pages 1–4, 2014. doi: 10.1109/ICHVE.2014.7035408.

[34] E. A. Morris and W. H. Siew. Partial discharge activity in polymeric cable insulation under high voltage ac and dc. In *2017 52nd International Universities Power Engineering Conference (UPEC)*, pages 1–4, 2017. doi: 10.1109/UPEC.2017.8231907.

[35] H. Niu, A. Cavallini, G. C. Montanari, and Y. Zhang. Noise rejection strategy and experimental research on partial discharge at dc voltage. In *2009 IEEE 9th International Conference on the Properties and Applications of Dielectric Materials*, pages 489–492, 2009. doi: 10.1109/ICPADM.2009.5252385.

[36] R. Guo, K. Wang, Z. Xu, J. Li, J. Sun, and H. Cheng. Partial discharge characteristics and classification in oil-paper insulation under dc voltage. In *2016 IEEE International Conference on High Voltage Engineering and Application (ICHVE)*, pages 1–4, 2016. doi: 10.1109/ICHVE.2016.7800629.

[37] T. Klueter, J. Wulff, and F. Jenau. Measurement and statistical analysis of partial discharges at dc voltage. In *2013 48th International Universities' Power Engineering Conference (UPEC)*, pages 1–5, 2013. doi: 10.1109/UPEC.2013.6714912.

[38] E. Corr and W. H. Siew. Analyses of partial discharges in dielectric samples under dc excitation. In *2015 50th International Universities Power Engineering Conference (UPEC)*, pages 1–6, 2015. doi: 10.1109/UPEC.2015.7339825.

[39] S. Li, W. Si, and Q. Li. Partition and recognition of partial discharge development stages in oil-pressboard insulation with needle-plate electrodes under combined ac-dc voltage stress. *IEEE Transactions on Dielectrics and Electrical Insulation*, 24(3):1781–1793, 2017. doi: 10.1109/TDEI.2017.006361.

[40] S. Li, Q. Li, W. Si, J. Yao, Y. Shi, and T. Zhang. Partial discharge characteristics in pre-breakdown processes of oil-pressboard insulation with needle-plate defect under ac-dc combined voltage. In *2018 IEEE Electrical Insulation Conference (EIC)*, pages 18–21, 2018. doi: 10.1109/EIC.2018.8481130.

[41] M. G. Niasar, X. Wang, and R. C. Kiiza. Review of partial discharge activity considering very-low frequency and damped applied voltage. *Energies*, 14(440), 2021. doi: 10.3390/en14020440.

[42] R. Bodega, A. Cavallini, P. H. F. Morshuis, and F. J. Wester. The effect of voltage frequency on partial discharge activity. In *Annual Report Conference on Electrical Insulation and Dielectric Phenomena*, pages 685–689, 2002. doi: 10.1109/CEIDP.2002.1048889.

[43] B. Florkowska, P. Zydron, and M. Florkowski. Analysis of pd phase-resolved images at low frequency of testing voltage. In *Conference Record of the 2004 IEEE International Symposium on Electrical Insulation*, pages 143–146, 2004. doi: 10.1109/ELINSL.2004.1380493.

[44] A. Eigner and K. Rethmeier. An overview on the current status of partial discharge measurements on ac high voltage cable accessories. *IEEE Electrical Insulation Magazine*, 32(2):48–55, March 2016. ISSN 0883-7554. doi: 10.1109/MEI.2016.7414231.

[45] L. W. van Veen. *Comparison of measurement methods for partial discharge measurement in power cables.* PhD thesis, Delft University of Technology, Netherlands, 2014.

[46] P. H. F. Morshuis, R. Bodega, M. Lazzaroni, and F. J. Wester. Partial discharge detection using oscillating voltage at different frequencies. In *IMTC/2002. Proceedings of the 19th IEEE Instrumentation and Measurement Technology Conference (IEEE Cat. No.00CH37276)*, volume 1, pages 431–435 vol.1, 2002. doi: 10.1109/IMTC.2002.1006880.

[47] Ieee guide for field testing of shielded power cable systems using very low frequency (vlf)(less than 1 hz). *IEEE Std 400.2-2013*, pages 1–60, 2013. doi: 10.1109/IEEESTD.2013.6517854.

[48] D. Fynes-Clinton and C. Nyamupangedengu. Partial discharge characterization of cross-linked polyethylene medium voltage power cable termination defects at very low frequency (0.1 hz) and power frequency test voltages. *IEEE Electrical Insulation Magazine*, 32(4):15–23, July 2016. ISSN 0883-7554. doi: 10.1109/MEI.2016.7528986.

[49] R. Bodega, P. H. F. Morshuis, M. Lazzaroni, and F. J. Wester. Pd recurrence in cavities at different energizing methods. *IEEE Transactions on Instrumentation and Measurement*, 53(2):251–258, April 2004. ISSN 0018-9456. doi: 10.1109/TIM.2003.822478.

[50] R. Miller and I. A. Black. Partial discharge measurements over the frequency range 0.1 hz to 50 hz. *IEEE Transactions on Electrical Insulation*, EI-12(3):224–233, June 1977. ISSN 0018-9367. doi: 10.1109/TEI.1977.298026.

[51] R. Miller and I. A. Black. Partial discharge energy measurements on electrical machine insulation when energized at frequencies between 0.1 hz and power frequency. *IEEE Transactions on Electrical Insulation*, EI-14(3):127–135, June 1979. ISSN 0018-9367. doi: 10.1109/TEI.1979.298212.

[52] E. Gockenbach and W. Hauschild. The selection of the frequency range for high-voltage on-site testing of extruded insulation cable systems. *IEEE Electrical Insulation Magazine*, 16(6):11–16, 2000. doi: 10.1109/57.887600.

[53] P. Coors and S. Schierig. Hv ac testing of super-long cables. In *Conference Record of the 2008 IEEE International Symposium on Electrical Insulation*, pages 636–640, 2008. doi: 10.1109/ELINSL.2008.4570412.

[54] W. Schufft, P. Coors, W. Hauschild, and J. Spiegelberg. Frequency-tuned resonant test systems for on-site testing and diagnostics of extruded cables. In *1999 Eleventh International Symposium on High Voltage Engineering*, volume 5, pages 335–339 vol.5, 1999. doi: 10.1049/cp:19990953.

[55] A. Cavallini, R. Ciani, M. Conti, P. F. H. Morshuis, and G. C. Montanari. Modeling memory phenomena for partial discharge processes in insulation cavities. In *2003 Annual Report Conference on Electrical Insulation and Dielectric Phenomena*, pages 723–727, Oct 2003. doi: 10.1109/CEIDP.2003.1254956.

[56] A. Cavallini, V. Krotov, G. C. Montanari, P. H. F. Morshuis, and L. E. Mariut. The role of supply frequency in the evaluation of partial discharge inception voltage in xlpe-embedded cavities. In *2012 Annual Report Conference on Electrical Insulation and Dielectric Phenomena*, pages 487–490, Oct 2012. doi: 10.1109/CEIDP.2012.6378826.

[57] W. Hauschild, A. Cavallini, and G. C. Montanari. Effect of supply voltage frequency on testing of insulation system. *IEEE Transactions on Dielectrics and Electrical Insulation*, 13(5):1189–1191, Oct 2006. ISSN 1070-9878. doi: 10.1109/TDEI.2006.247849.

[58] C. Forssen and H. Edin. Influence of cavity size and cavity location on partial discharge frequency dependence [polymer insulation]. In *The 17th Annual Meeting of the IEEE Lasers and Electro-Optics Society, 2004. LEOS 2004.*, pages 438–441, Oct 2004. doi: 10.1109/CEIDP.2004.1364281.

[59] C. Forssen and H. Edin. Partial discharges in a cavity at variable applied frequency part 2: measurements and modeling. *IEEE Transactions on Dielectrics and Electrical Insulation*, 15(6):1610–1616, December 2008. ISSN 1070-9878. doi: 10.1109/TDEI.2008.4712664.

[60] H. A. Illias, G. Chen, and P. L. Lewin. Modeling of partial discharges from a spherical cavity within a dielectric material under variable frequency electric fields. In *2008 Annual Report Conference on Electrical Insulation and Dielectric Phenomena*, pages 447–450, Oct 2008. doi: 10.1109/CEIDP.2008.4772896.

[61] G. Chen and F. Baharudin. Partial discharge modelling based on a cylindrical model in solid dielectrics. In *2008 International Conference on Condition Monitoring and Diagnosis*, pages 74–78, April 2008. doi: 10.1109/CMD.2008.4580233.

[62] U. Gafvert, H. Edin, and C. Forssen. Modelling of partial discharge spectra measured with variable applied frequency. In *Proceedings of the 7th International Conference on Properties and Applications of Dielectric Materials (Cat. No.03CH37417)*, volume 3, pages 839–842 vol.3, June 2003. doi: 10.1109/ICPADM.2003.1218552.

[63] F. Mauseth, H. Tollefsen, and S. Hvidsten. Effect of test voltage frequency on pd inception in service aged cable joints. In *2014 ICHVE International Conference on High Voltage Engineering and Application*, pages 1–4, Sept 2014. doi: 10.1109/ICHVE.2014.7035487.

[64] C. Forssen and H. Edin. Modeling partial discharges in a cavity at different applied frequencies. In *2007 Annual Report - Conference on Electrical Insulation*

and Dielectric Phenomena, pages 132–135, Oct 2007. doi: 10.1109/CEIDP.2007.4451518.

[65] C. Forssen. *Modelling of cavity partial discharges at variable applied frequency.* PhD thesis, Kungl Tekniska Hogskolan (KTH), Stockholm (Sweden), June 2008.

[66] P. Seri, H. Naderiallaf, and G. C. Montanari. Modelling of supply voltage frequency effect on partial discharge repetition rate and charge amplitude from ac to dc at room temperature. *IEEE Transactions on Dielectrics and Electrical Insulation*, 27 (3):764–772, 2020.

[67] H. A. Illias, G. Chen, and P. L. Lewin. Partial discharge modelling in a spherical cavity within a dielectric insulation material as a function of frequency. In *2009 IEEE Electrical Insulation Conference*, pages 55–59, May 2009. doi: 10.1109/EIC.2009.5166323.

[68] H. A. Illias, G. Chen, and P. L. Lewin. Partial discharge measurements for spherical cavities within solid dielectric materials under different stress and cavity conditions. In *2009 IEEE Conference on Electrical Insulation and Dielectric Phenomena*, pages 388–391, Oct 2009. doi: 10.1109/CEIDP.2009.5377831.

[69] H. A. Illias, G. Chen, and P. L. Lewin. Comparison of partial discharge measurement and simulation results for spherical cavities within solid dielectric materials as a function of frequency using finite element analysis method. In *2010 IEEE International Symposium on Electrical Insulation*, pages 1–5, June 2010. doi: 10.1109/ELINSL.2010.5549733.

[70] H. Illias, G. Chen, and P. L. Lewin. Partial discharge behavior within a spherical cavity in a solid dielectric material as a function of frequency and amplitude of the applied voltage. *IEEE Transactions on Dielectrics and Electrical Insulation*, 18(2):432–443, April 2011. ISSN 1070-9878. doi: 10.1109/TDEI.2011.5739447.

[71] J. Senoamadi, R. Mabodi, and C. Nyamupangedengu. The effect of supply voltage frequency on cavity partial discharge mechanisms. In *2018 26th Southern African Universities Power Engineering Conference (SAUPEC)*, Jan 2018.

[72] K. Mosito, M. Dlamini, and C. Nyamupangedengu. A comparative study of cavity partial discharge parameters at vlf and at 50 hz test voltages. In *2015 23rd*

Southern African Universities Power Engineering Conference (SAUPEC), pages 261–266, Jan 2015.

[73] H. V. P. Nguyen, B. T. Phung, and S. Morsalin. Modelling partial discharges in an insulation material at very low frequency. In *2017 International Conference on High Voltage Engineering and Power Systems (ICHVEPS)*, pages 451–454, Oct 2017. doi: 10.1109/ICHVEPS.2017.8225888.

[74] H. V. P. Nguyen, B. T. Phung, and T. Blackburn. Effects of aging on partial discharge patterns in voids under very low frequency excitation. In *2016 IEEE International Conference on Dielectrics (ICD)*, volume 1, pages 524–527, July 2016. doi: 10.1109/ICD.2016.7547657.

[75] H. V. P. Nguyen and B. T. Phung. Void discharge behaviours as a function of cavity size and voltage waveform under very low-frequency excitation. *High Voltage*, 3 (2):96–102, 2018. ISSN 2397-7264. doi: 10.1049/hve.2017.0174.

[76] T. S. Negm, M. Refaey, and A. A. Hossam-Eldin. Modeling and simulation of internal partial discharges in solid dielectrics under variable applied frequencies. In *2016 Eighteenth International Middle East Power Systems Conference (MEPCON)*, pages 639–644, Dec 2016. doi: 10.1109/MEPCON.2016.7836959.

[77] T. S. Negm, M. Refaey, and A. A. Hossam-Eldin. Investigation of partial discharge frequency dependence in distribution system cables. *CIRED - Open Access Proceedings Journal*, 2017(1):268–272, 2017. ISSN 2515-0855. doi: 10.1049/oap-cired.2017.0532.

[78] F Haghjoo, Esmaeel Khanahmadloo, and S. Mohammad Shahrtash. Comprehensive 3-capacitors model for partial discharge in power cables. *COMPEL: The International Journal for Computation and Mathematics in Electrical and Electronic Engineering*, 31:346–368, Mar 2012.

[79] R. Plessow and W. Pfeiffer. Influence of the frequency on the partial discharge inception voltage. In *Electrical Insulation and Dielectric Phenomena, 1994., IEEE 1994 Annual Report., Conference on*, pages 97–102, Oct 1994. doi: 10.1109/CEIDP.1994.591699.

[80] H. A. Illias, G. Chen, and P. L. Lewin. Comparison between three-capacitance, analytical-based and finite element analysis partial discharge models in condition

monitoring. *IEEE Transactions on Dielectrics and Electrical Insulation*, 24(1): 99–109, Feb 2017. ISSN 1070-9878. doi: 10.1109/TDEI.2016.005971.

[81] C. Pan, G. Chen, J. Tang, and K. Wu. Numerical modeling of partial discharges in a solid dielectric-bounded cavity: A review. *IEEE Transactions on Dielectrics and Electrical Insulation*, 26(3):981–1000, June 2019. doi: 10.1109/TDEI.2019.007945.

[82] G. Paolitti and A. Golubev. Partial discharge theory and technologies related to traditional testing methods of large rotating apparatus. In *Conference Record of the 1999 IEEE Industry Applications Conference. Thirty-Forth IAS Annual Meeting (Cat. No.99CH36370)*, volume 2, pages 967–981 vol.2, 1999. doi: 10.1109/IAS.1999.801624.

[83] H. Suzuki, K. Aihara, T. Takahashi, and T. Okamoto. Deterministic partial discharge model with dissipation. *IEICE International Symposium on Nonlinear Theory and its Applications (NOLTA2004)*, pages 143–146, Nov 2004. doi: 10.1109/14.90292.

[84] D. Gowda and Anandraj. Modeling of partial discharge (pd) for solid insulation with void and building a hardware setup to measure partial discharge. In *2016 Biennial International Conference on Power and Energy Systems: Towards Sustainable Energy (PESTSE)*, pages 1–7, Jan 2016. doi: 10.1109/PESTSE.2016.7516414.

[85] X. Chen, M. Bi, T. Jiang, and Y. Wang. An equivalent circuit model for partial discharge occuring in transformer oil bubbles. In *2016 IEEE International Conference on High Voltage Engineering and Application (ICHVE)*, pages 1–4, Sept 2016. doi: 10.1109/ICHVE.2016.7800911.

[86] R. Patsch and F. Berton. The role of space charges in pd-processes. In *Proceedings of 2001 International Symposium on Electrical Insulating Materials (ISEIM 2001). 2001 Asian Conference on Electrical Insulating Diagnosis (ACEID 2001). 33rd Symposium on Electrical and Ele*, pages 21–24, Nov 2001. doi: 10.1109/ISEIM.2001.973547.

[87] R. Patsch, J. Menzel, and D. Benzerouk. The analysis of pd-sequences from different defects. In *2006 IEEE 8th International Conference on Properties applications of Dielectric Materials*, pages 31–35, June 2006. doi: 10.1109/ICPADM.2006.284110.

[88] R. Patsch, Y. Z. Arief, D. Benzerouk, and J. Menzel. Space charges in polymers and their influence on electrical treeing. In *2007 Annual Report - Conference on Electrical Insulation and Dielectric Phenomena*, pages 208–212, 2007.

[89] S. A. Boggs. Partial discharge. iii. cavity-induced pd in solid dielectrics. *IEEE Electrical Insulation Magazine*, 6(6):11–16, Nov 1990. ISSN 0883-7554. doi: 10.1109/57.63094.

[90] A. J. Christina, M. A. Salam, Q. M. Rahman, M. S. Arifin, F. Wen, S. P. Ang, and S. Hasan. Partial discharge modeling with increasing applied voltages across different void sizes. In *2017 4th International Conference on Advances in Electrical Engineering (ICAEE)*, pages 22–25, Sept 2017. doi: 10.1109/ICAEE.2017.8255320.

[91] T. G. Aakre, E. Ildstad, and S. Hvidsten. Partial discharge inception voltage of voids enclosed in epoxy/mica versus voltage frequency and temperature. *IEEE Transactions on Dielectrics and Electrical Insulation*, 27(1):214–221, 2020.

[92] N. P. Kolev, M. G. Danikas, E. D. Gadjeva, and N. R. Gourov. Development of partial discharge model, simulation and measurement. In *1999 Annual Report Conference on Electrical Insulation and Dielectric Phenomena (Cat. No.99CH36319)*, pages 214–217 vol.1, 1999. doi: 10.1109/CEIDP.1999.804629.

[93] D. P. Agoris and N. D. Hatziargyriou. Approach to partial discharge development in closely coupled cavities embedded in solid dielectrics by the lumped capacitance model. *IEE Proceedings A - Science, Measurement and Technology*, 140(2):131–134, March 1993. ISSN 0960-7641. doi: 10.1049/ip-a-3.1993.0021.

[94] C. Y. Ren, Y. H. Cheng, P. Yan, Y. H. Sun, and T. Shao. Simulation of partial discharges in single and double voids using simulink. In *Conference Record of the 2006 Twenty-Seventh International Power Modulator Symposium*, pages 120–123, 2006.

[95] P. Y. Chia and A. C. Liew. Novel approach to partial discharge signals modeling in dielectric insulation void using extension of lumped capacitance model. In *PowerCon 2000. 2000 International Conference on Power System Technology. Proceedings (Cat. No.00EX409)*, volume 3, pages 1207–1212 vol.3, Dec 2000. doi: 10.1109/ICPST.2000.898141.

[96] High-voltage test techniques part 1: General definitons and test requirements. *SANS 60060-1:2011 (IEC 60060:2010)*, pages 1–77, 2011.

[97] G. Callender and P. L. Lewin. Modeling partial discharge phenomena. *IEEE Electrical Insulation Magazine*, 36(2):29–36, 2020.

[98] Chegg Study. Paschen curve: The value of townsend's second ionization coefficient. https://www.chegg.com/homework-help/questions-and-answers/value-townsend-s-second-ionization-coefficient-0111-cm-calculate-/breakdown-voltage-air-gap-q24785794. Accessed: 2021.03.12.

[99] C. Hudon, R. Bartnikas, and M. R. Wertheimer. Spark-to-glow discharge transition due to increased surface conductivity on epoxy resin specimens. *IEEE Transactions on Electrical Insulation*, 28(1):1–8, 1993.

[100] P. H. F. Morshuis. Degradation of solid dielectrics due to internal partial discharge: some thoughts on progress made and where to go now. *IEEE Transactions on Dielectrics and Electrical Insulation*, 12(5):905–913, 2005.

[101] S. S. Samat, I. Musirin, and A. S. Kusim. The effect of supply voltage on partial discharge properties in solid dielectric. In *2012 IEEE International Power Engineering and Optimization Conference Melaka, Malaysia*, pages 490–495, 2012.

Appendix A

SAUPEC 2019 Conference Paper

This appendix contains a publication handed in to the South African Universities Power Engineering Conference (SAUPEC/RobMech/PRASA) in 2019.

2019 SAUPEC/RobMech/PRASA Conference
Bloemfontein, South Africa, January 28-30, 2019

Influence of Variable Frequency of the Applied Voltage on Cavity Partial Discharge Parameters: A Critical Review

Tapiwa Venge
School of Electrical and Information Engineering
University of the Witwatersrand
Johannesburg, South Africa
tapiwa.venge@students.wits.ac.za

Cuthbert Nyamupangedengu
School of Electrical and Information Engineering
University of the Witwatersrand
Johannesburg, South Africa
cuthbert.nyamupangedengu@wits.ac.za

***Abstract*—This paper presents a critical literature review on the influence of supply voltage frequency on partial discharges activity in an air-filled cavity. A wide range of voltages and frequencies are used for different applications. For instance, very low frequencies are used to test capacitive equipment so as to save cost and power losses since it may not be technically feasible to use power frequencies (50/60Hz). In literature review; different parameters, frequency ranges, defect types and key findings has been noted. A lot of agreements and inconsistencies have been found when it comes to key findings. The only agreements found are on partial discharge inception voltage, and delay and rise times that decrease as frequency is increased. Major reasons and explanations related to frequency dependence of partial discharges in cavities have been identified as statistical time lags, surface and bulk conductivity, and surface charge decay times. Due to the inconsistencies in results, more work and modeling need to be done in understanding the theory of PD phenomena.**

***Index Terms*—cavity, disharges, equipment failure, supply frequency, parameters, PD magnitude, PRPDP**

I. Introduction

Electrical equipment insulation design, protection, defect detection and measurement are important in the management of high voltage (HV) equipment that includes transformers, solid dielectric castings and power cables [1]. HV equipment diagnosis reveals that insulation failure is the major cause of more than 60% of HV equipment damage [2]. The insulation quality is correlated to the pattern of partial discharges (PD) hence it is important to understand the PD phenomena.

A PD is a localised discharge that partially bridges insulation between electrodes [3]. It results from the electrical breakdown of a gas contained in a highly non-uniform electric field [4]. For a PD to occur there must be significantly high electric field or voltage at the defect and a presence of a starting or initiating electron. Although the magnitude of such discharges are short-living (nano to micro seconds), they cause slow progressive deterioration of insulation quality [5], [6]. Hence, with time, they may lead to a reduced lifespan and ultimate failure of the HV equipment.

The work reviewed in this paper is in relation to PDs in cavities due to the knowledge that discharges in voids are among the common sources of PDs in insulation [5]. Partial discharges in voids are affected and influenced by many factors including cavity size and location, humidity, temperature, altitude, supply voltage amplitude and frequency, etc. This paper focusses on the frequency attribute of the applied voltage.

Frequency has become an important aspect in the study of PD activities and mechanisms. For instance, the incorporation of renewable energy especially solar energy into grid-ties has led to the addition of harmonics, which are a component of frequency, into the electrical systems [8]. Solar power stations, in particular, aid to these harmonics and other frequencies due to the use of inverters. The presence of harmonics and other frequencies has an effect on dielectric stressing that need to be understood [9]. Hence, the influence of harmonics on partial discharges has become a major concern as renewable energy is increasingly being used as an alternative source of power supply.

A wide range of voltages and frequencies is used for different applications depending on the equipment being measured or tested. As much as most HV equipment operates at power frequency (50/60 Hz), they get tested at different frequencies. The use of very low frequency for capacitive objects reduces power, size, cost, volume and weight of the power supplying equipment [10]. It is not technically and/or economically feasible to test some of the equipment at power frequency. For instance, low frequencies are used for capacitive components like power cables and rotating machines (0.1 Hz), and higher frequencies are used for inductive equipment like transformers (150 - 400 Hz) [10]–[12].

By varying the frequency, local conditions in the cavities and defects are altered. Some of the conditions that can be altered are: the statistical nature of PDs, electric field distribution and controlled relaxation times [13]. Hence, in most laboratory experiments, varying frequency is used for accelerating PD ageing tests as in real-life set-ups the effect of ageing might take longer durations.

Section II reviews the work that has been done as published in literature, including the parameters tested, cavity sizes and key findings in helping with contextualisation. Critical analysis

978-1-7281-0369-3/19/$31.00 ©2019 IEEE

of literature review is detailed in Section III whereas the recommendations and conclusion, are in Section IV and V, respectively.

II. Literature Review

Various studies and researches have been done on the influence of frequencies (of different ranges) of the supply voltage on PD mechanisms and parameters. The influence has been investigated on different parameters including the PD magnitude, PD patterns, number of PDs per cycle etc, as shown in the fourth column of Table I. The second and third columns show the frequency ranges and types of defects studied by different researchers. Table I highlights the summary and key findings, in the literature, that are related to the dependency of PDs due to variable frequency of the supply voltage.

Despite the significant amount of research done on the frequency dependence of PD mechanisms, there has been some inconsistencies in terms of key findings and conclusions by different researchers. However, there also has been notable consistencies in some of the PD parameter results found.

A common agreement by most researchers is that partial discharge inception voltage (PDIV) either slightly increases with increase of frequency or is independent of frequency change. This slight increase may be explained by the influence of the statistical time lag [14]. Plessow et al [7] and Forssen et al [12] have shown that PDIV is mainly dependent on the supply voltage magnitude and the void size. Another general consensus is that minimal PD magnitude remains approximately constant and is independent from the influence of variable frequency. Lastly, on the researchers that have dealt with delay, width and rise time [15]–[17], there is a consistency that these parameters reduce as the frequency is increased.

The phase-resolved-partial discharge pattern (PRPDP) parameter has led to a rise of different disagreements and inconsistencies on its dependency on variable frequency of the supply voltage. Bodega et al [18] and Morshuis et al [19] concluded that the PRPDP shape is generally independent on the change of supply voltage frequency. In addition, Nyamupangedengu & Jandrell [20] came to a similar conclusion on the pulse shape of the partial discharges. Other researchers have disagreed to the above conclusions. Cavallini & Montanari [10] found that the PRPDP gets closer to zero crossing as frequency is increased. Edin & Forssen [21] concluded that PRPDP changes with supply voltage frequency without specifying how but on analysing their results it is noted that the patterns are opposite to those by Cavallini and Montanari. Other conclusions from literature include that PRPDP parameter has a wider shift and shape at higher frequencies and that the shape is generally independent of frequency change; which are in agreement with some of the above disagreements. The above analysis indicates that there is more work to be on the PD cavity parameters in relation to the variable frequency component.

The other two parameters studied in literature as shown in the fourth column include the pulse repetition rate (PRR) and the PD magnitude (some with the mean, maximal and minimal magnitude in depth). When referring to the 'Key Findings' in the table it is noted that there is a somewhat balanced mixture of agreements and inconsistencies whereby various researchers agree that increasing supply frequency increases PRR. The others however, disagree to this and concluded that increasing supply frequency decreases PRR. This further shows that more work has to be done on the frequency dependence of PD cavity parameters.

III. Critical Analysis and Discussion

Although there has been agreements and inconsistencies in terms of the key results and findings of the PD activity due to frequency dependence, the factors that are related to how frequency affects PD activity have been the same. The major influence has been found to be the statistical time lag followed by the conductivity of the bulk insulation and surface conductivity of the cavity walls [22], [23].

Important to note is that the frequency ranges that were used by various researchers are not the same. Some used frequency range between 0 to 50 Hz, others between 0 to 300 Hz and 0 to 100 Hz, whereas some used only two frequency values (e.g 0.2 Hz and 100 Hz). This widely varying spectrum of frequencies also led to why some of the key findings had inconsistencies.

For example, taking only two frequency points and them generalising the PD behaviour as a function of frequency is misleading. In addition, considering only the frequency range between 0 to 50 Hz does not necessarily give reliable conclusions about the effect of changing frequency since some of the tests are done in frequencies greater than 50/60 Hz. Only taking frequency above 50 Hz also misses the behaviour of PDs at very low frequencies which is important since some equipment is tested and operate at these low frequencies. Therefore, having a more comprehensive range from very low frequencies up to frequencies greater than 50 Hz gives a better indication of the influence of frequency on PD activity. As a result, PD activity found at frequencies other than the power frequency can be interpreted based on the relationship shared.

Referring to Table I, it is noted that the experiments were carried out on defect types of different sizes and insulation material. This affects results due to the difference in permittivity of material which has an effect on PD activity. Moreover, the use of damped alternating current (DAC) power supply has the potential of leading to changes in the conclusions found. Different shapes (cylindrical, spherical etc) and sizes of voids are used in literature hence it might have contributed to some marginal inconsistencies. Thus, results will have some inconclusive findings.

In addition, to the above highlighted observations and interpretation of literature review (Table I), the last part of this section outlines the common reasons and explanations stated by most researchers.

TABLE I: Key findings on the effect of supply voltage frequency on PD parameters

Researchers	**Frequency Ranges**	**Defect Types**	**Parameters**	**Key Findings**
Bodega et al [18], [24]; Morshuis et al [19]	0.1 Hz; 50 Hz; DAC(260, 520 , 930)	2 - 3 mm diameter spherical cavities in cast polyester resin	- PD magnitude - PRPDP - PDIV	- PD maximal magnitude decrease with increase of frequency (above 200 Hz). - PRPDP shape generally independent of change of frequency. - minimal PD independent of frequency.
Forssen & Edin [12], [21], [25]	0.01 to 100 Hz	1.5 - 10 mm diameter disc-shaped cavities in polycarbonate	- PRR - PD magnitude (max, min, mean) - PD phase - PDIV	- maximal magnitude decrease with decrease of frequency. - minimal magnitude approximately constant with frequency. - PRR decrease with decrease of frequency. - PRPDP changed.
Forssen & Edin [26]	0.02 and 100 Hz	1.5 - 10 mm diameter disc-shaped cavities in polycarbonate	- PD magnitude - PRR	- PRR decrease with increase of frequency. - PRPDP changed. - maximal magnitude decreases with increase of frequency.
Illias et al [23]	0.01 to 100 Hz	1 mm diameter spherical cavity in epoxy resin	- PD charge (mean and maximum) - PRR	- PRR decrease with increase of frequency. - PD magnitude decrease with increase of frequency.
Illias et al [27]–[30]	0.5 to 50 Hz; 0.1 and 50 Hz	1 - 2.3 mm diameter spherical cavity in epoxy resin	- PRR - total apparent charge - PD magnitude	- PRR increase with increase of frequency. - maximal PD magnitude decrease with decrease of frequency. - Total apparent change decrease with decrease of frequency. - mean charge decrease with increase of frequency.
Miller & Black [31], [32]	0.1 to 50 Hz	4 mm diameter cylindrical cavity in epoxy resin	- PDIV - PD magnitude	- PDIV independent of change of varying frequency. - smaller PD magnitudes at lower frequencies than at higher.
Cavallini et al [10], [33]; Hauschild et al [34]	0.1 to 300 Hz	2 mm diameter spherical cavity in epoxy resin	- PRPDP - PDIV - PRR - maximal magnitude	- maximal magnitude decrease with increase in frequency. - PDIV slightly increase with increase in frequency. - PRPDP closer to zero crossing with increase of frequency.
Fynes-Clinton & Nyamupangedengu [35]	0.1 and 50 Hz	1 - 2 mm v-shaped cavity in XLPE	- PDIV - apparent magnitude - PRPDP	- PRPDP independent of frequency change. - apparent PD magnitude increase with increase in frequency. - PDIV increase with increase in frequency.
Negm et al [8]	50 to 1 000 Hz	1.5 mm diameter cavity	- PRR - PRPDP - PD charge	- PRR and PD charge decrease with increase of frequency. - PRPDP has a wider shift from zero crossing at higher frequencies.
Haghjoo et al [36]	50 and 100 Hz	1 mm diameter cavity	- PRPDP - PRR - apparent charge	- PRR decrease with increase of frequency. - Apparent charge increase as frequency increase. - Patterns wider from zero crossing at higher frequencies.

Table I continued from previous page

Researchers	Frequency Ranges	Defect Types	Parameters	Key Findings
Nguyen et al [37]	0.1 and 50 Hz	2 mm diameter cylindrical void	- PRR - PD magnitude (mean and max)	- PRR increase with increase in frequency. - mean PD magnitude increase with increase in frequency. - max PD magnitude increase with increase in frequency.
Nyamupangedengu & Jandrell [15], [20]	10 to 400 Hz	0.5 - 2 mm diameter in polyethylene discs	- Pulse shape - Pulse height	- Void defect pulse shape independent of change of frequency. - Negative pulse height decrease with increase of frequency.
Senoamadi et al [38]	0.02, 0.1 and 50 Hz	5 mm diameter cylindrical cavity in polyethylene	- PRR - PD magnitude - PRPDP - PDIV	- PRR increase with increase in frequency. - No trend for PDIV with change of frequency. - PD magnitude decrease with decrease of frequency. - PRPDP are away from zero crossing at lower frequency.
Mosito et al [39]	0.02, 0.1 and 50 Hz	1 mm diameter disc shaped cavity in polyethylene	- PDEV & PDIV - PRPDP - apparent charge	- PDIV and PDEV increase with increase in frequency. - PRPDP shift from zero crossing as frequency increase. - apparent charge magnitude increase with frequency increase.
Zhou et al [40], [41]	5 to 50 Hz	Tip - plate electrode setup	- PDIV - PRR - PRPDP - PD magnitude (mean and max)	- PDIV slightly changes with change of frequency. - PRR and PD magnitude varies with change of frequency. - PRPDP distribution in positive half cycle increases with decrease of frequency.
Wang [17]	2 to 5 000 Hz	single PD model	- PRR - PD magnitude (total, min, max) - delay time	- PRR decrease significantly with increase of frequency. - min PD magnitude independent with frequency change. - max PD magnitude decrease with increase of frequency. - total PD magnitude decrease with increase of frequency. - delay time decreases as frequency is increased.
Radu et al [16]	1 kHz to 30 kHz	0.5 mm gap between dielectric (@ atm)	- Pulse height - PRR -Width & rise times	- Pulse height constant with change of frequency - PRR reduce with increase of frequency. - Width and rise times reduce with increase of frequency.
Edin Thesis [22]	0.1 to 100 Hz	cable (void) model (CBM1)	- PRR - total charge - mean charge	- total charge independent of frequency. - mean charge increase with increase of frequency. - +ve and -ve charges symmetrical on both polarities. - PD activity decrease with decreasing frequency. - mean phase of discharges increase with decreasing frequency. - PRR slightly decrease as frequency is increased.
Forssen Thesis [14]	0.01 and 100 Hz	4 mm diameter void	- PRR - PD magnitude (total, min, max)	- total charge increase with increase of frequency. - maximum PD magnitude increase with increase of frequency. - minimum PD magnitude independent of frequency change. - wider spread in PD magnitude at higher frequencies. - PRR increase with increase in frequency.

Among the rest of the researchers, Illias et al [23], [30] explained that the repetition rate decrease as the supply frequency is increased is due to the shielding and statistical time lag effect caused by increased cavity surface conductivity, also causing the PD magnitude to decrease. Negm et al [42] explained the influence of charge decrease with increase in frequency due to the accumulation of charges on cavity walls. He then goes further stating that the time constants related to the type of insulation material and cavity wall conductivity properties also have an effect on the frequency dependence of PD activity in a void.

IV. Recommendations

This critical review of the available knowledge in literature has shown that more work need to be done in understanding the PD phenomena, especially with regard to the frequency dependence of the mechanisms. Thus, it will help in explaining how and why PD activity change the way it does when applied voltage frequency is varied. Different ranges of frequencies have been used and experimented by various researchers. Hence, a specific range that covers all the ranges according to the IEC60270 standard PD experiment set-up of 0 - 400 Hz needs to be experimentally investigated. In addition, it is important to investigate how the PD activity will behave under DC conditions i.e, 0 Hz. Modeling must be done to validate explanation and interpretation of experimentally obtained results on PD activity particularly on how it is affected by the changes in the test voltage frequency.

V. Conclusion

A critical review of the influence of supply voltage frequency of cavity PD parameters has been presented. The parameters in literature that has been reviewed, among the rest, include PDIV, PRR, PRPDP, PD magnitude etc. There has been general agreements and controversies in terms of key findings among researchers. This has been as a result of different materials, cavity sizes, power supply types used when experiments were taken. Major reasons and explanations related to frequency dependence of PDs in cavities has been noted to be statistical time lags, surface and bulk conductivity, and surface charge decay times. Based on the review and key findings in literature, a more in-depth analysis for the theory of cavity PD mechanism in context of frequency dependence behaviour is required. This analyis will give better insight of why and how cavity PDs behave with change of variable supply frequency. Therefore, more work is required since there are no general agreements on some of PD behaviour. PD modeling can be used to gain more understanding of the PD phenomenon.

References

[1] S. A. Boggs, "Partial discharge. iii. cavity-induced pd in solid dielectrics," *IEEE Electrical Insulation Magazine*, vol. 6, no. 6, pp. 11–16, Nov 1990.

[2] W. J. K. Raymond, H. A. Illias, A. H. A. Bakar, and H. Mokhlis, "Partial discharge classifications: Review of recent progress," *Measurement*, vol. 68, pp. 164 – 181, 2015. [Online]. Available: http://www.sciencedirect.com/science/article/pii/S0263224115000901

[3] H. A. Illias, M. E. Othman, M. A. Tunio, A. H. A. Bakar, H. Mokhlis, G. Chen, P. L. Lewin, and A. M. Ariffin, "Measurement and simulation of partial discharge activity within a void cavity in a polymeric power cable model," in *2013 IEEE International Conference on Solid Dielectrics (ICSD)*, June 2013, pp. 105–108.

[4] G. C. Stone, "Partial discharge diagnostics and electrical equipment insulation condition assessment," *IEEE Transactions on Dielectrics and Electrical Insulation*, vol. 12, no. 5, pp. 891–904, Oct 2005.

[5] S. A. Boggs, "Partial discharge: overview and signal generation," *IEEE Electrical Insulation Magazine*, vol. 6, no. 4, pp. 33–39, July 1990.

[6] F. H. Kreuger, *Partial Discharge Detection in High-Voltage Equipment*, 1st ed. London: Butterworth & Co. (Publishers) Ltd, 1989, ch. 1, pp. 1–14.

[7] R. Plessow and W. Pfeiffer, "Influence of the frequency on the partial discharge inception voltage," in *Electrical Insulation and Dielectric Phenomena, 1994., IEEE 1994 Annual Report., Conference on*, Oct 1994, pp. 97–102.

[8] T. S. Negm, M. Refaey, and A. A. Hossam-Eldin, "Modeling and simulation of internal partial discharges in solid dielectrics under variable applied frequencies," in *2016 Eighteenth International Middle East Power Systems Conference (MEPCON)*, Dec 2016, pp. 639–644.

[9] P. Romano, "Influence on pd parameters due to voltage conducted disturbances," *IEEE Transactions on Dielectrics and Electrical Insulation*, vol. 11, no. 1, pp. 160–165, Feb 2004.

[10] A. Cavallini and G. C. Montanari, "Effect of supply voltage frequency on testing of insulation system," *IEEE Transactions on Dielectrics and Electrical Insulation*, vol. 13, no. 1, pp. 111–121, Feb 2006.

[11] J. Giddens, H. Edin, and U. Gafvert, "Measuring system for phase-resolved partial discharge detection at low frequencies," in *1999 Eleventh International Symposium on High Voltage Engineering*, vol. 5, 1999, pp. 228–231 vol.5.

[12] C. Forssen and H. Edin, "Partial discharges in a cavity at variable applied frequency part 1: measurements," *IEEE Transactions on Dielectrics and Electrical Insulation*, vol. 15, no. 6, pp. 1601–1609, December 2008.

[13] U. Gafvert, H. Edin, and C. Forssen, "Modelling of partial discharge spectra measured with variable applied frequency," in *Proceedings of the 7th International Conference on Properties and Applications of Dielectric Materials (Cat. No.03CH37417)*, vol. 3, June 2003, pp. 839–842 vol.3.

[14] C. Forssen, "Modelling of cavity partial discharges at variable applied frequency," Ph.D. dissertation, Kungl Tekniska Hogskolan (KTH), June 2008.

[15] C. Nyamupangedengu and I. R. Jandrell, "Partial discharge spectral response to variations in the supply voltage frequency," *IEEE Transactions on Dielectrics and Electrical Insulation*, vol. 19, no. 2, pp. 521–532, April 2012.

[16] I. Radu, R. Bartnikas, and M. R. Wertheimer, "Frequency and voltage dependence of glow and pseudoglow discharges in helium under atmospheric pressure," *IEEE Transactions on Plasma Science*, vol. 31, no. 6, pp. 1363–1378, Dec 2003.

[17] P. Wang, N. Yang, C. Zheng, and Y. Li, "Effect of repetitive impulsive and square wave voltage frequency on partial discharge features," in *2018 12th International Conference on the Properties and Applications of Dielectric Materials (ICPADM)*, May 2018, pp. 152–155.

[18] R. Bodega, A. Cavallini, P. H. F. Morshuis, and F. J. Wester, "The effect of voltage frequency on partial discharge activity," in *Annual Report Conference on Electrical Insulation and Dielectric Phenomena*, 2002, pp. 685–689.

[19] P. H. F. Morshuis, R. Bodega, M. Lazzaroni, and F. J. Wester, "Partial discharge detection using oscillating voltage at different frequencies," in *IMTC/2002. Proceedings of the 19th IEEE Instrumentation and Measurement Technology Conference (IEEE Cat. No.00CH37276)*, vol. 1, 2002, pp. 431–435 vol.1.

[20] C. Nyamupangedengu and I. R. Jandrell, "Influence of supply voltage frequency and magnitude on pd pulse parameters," *IEEE Transactions on Dielectrics and Electrical Insulation*, vol. 15, no. 6, pp. 1590–1600, December 2008.

[21] C. Forssen and H. Edin, "Partial discharges in a cavity at variable applied frequency part 2: measurements and modeling," *IEEE Transactions on Dielectrics and Electrical Insulation*, vol. 15, no. 6, pp. 1610–1616, December 2008.

[22] H. Edin, "Partial discharges studied with variable frequency of the applied voltage," Ph.D. dissertation, Kungl Tekniska Hogskolan (KTH), September 2001.

[23] H. A. Illias, G. Chen, and P. L. Lewin, "Modeling of partial discharges from a spherical cavity within a dielectric material under variable frequency electric fields," in *2008 Annual Report Conference on Electrical Insulation and Dielectric Phenomena*, Oct 2008, pp. 447–450.

[24] R. Bodega, P. H. F. Morshuis, M. Lazzaroni, and F. J. Wester, "Pd recurrence in cavities at different energizing methods," *IEEE Transactions on Instrumentation and Measurement*, vol. 53, no. 2, pp. 251–258, April 2004.

[25] C. Forssen and H. Edin, "Influence of cavity size and cavity location on partial discharge frequency dependence [polymer insulation]," in *The 17th Annual Meeting of the IEEE Lasers and Electro-Optics Society, 2004. LEOS 2004.*, Oct 2004, pp. 438–441.

[26] ——, "Modeling partial discharges in a cavity at different applied frequencies," in *2007 Annual Report - Conference on Electrical Insulation and Dielectric Phenomena*, Oct 2007, pp. 132–135.

[27] H. A. Illias, G. Chen, and P. L. Lewin, "Partial discharge modelling in a spherical cavity within a dielectric insulation material as a function of frequency," in *2009 IEEE Electrical Insulation Conference*, May 2009, pp. 55–59.

[28] ——, "Partial discharge measurements for spherical cavities within solid dielectric materials under different stress and cavity conditions," in *2009 IEEE Conference on Electrical Insulation and Dielectric Phenomena*, Oct 2009, pp. 388–391.

[29] ——, "Comparison of partial discharge measurement and simulation results for spherical cavities within solid dielectric materials as a function of frequency using finite element analysis method," in *2010 IEEE International Symposium on Electrical Insulation*, June 2010, pp. 1–5.

[30] H. Illias, G. Chen, and P. L. Lewin, "Partial discharge behavior within a spherical cavity in a solid dielectric material as a function of frequency and amplitude of the applied voltage," *IEEE Transactions on Dielectrics and Electrical Insulation*, vol. 18, no. 2, pp. 432–443, April 2011.

[31] R. Miller and I. A. Black, "Partial discharge measurements over the frequency range 0.1 hz to 50 hz," *IEEE Transactions on Electrical Insulation*, vol. EI-12, no. 3, pp. 224–233, June 1977.

[32] ——, "Partial discharge energy measurements on electrical machine insulation when energized at frequencies between 0.1 hz and power frequency," *IEEE Transactions on Electrical Insulation*, vol. EI-14, no. 3, pp. 127–135, June 1979.

[33] A. Cavallini, R. Ciani, M. Conti, P. F. H. Morshuis, and G. C. Montanari, "Modeling memory phenomena for partial discharge processes in insulation cavities," in *2003 Annual Report Conference on Electrical Insulation and Dielectric Phenomena*, Oct 2003, pp. 723–727.

[34] W. Hauschild, A. Cavallini, and G. C. Montanari, "Effect of supply voltage frequency on testing of insulation system," *IEEE Transactions on Dielectrics and Electrical Insulation*, vol. 13, no. 5, pp. 1189–1191, Oct 2006.

[35] D. Fynes-Clinton and C. Nyamupangedengu, "Partial discharge characterization of cross-linked polyethylene medium voltage power cable termination defects at very low frequency (0.1 hz) and power frequency test voltages," *IEEE Electrical Insulation Magazine*, vol. 32, no. 4, pp. 15–23, July 2016.

[36] F. Haghjoo, E. Khanahmadloo, and S. M. Shahrtash, "Comprehensive 3-capacitors model for partial discharge in power cables," *COMPEL: The International Journal for Computation and Mathematics in Electrical and Electronic Engineering*, vol. 31, pp. 346–368, Mar 2012.

[37] H. V. P. Nguyen, B. T. Phung, and S. Morsalin, "Modelling partial discharges in an insulation material at very low frequency," in *2017 International Conference on High Voltage Engineering and Power Systems (ICHVEPS)*, Oct 2017, pp. 451–454.

[38] J. Senoamadi, R. Mabodi, and C. Nyamupangedengu, "The effect of supply voltage frequency on cavity partial discharge mechanisms," in *2018 26th Southern African Universities Power Engineering Conference (SAUPEC)*, Jan 2018.

[39] K. Mosito, M. Dlamini, and C. Nyamupangedengu, "A comparative study of cavity partial discharge parameters at vlf and at 50 hz test voltages," in *2015 23rd Southern African Universities Power Engineering Conference (SAUPEC)*, Jan 2015, pp. 261–266.

[40] Y. Zhou, Z. Zhou, S. Guo, Z. Niu, M. Huang, and S. Li, "Comparison of air corona pd characteristics under low and power frequency voltage by impulse-current method," in *2017 IEEE Conference on Electrical Insulation and Dielectric Phenomenon (CEIDP)*, Oct 2017, pp. 339–342.

[41] Y. Zhou, Z. Zhou, L. Zhang, Y. Zhang, Y. Mo, and J. Sun, "Characterization and comprehension of corona partial discharge in air under power frequency to very low frequency voltage," *Plasma Science and Technology*, vol. 20, no. 5, pp. 1–9, 2018. [Online]. Available: http://stacks.iop.org/1009-0630/20/i=5/a=054016

[42] T. S. Negm, M. Refaey, and A. A. Hossam-Eldin, "Investigation of partial discharge frequency dependence in distribution system cables," *CIRED - Open Access Proceedings Journal*, vol. 2017, no. 1, pp. 268–272, 2017.

Appendix B

SAUPEC 2020 Conference Paper

This appendix contains a publication handed in to the South African Universities Power Engineering Conference (SAUPEC/RobMech/PRASA) in 2020.

Influence of Supply Voltage Frequency on Cavity Partial Discharge Parameters: Simulation Results

Tapiwa Venge
School of Electrical and Information Engineering
University of the Witwatersrand,
Johannesburg, South Africa
tapiwa.venge@students.wits.ac.za

Cuthbert Nyamupangedengu
School of Electrical and Information Engineering
University of the Witwatersrand,
Johannesburg, South Africa
cuthbert.nyamupangedengu@wits.ac.za

***Abstract*—This paper presents simulation results on the influence of supply voltage frequency on cavity partial discharges (PD) parameters. The capacitance equivalent model is implemented in MATLAB® Simulink® to achieve the results. Frequency dependent mechanisms responsible for this influence are the statistical time lag, surface and bulk conductivity, and surface charge decay and electron de-trapping. Only the first two of these mechanisms are implemented in the model to get their effect on partial discharge inception voltage (PDIV) as well as the phase-resolved partial discharge patterns. PDIV and PD magnitude increase as the supply voltage frequency is increased. Pulse repetition rate (PRR) has two trends whereby for frequencies between very low frequency to 50 Hz it increases whereas for frequencies above 50 Hz it decreases. More analysis is required to understand why these two trends behave the way they do. Modeling of the surface charge decay and electron de-trapping factor, and experimental results is recommended to validate and give more confidence and reliability to the simulation results.**

***Index Terms*—capacitance, cavity, discharges, modeling, PDIV, PRPDP, supply voltage frequency**

I. Introduction

Partial discharge (PD) activity is a complex process as it is influenced by many mechanisms and parameters. Many of these parameters are critical in influencing how partial discharges occur and behave under a wide range of conditions and stresses. More insight in understanding how each mechanism and parameter contributes to the phenomenon can be attained through modeling. Consequently, modeling can be used to confirm theories as well as validate experimental results. Therefore, modeling becomes a vital tool in facilitating a better understanding on the complexity of PD activity. Illias et al [1] echo the above and stated the main objectives of PD modeling as: (i) to increase the understanding of PD phenomena and behavior, (ii) to identify critical parameters and physical mechanisms influencing PD events, such as electron generation and surface charge distribution, and (iii) to derive relations of defect characteristics, insulation design parameters, and test conditions with PD activities.

In agreement with Illias at al [1], Niemeyer [2] had stated that PD modeling allows understanding and approximation of the objectives listed above. Niemeyer [2] presented a generalized PD model that can be applied to any arbitrary insulation defects. It is general because it approximates the relationships between defect size and location, insulation thickness and permittivity, and PD characteristics such as electron generation and field enhancement.

978-1-7281-4162-6/20/$31.00 ©2020 IEEE

A review done by the authors [3] on the influence of variable supply voltage frequency on cavity PDs showed that more work and modeling need to be done in understanding the PD phenomena. The work presented in this paper uses PD modeling to facilitate a better and insightful understanding on the behavior of partial discharge parameters, especially with regards to the applied voltage frequency.

The incorporation of solar energy into grid-ties has led to the addition of harmonics, which are a component of frequency, into the electrical system network [4]. Solar power stations are a source of harmonics and other frequencies due to the use of inverters which have an effect on dielectric stressing that still need to be understood [5]. Hence, the influence of supply frequency on PD has become a major concern as solar is increasingly being used as an alternative source of energy.

Section II details on the frequency dependent mechanisms (statistical time lag, surface and bulk conductivity, and surface charge decay and electron de-trapping) that are responsible for how PDs change with respect to the supply frequency. Section III presents a background and review of the capacitance model as well as the implemented equivalent circuit. Results and discussion are shown in Section IV. Lastly, recommendations and conclusion are presented in Section V and VI, respectively.

II. Frequency Dependent Mechanisms

This section presents a qualitative insight based on literature review on the factors that give rise to frequency dependence of partial discharges.

Cavity geometry and location, insulation material, characteristic times and charge decay processes are mainly responsible for effects that arise from the rate of change of the applied voltage [4], [6]–[8]. They are dependent on surface and bulk conductivity properties i.e cavity walls and insulation material properties [4]. The charge transport process and characteristic times are statistical time lag (τ_{stat}), void relaxation time (τ_{void}), dielectric time constant ($\tau_{material}$), decay time constant (τ_{decay}), and trap time constant (τ_{trap}). It is the relation between these constants and the period time of the applied voltage (T), and therefore the supply voltage frequency due

to the relationship between time and frequency, that result in the frequency dependence effect of partial discharge activity and its patterns [6], [9].

A. Statistical Time Lag (τ_{stat})

Statistical time lag is the time it takes for the seed electron to be available after the critical inception voltage or electric field has been satisfied. In other words, it is the time it takes for the two conditions necessary for a PD to occur to be both satisfied. If the applied voltage period (T) is short such that τ_{stat} is in the order of T, then its effect in contributing to frequency dependence is insignificant. The reverse is true. This condition means that there will be time delay for a partial discharge to occur after the critical electric field has been satisfied. As a result, PDs are shifted forward and occur at higher magnitudes due to the lack of seed electrons, a phenomena known as the statistical effect [10]. Hence, the statistical time lag can be further be divided into inception delay and phase lag which are responsible for discharge gap over-voltage and phase forward shift, respectively [8]. The influence of the statistical time lag becomes less significant at lower frequencies when the period time becomes longer, and more significant with increased applied voltage frequency as the period time becomes shorter. Therefore, that is how the statistical time lag influences PD frequency dependence.

B. Surface and Bulk Conductivity vis-à-vis (τ_{void} & $\tau_{material}$)

The characteristic constants that are dependent on the distribution of the electric field on cavity surface and bulk conductivity are the void relaxation time and the dielectric time constant. The void relaxation time (τ_{void}) and the dielectric time constant ($\tau_{material}$) are associated with the redistribution of charge on the cavity's surface walls and bulk insulation material, respectively [7]. These constants have a behavioral effect on each other that leads to how they contribute to the frequency dependence of PD activity. The first relationship is when the void relaxation time is shorter than the dielectric time constant ($\tau_{void} < \tau_{material}$). This condition is as a result of the inner surface walls of the void being more conducting due to repetitive PD activity and ageing. Therefore, the number of partial discharges per cycle will decrease with decreasing frequency due to the screening effect of void surface conductivity at low frequencies [6]. The second relationship when the void relaxation time takes longer or is greater than the dielectric time constant ($\tau_{void} > \tau_{material}$). This leads to an increased number of partial discharges per cycle at low frequencies due to the slow incremental rate of change of the applied voltage.

C. Surface Charge Decay (τ_{decay}) and Electron De-trapping (τ_{trap})

The last two characteristic constants contributing to the frequency dependence effect on PD activity are the decay time (τ_{decay}) and trap time (τ_{trap}) constants. They are a result of charge transport process in insulation material and correlate with the previously mentioned times and constants. It is important to note how these two come to be significant by briefly looking at what happens as the charge is transported on the surface and material insulation. When a PD occurs, the resultant charge, Q_{res}, moves in the direction of the electric field and is trapped at the opposite cavity walls as the insulation is non-conducting.

The charge trapped at the cavity walls establish a residual field that opposes the applied electric field [9]. The trapped charge at the void surface walls establishes an electric field in the cavity at zero crossings resulting in PDs occurring earlier in the circle. The earlier appearance of PDs in the cycle can result in the increase of number of PDs per voltage cycle.

After the PD activity from trapped charge has occurred and applied voltage field is increased (to enhance the field) in the cavity, the trapped charge decays due to recombination at surface conductivity and diffusion into shallow traps of the charge surface. This aids to the extinction of a discharge from resultant electric field. This decay reduces electron generation from surface emission as the diffusion of electrons into shallow and/or deep traps leads to a less likely availability of initiating electrons.

If the surface charge decays slower than the rate of change of applied voltage ($\tau_{decay} > T$), its frequency dependence contribution is insignificant since the applied voltage will rise faster than the decaying of the surface charge. However, if the surface charge decays faster or equal to the magnitude of the period time of the applied voltage ($\tau_{decay} \leq T$) then the total field in the cavity decreases. This condition is more significant at lower frequencies where the periodic time is longer therefore decreasing the number of discharges per voltage cycle.

In addition and in relation to the decay time constant, the diffused electrons in the shallow traps of the cavity surface are further transported into deeper traps of the bulk insulation. If the decaying of trapped charge on cavity surface into deeper traps is in the range of periodic time of the applied voltage ($\tau_{trap} \approx T$), it will reduce the electron generation especially from surface irradiation hence an increased statistical time lag. The effect statistical time lag has on frequency dependence of PD activity has been outlined in Section II-A.

III. Capacitance Model

A. Background and Review

Achillides [11] presented the history of the birth of an electrical representation of the capacitive model that was created in 1932 by Germant and Philippoff. In this model, the void is simply represented by a capacitor and a spark gap only hence the discharges were represented as the discharges that happened across this capacitor. Whitehead in 1952 improved the model by replacing the spark gap with an electrically controlled device so as to represent the discharges better [12]. Many adjustments and improvements have been done to this model in order to gain more reliable results on respective PD parameters and factors.

Paoletti and Golubev [13], [14] presented a modified model to the classical one. They divided the full model into two simplified models: insulation and void. The insulation model

is represented by a capacitor and resistor in parallel with each other [15]. The void model is represented also by a capacitor in parallel with a resistor. The resistor in the void model was as a result of the observation and analysis of progressive failure that shows that there is resistance in parallel with the capacitor.

Achillides [11], [16] critically analyzed both models and the criticism that the ABC model was getting from the dipole model and agreed that the spark gap of the three capacitance cannot represent the physics and magnitude in a void. However, on the contrary, he stated that the ABC model is capable of representing PDs based on the change of capacitances. The other argument that was raised against the classical ABC model was that the surface is not equipontential [17]. This argument is opposed as the non-equipotential of surface walls is just a geometrical constraint and does not affect the presence of the cavity in an insulation [11]. The geometric constraint can be addressed by arranging arrays of capacitors. Furthermore, it is concluded that the change in capacitance in the ABC model is the same as the induced charge concept. With the application and analysis of the electromagnetic theory and other factors it is concluded by various researchers that the three capacitance model is a valid and powerful tool in analyzing PD transients in insulation material of any equipment [11], [12], [16].

Haghjoo et al [12] presented a comprehensive three-capacitance model of the general ABC model for PDs in single voids in insulation of medium and high voltage cables. This model is stated to be complete, reliable and flexible as it provides insight in the influence of void location and size, applied voltage amplitude and frequency, pressure and temperature in the cavity, number of initiating electrons and statistical occurrence on PD activity. Moreover, switching operation with opening and closing modes is implemented to represent the inception and extinction of the discharges.

Pan et al [18] in the numerical modeling review of PDs in dielectric-bounded cavities summarises the various capacitance models used for PD simulation. He presented circuit structures, characteristics and explanations on each of the capacitance models. These included how the capacitance model is used in considering two or more cavities, the effect of space charges and insulation resistance, cavity and surface discharge, as well as the resistance of the discharge channel.

Lastly, from the above background and review of PD models stated in literature, especially in reference to the capacitance model, the choice on which structure model is the best to implement depends on the requirements and area of focus that a user wants to simulate [1].

B. Implemented Model

The implemented model focuses on two of the three frequency dependent mechanisms: statistical time lag, and surface and bulk conductivity. The equivalent circuit of the three-capacitance model (Fig. 1) is used in the creation of the model in MATLAB® Simulink®.

Fig. 2 presents the flow diagram of how the model is executed. Referring to Figure 1, C_a is the equivalent capacitor

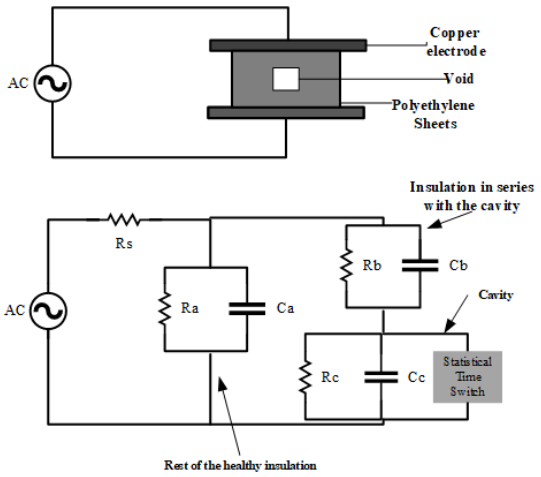


Fig. 1. Capacitance Model Equivalent Circuit

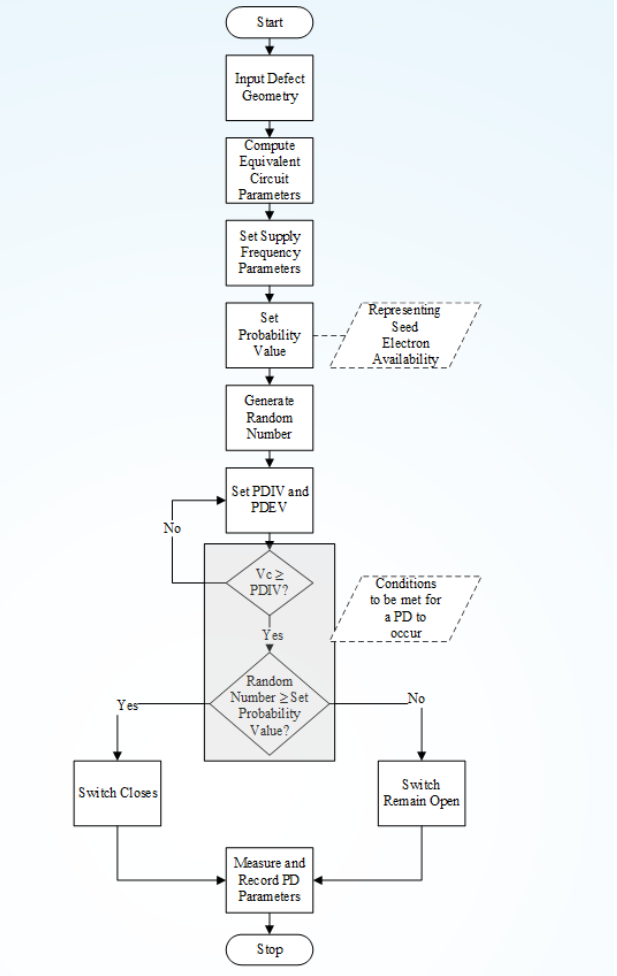


Fig. 2. Flow Diagram of the Implemented Model

of the whole insulation , C_b is the other equivalent capacitor in series above and below the void, and C_c is the equivalent capacitor representing the cavity; hence the 'a-b-c' which

is named after the capacitors arrangement in the electrical circuit. R_a represents the conductivity of healthy part of the insulation, R_b represents the series conductivity below and above the void, and R_c is the conductivity in the void. The resistors in parallel with the capacitors are the ones that are equivalent and represent the surface and bulk conductivity of the insulation. The PD signal detection implemented in the model is generated using an R-L-C impedance circuit connected in parallel [19].

IV. Results and Discussion

A. Partial Discharge Inception Voltage (PDIV)

With the PDIV set at 8 kV in the implemented model, the simulated results (Fig. 3 to 10) show that the inception voltage slightly increases as frequency is increased e.g PDIV at 10 Hz is $\approx$ 9 kV (Fig. 4) and at 75 Hz is $\approx$ 12 kV (Fig. 7). This is in agreement with the consensus conclusion by most researchers [10], [20]–[22]. This behavior can be explained by the frequency dependent factor of the statistical time lag. At low frequencies, this effect is negligible due to a larger period time of the applied voltage. However, at higher frequencies the statistical time lag effect is significant as the period time of the applied voltage is smaller hence satisfying the condition $\tau_{stat} > T$ as explained in Section II-A.

B. Phase-Resolved Partial Discharge Pattern (PRPDP)

A PRPDP consists of three components: pulse repetition rate (PRR), PD magnitude and the phase distribution of the PD pattern. The PRR can be interpreted as the number of PDs per cycle.

The simulated results (Fig. 3 to 10) have highlighted that the PD magnitude increase with frequency increase of the applied voltage. This is also concluded by other researchers [9], [22]–[24]. In addition, the preceding discharges are not closely packed as the frequency is increased hence a wider spaced phase-resolved pattern. The increase of PD magnitude and wider spaced pattern of preceding discharges due to the increase of the supply frequency is attributed to the statistical time lag effect of the condition ($\tau_{stat} \geq T$). It is more significant at increased and high supply frequencies as the period of the applied voltage is reduced.

However, if close attention and analysis is applied on the occurrence of the number of PDs per voltage cycle, two observations are noted when it comes to the influence variable

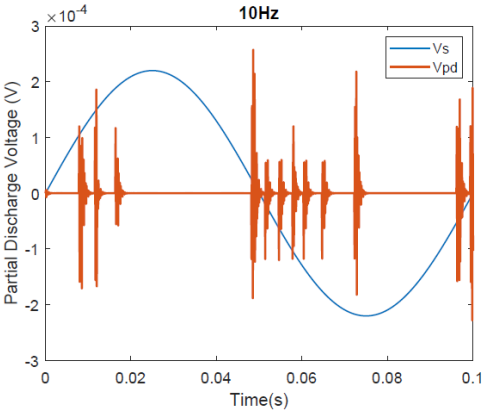


Fig. 4. 10 Hz Supply Frequency

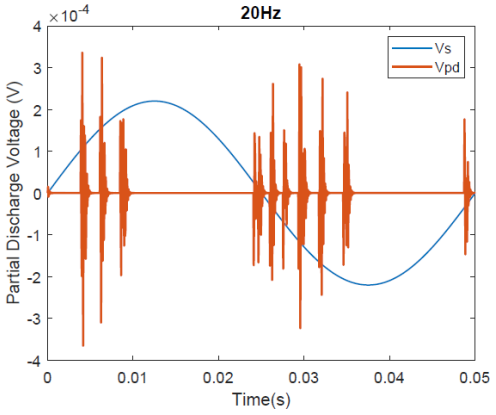


Fig. 5. 20 Hz Supply Frequency

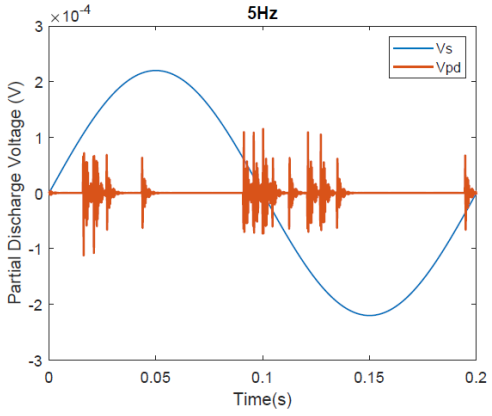


Fig. 3. 5 Hz Supply Frequency

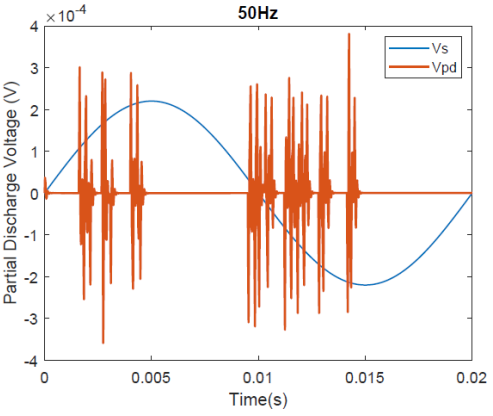


Fig. 6. 50 Hz Supply Frequency

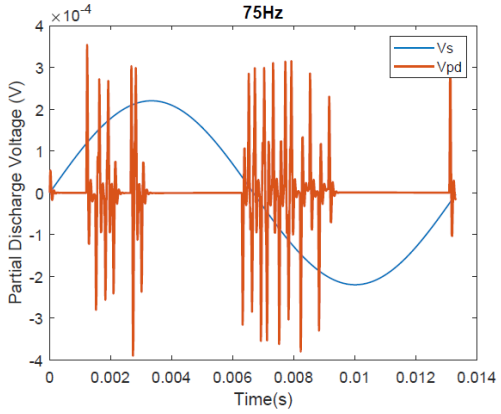


Fig. 7. 75 Hz Supply Frequency

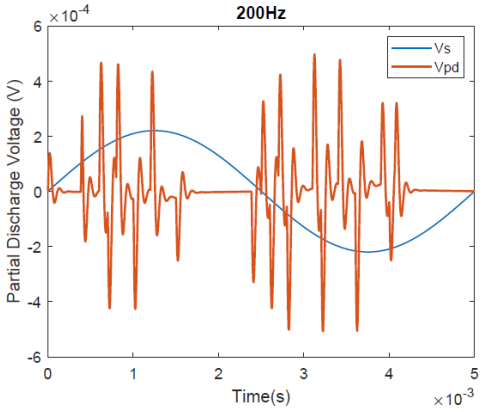


Fig. 9. 200 Hz Supply Frequency

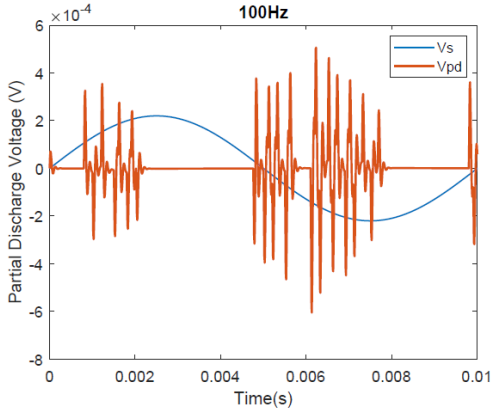


Fig. 8. 100 Hz Supply Frequency

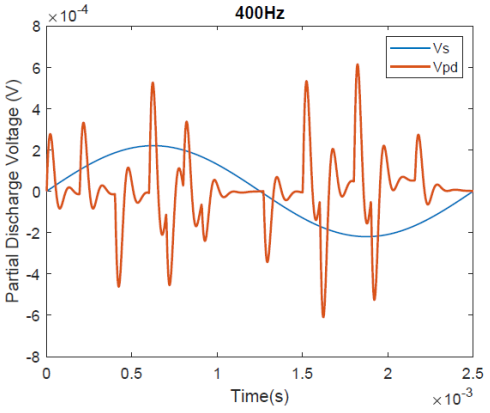


Fig. 10. 400 Hz Supply Frequency

frequency of the applied voltage has on the behavior of PRR. The two observations are frequency range dependent i.e between Very Low Frequency (VLF) to 50 Hz range, and the range above 50 Hz. Results have shown that PRR increases when frequency is increased from VLF to 50 Hz and decreases from 50 Hz and above. In addition to this observed trending, Cavallini and Montanari [20] also came up to the same conclusion about this behavior based on their experimental results on the PRR.

Frequency increase from very low frequencies to 50 Hz results in the increase in the number of PDs per voltage cycle. This behavior has been noted by a notable amount of researchers as most researchers have dealt with this frequency range [10], [24]–[28]. The increase in the PRR with supply frequency increase is more due to τ_{stat}, and the surface and bulk conductivity condition whereby ($\tau_{void} < \tau_{material}$). As outlined in Section II based on the mentioned condition, Nguyen [24] states that PRR increase with increasing supply frequency will be due to the screening effect of void surface conductivity at low supply voltage frequencies.

Frequency increase from 50 Hz going forward (till 400 Hz) result in the decrease of PRR. This behavior has been noted by some of the researchers who have dealt with frequency ranges that are above 50 Hz. Important to note is that not many researchers studied this range. The others studied till 100 Hz [7], [12], [29] and in some instances some have only taken two supply frequency points and/or values to come up with their conclusions, hence the work presented is observing PD activity at the skipped frequency ranges.

Negm et al [4] only took the frequency range that was greater than 50 Hz only (50 - 600 Hz). Despite the missing frequency range below 50 Hz, the authors agreed, on the range that they investigated, that increase in frequency decrease the rate at which pulse repetitions occurs, which is in agreement with the presented simulation results. The decrease in PRR as supply frequency is increased is due to the surface and bulk conductivity condition whereby ($\tau_{void} > \tau_{material}$). In addition, it is due to the shielding and statistical time lag effect caused by increased surface conductivity [7].

V. Recommendations

The other frequency dependent mechanism factor, surface charge decay and electron de-trapping, that is not incorporated in the implemented model need to be added so as to gain full

insight on the effect supply frequency has as a whole to PD activity. This factor, to the best of the authors' knowledge is responsible for residual charge and memory effects. Hence, it is of importance to include it in the modeling. More analysis on why the PRR increases and decreases as frequency is changed need to be carried out. In addition, experimental results need to be carried out so as to validate the simulation results thereby giving more confidence and reliability into the simulated results. This will result in a base of confidence on the explanations given on the results as well as clear analysis on the shortcomings that have been noted in literature.

VI. Conclusion

Simulation results on the influence of supply voltage frequency on cavity PD parameters have been presented. The frequency dependent factors responsible for influencing PD activity are the statistical time lag, and surface and bulk conductivity. The parameters observed are PDIV and PRPDP which constitutes of PD magnitude and PRR. It is shown that PDIV and PD magnitude increase with increase of supply frequency as well as PRR of frequencies between VLF and 50 Hz. However, PRR of frequencies above 50 Hz decreases with increase of supply frequency. Modeling of the surface charge decay and electron de-trapping factor, and experimental results is recommended to validate and give more confidence and reliability to the simulation results.

References

[1] H. A. Illias, G. Chen, and P. L. Lewin, "Comparison between three-capacitance, analytical-based and finite element analysis partial discharge models in condition monitoring," *IEEE Transactions on Dielectrics and Electrical Insulation*, vol. 24, no. 1, pp. 99–109, Feb 2017.

[2] L. Niemeyer, "A generalized approach to partial discharge modeling," *IEEE Transactions on Dielectrics and Electrical Insulation*, vol. 2, no. 4, pp. 510–528, Aug 1995.

[3] T. Venge and C. Nyamupangedengu, "Influence of variable frequency of the applied voltage on cavity partial discharge parameters: A critical review," in *2019 Southern African Universities Power Engineering Conference/Robotics and Mechatronics/Pattern Recognition Association of South Africa (SAUPEC/RobMech/PRASA)*, Jan 2019, pp. 582–587.

[4] T. S. Negm, M. Refaey, and A. A. Hossam-Eldin, "Modeling and simulation of internal partial discharges in solid dielectrics under variable applied frequencies," in *2016 Eighteenth International Middle East Power Systems Conference (MEPCON)*, Dec 2016, pp. 639–644.

[5] P. Romano, "Influence on pd parameters due to voltage conducted disturbances," *IEEE Transactions on Dielectrics and Electrical Insulation*, vol. 11, no. 1, pp. 160–165, Feb 2004.

[6] U. Gafvert, H. Edin, and C. Forssen, "Modelling of partial discharge spectra measured with variable applied frequency," in *Proceedings of the 7th International Conference on Properties and Applications of Dielectric Materials (Cat. No.03CH37417)*, vol. 3, June 2003, pp. 839–842 vol.3.

[7] H. A. Illias, G. Chen, and P. L. Lewin, "Modeling of partial discharges from a spherical cavity within a dielectric material under variable frequency electric fields," in *2008 Annual Report Conference on Electrical Insulation and Dielectric Phenomena*, Oct 2008, pp. 447–450.

[8] H. Edin, "Partial discharges studied with variable frequency of the applied voltage," Ph.D. dissertation, Kungl Tekniska Hogskolan (KTH), Stockholm (Sweden), September 2001.

[9] C. Forssen, "Modelling of cavity partial discharges at variable applied frequency," Ph.D. dissertation, Kungl Tekniska Hogskolan (KTH), Stockholm (Sweden), June 2008.

[10] C. Forssen and H. Edin, "Partial discharges in a cavity at variable applied frequency part 1: measurements," *IEEE Transactions on Dielectrics and Electrical Insulation*, vol. 15, no. 6, pp. 1601–1609, December 2008.

[11] Z. Achillides, G. E. Georghiou, and E. Kyriakides, "Partial discharges and associated transients: the induced charge concept versus capacitive modeling," *IEEE Transactions on Dielectrics and Electrical Insulation*, vol. 15, no. 6, pp. 1507–1516, December 2008.

[12] F. Haghjoo, E. Khanahmadloo, and S. M. Shahrtash, "Comprehensive 3-capacitors model for partial discharge in power cables," *COMPEL: The International Journal for Computation and Mathematics in Electrical and Electronic Engineering*, vol. 31, pp. 346–368, Mar 2012.

[13] G. Paoletti and A. Golubev, "Partial discharge theory and applications to electrical systems," in *Conference Record of 1999 Annual Pulp and Paper Industry Technical Conference (Cat. No.99CH36338)*, June 1999, pp. 124–138.

[14] G. J. Paoletti and A. Golubev, "Partial discharge theory and technologies related to medium-voltage electrical equipment," *IEEE Transactions on Industry Applications*, vol. 37, no. 1, pp. 90–103, Jan 2001.

[15] K. Yue, J. Chen, H. Ruan, and C. Qian, "Study on partial discharge model of solid insulator," in *2016 IEEE International Conference on High Voltage Engineering and Application (ICHVE)*, Sept 2016, pp. 1–4.

[16] Z. Achillides, M. G. Danikas, and E. Kyriakides, "Partial discharge modeling and induced charge concept: Comments and criticism of pedersen's model and associated measured transients," *IEEE Transactions on Dielectrics and Electrical Insulation*, vol. 24, no. 2, pp. 1118–1122, April 2017.

[17] I. W. McAllister, "Electric field theory and the fallacy of void capacitance," *IEEE Transactions on Electrical Insulation*, vol. 26, no. 3, pp. 458–459, Jun 1991.

[18] C. Pan, G. Chen, J. Tang, and K. Wu, "Numerical modeling of partial discharges in a solid dielectric-bounded cavity: A review," *IEEE Transactions on Dielectrics and Electrical Insulation*, vol. 26, no. 3, pp. 981–1000, June 2019.

[19] J. van Jaarsveldt, "Non-intrusive condition monitoring of power cables within the industrial sector," Master's thesis, North West University, Potchefstroom (South africa), May 2015.

[20] A. Cavallini and G. C. Montanari, "Effect of supply voltage frequency on testing of insulation system," *IEEE Transactions on Dielectrics and Electrical Insulation*, vol. 13, no. 1, pp. 111–121, Feb 2006.

[21] A. Cavallini, R. Ciani, M. Conti, P. F. H. Morshuis, and G. C. Montanari, "Modeling memory phenomena for partial discharge processes in insulation cavities," in *2003 Annual Report Conference on Electrical Insulation and Dielectric Phenomena*, Oct 2003, pp. 723–727.

[22] D. Fynes-Clinton and C. Nyamupangedengu, "Partial discharge characterization of cross-linked polyethylene medium voltage power cable termination defects at very low frequency (0.1 hz) and power frequency test voltages," *IEEE Electrical Insulation Magazine*, vol. 32, no. 4, pp. 15–23, July 2016.

[23] R. Miller and I. A. Black, "Partial discharge measurements over the frequency range 0.1 hz to 50 hz," *IEEE Transactions on Electrical Insulation*, vol. EI-12, no. 3, pp. 224–233, June 1977.

[24] H. V. P. Nguyen, B. T. Phung, and S. Morsalin, "Modelling partial discharges in an insulation material at very low frequency," in *2017 International Conference on High Voltage Engineering and Power Systems (ICHVEPS)*, Oct 2017, pp. 451–454.

[25] C. Forssen and H. Edin, "Partial discharges in a cavity at variable applied frequency part 2: measurements and modeling," *IEEE Transactions on Dielectrics and Electrical Insulation*, vol. 15, no. 6, pp. 1610–1616, December 2008.

[26] H. A. Illias, G. Chen, and P. L. Lewin, "Partial discharge modelling in a spherical cavity within a dielectric insulation material as a function of frequency," in *2009 IEEE Electrical Insulation Conference*, May 2009, pp. 55–59.

[27] ——, "Comparison of partial discharge measurement and simulation results for spherical cavities within solid dielectric materials as a function of frequency using finite element analysis method," in *2010 IEEE International Symposium on Electrical Insulation*, June 2010, pp. 1–5.

[28] H. Illias, G. Chen, and P. L. Lewin, "Partial discharge behavior within a spherical cavity in a solid dielectric material as a function of frequency and amplitude of the applied voltage," *IEEE Transactions on Dielectrics and Electrical Insulation*, vol. 18, no. 2, pp. 432–443, April 2011.

[29] C. Forssen and H. Edin, "Modeling partial discharges in a cavity at different applied frequencies," in *2007 Annual Report - Conference on Electrical Insulation and Dielectric Phenomena*, Oct 2007, pp. 132–135.

Appendix C

MDPI 2021 Energies Journal Article

This appendix contains an article published in the MDPI Energies journal as part of the Special Issue *Partial Discharge Monitoring and Analysis* edition.

energies

MDPI

Article

Analysis of Cavity PD Characteristics' Sensitivity to Changes in the Supply Voltage Frequency

Tapiwa Venge * and Cuthbert Nyamupangedengu *

School of Electrical and Information Engineering (EIE), Faculty of Engineering and the Built Environment (EBE), University of the Witwatersrand Johannesburg, Private Bag 3, Johannesburg 2050, South Africa
* Correspondence: tapiwa.venge@students.wits.ac.za (T.V.); cuthbert.nyamupangedengu@wits.ac.za (C.N.)

Abstract: The supply voltage frequency effect on partial discharge (PD) phenomena has continued to draw research interest. Although most high voltage equipment operates at power frequency (50/60 Hz), testing is often done at different frequencies for various reasons. Despite some agreements and inconsistencies for the research findings of PD activity's frequency dependence, there has been consensus on the recognition of the discharge mechanism parameters that influence how the supply voltage frequency affects PD activity. These parameters include statistical time lag, discharge area surface conductivity, and the residual charge decay. In this paper, a 3-capacitor model (ABC) is used to simulate how the changes in the discharge mechanism parameters influence PD characteristics as a function of the supply voltage frequency. The findings are that the phase-resolved partial discharge pattern (PRPDP) and PD repetition rate (PDRR) characteristics are more sensitive to variations in the probability of the seed electron availability at higher frequencies of the supply voltage. The opposite trend is observed for the cavity surface resistance. At lower resistance of cavity surface, the PRPDP and PDRR characteristics are more sensitive to changes in the supply voltage frequency than at higher resistances. The paper also confirms that incorporating equivalent resistances in the ABC model makes it more authentic than the model comprising of capacitors only.

Keywords: 3-capacitor model; ABC model; frequent dependent mechanisms; partial discharges; statistical time lag; supply voltage frequency; surface conductivity

check for updates

Citation: Venge, T.; Nyamupangedengu, C. Analysis of Cavity PD Characteristics' Sensitivity to Changes in the Supply Voltage Frequency. *Energies* **2021**, *14*, 478. https://doi.org/10.3390/en14020478

Received: 3 December 2020
Accepted: 13 January 2021
Published: 18 January 2021

Publisher's Note: MDPI stays neutral with regard to jurisdictional claims in published maps and institutional affiliations.

Copyright: © 2021 by the authors. Licensee MDPI, Basel, Switzerland. This article is an open access article distributed under the terms and conditions of the Creative Commons Attribution (CC BY) license (https://creativecommons.org/licenses/by/4.0/).

1. Introduction

Insulation is often regarded as the weakest part of high voltage and medium voltage equipment [1]. As an example, according to the IEEE Recommended Practice for the Design of Reliable Industrial and Commercial Power Systems (Gold Book) standard [2], about 60% of failure-initiating causes in power transformers occur in the insulation. In addition, it has been reported that 30% of motor damage relates to insulation failure [3]. The problems associated with electrical insulation failure arise from progressive deterioration of the insulation quality under operational stresses [4]. Electrical insulation systems are therefore designed to sustain failures caused by environmental conditions, electrical as well as mechanical and chemical stresses for reliable operation over the equipment lifespan [5,6].

Partial discharge (PD) activity in or on the insulation is one of the main indicators used to assess electrical insulation system quality. Hence, understanding PD phenomena allows corrective measures to be planned and implemented timely and cost effectively [7]. In the past few decades, there has been sustained progressive evolution in the researched and experienced knowledge on PD phenomena.

PD activity is influenced by many factors. These factors include humidity, temperature, altitude (air density), equipment type, and types of supply voltage. Significant research has been done on most of these factors such that there is a common understanding on how each influences PD activity. However, with regard to the supply voltage frequency, there has not been consensus on the understanding of PD characteristics' response to changes in the supply voltage frequency over a wider frequency range.

Supply voltage frequency (SVF) versus PD mechanisms has therefore been a sustained ongoing area of PD research. The depletion of coal-based electrical energy and the emergence of grid-tied inverter-based renewable energy (solar and wind) has increased the presence of harmonics in electrical systems [8]. Harmonics and other non-power supply voltage frequencies have adverse effects on dielectric stress that still need to be fully understood [9]. Consequently, there has been sustained research on how harmonics affect PD activity [10]. On the other hand, there has been cumulative research on the influence of supply voltage frequency on partial discharges, and this is the focus of the present work.

One of the reasons why there is interest in PD behavior under different supply voltage frequencies is that there is a wide range of types of test voltages used in testing power equipment. Although most high voltage equipment operates at power frequency (50/60 Hz), the test voltage frequencies may be different. Very low frequency is preferred for testing highly capacitive equipment such as power cables. Very low frequency testing helps in reducing the power rating, cost, volume, and weight of the test equipment [11]. Inductive equipment such as power transformers are often tested at higher frequencies (150–400 Hz) [11,12] for reasons such as avoiding saturation in the magnetic core. Oscillating Wave Test Sets technology is also an alternative non-power frequency technique with a reduced test voltage source power rating [6,13–15]. Therefore, the question is: to what extent do PD mechanisms respond to changes in the fundamental frequency of the supply voltage?

There is no consensus among researchers, especially with regard to the effect of supply voltage frequencies on the PD mechanism. Various researchers have investigated different test voltage frequencies. Some have only investigated two frequency points such as 0.1 Hz and 100 Hz and some just 50 Hz and 100 Hz. Generalized conclusions are often drawn up which can be regarded as being too brave to deduce trends from the few and too far apart data points. Due to the gaps in frequency ranges and few researchers having dealt with frequencies that are above 50 Hz, the present paper deals with frequencies of the range from low frequencies (1 Hz) up to 200 Hz.

The study approach in the present work is that of simulations. The results are validated through comparisons with measurement results obtained from the literature on similar experimental conditions. In the next section, the relevant literature is critically reviewed. The review highlights the knowledge gaps and also provides the experimentally obtained data that is then used for validating the model developed in the present work. The literature review also establishes the basis for choosing the 3-capacitor model for use in simulating PD supply voltage frequency dependency.

2. Literature Review on the Relationship between SVF and PD Characteristics

2.1. The Supply Voltage Frequency (SVF)

Various studies have been done on the influence of SVF (of different ranges) on PD mechanisms and the various parameters that influence PD characteristics. The commonly investigated PD characteristics include PD magnitude, Phase-Resolved Partial Discharge Patterns (PRPDP), PD Repetition Rate (PDRR), and PD Inception Voltage (PDIV). Significant knowledge has accumulated from research on the understanding of the relationship between SVF and PD phenomena. However, in the knowledge body, there are some inconsistencies that still need research.

It can be argued that contributing to the inconsistencies in research findings in the literature is the fact that the ranges of the supply voltages frequencies investigated vary widely. It is therefore necessary to be more comprehensive by considering a wider frequency ranging from very low frequencies through 50 Hz onto higher frequencies. Table 1 summarizes the landscape of the commonly used research findings in the literature.

Table 1. Key findings in the literature on the effect of supply voltage frequency on cavity PD characteristics [16].

Researchers	Frequency Ranges	Defect Types	Parameters	Key Findings
Seri et al. [17]	DC to 60 Hz	disc-shaped cavity embedded in polymeric insulation	- PDRR - PD amplitude	- PDRR increases due to increase in SVF. - PD charge amplitude increases due to increase in SVF.
Forssen & Edin [18–20]	0.01 to 100 Hz	1.5–10 mm depth disc-shaped cavities in polycarbonate	- PDRR - PD magnitude (max, min, mean)	- maximum PD magnitude decreases, with decrease in SVF. - minimum PD magnitude invariant with changes in SVF. - PDRR decreases with decrease in SVF.
Forssen & Edin [21]	0.02 and 100 Hz	1.5–10 mm depth disc-shaped cavities in polycarbonate	- PD magnitude - PRR	- PDRR decreases with increase in SVF. - PRPDP changed. - maximum PD magnitude reduces due to increase in SVF.
Illias et al. [22]	0.01 to 100 Hz	1 mm depth spherical cavity in epoxy resin	- PD charge (mean and maximum) - PDRR	- PDRR decreases due to increase in SVF. - PD magnitude reduces due to increase in SVF.
Illias et al. [23–26]	0.5 to 50 Hz; 0.1 and 50 Hz	1–2.3 mm depth spherical cavity in epoxy resin	- PDRR - total apparent charge - PD magnitude	- PDRR increases due to increase in SVF. - maximum PD magnitude reduces due to decrease in SVF. - mean charge reduces with increased SVF.
Miller & Black [27,28]	0.1 to 50 Hz	4 mm diameter cylindrical cavity in epoxy resin	- PDIV - PD magnitude	- PDIV invariant with changes in SVF. - reduced PD magnitudes at lower SVF than at higher SVF.
Fynes-Clinton & Nyamupangedengu [29]	0.1 and 50 Hz	1–2 mm v-shaped cavity in XLPE	- PDIV - apparent magnitude - PRPDP	- PRPDP not affected by SVF. - increasing SVF causes bigger apparent PD magnitudes. - higher PDIV due to increased SVF.
Cavallini et al. [11,30]; Hauschild et al. [31]	0.1 to 300 Hz	2 mm diameter spherical cavity in epoxy resin	- PRPDP - PDIV - maximum magnitude	- maximum PD magnitude reduces due to increase in SVF. - slight increase in PDIV due to increase in SVF. - overall shape of PRPDP shifts towards zero-crossing due to increase of SVF.
Negm et al. [8]	50 to 1000 Hz	1.5 mm diameter cavity	- PDRR - PRPDP - PD charge	- PDRR and PD magnitude decreases due to increase in SVF. - PRPDP overall shape has a wider spread at higher SVF.
Haghjoo et al. [32]	50 and 100 Hz	1 mm diameter cavity	- PRPDP - PDRR - apparent charge	- PDRR decreases due to increase in SVF. - PD magnitude increases due to increased SVF. - PRPDP overall shape has a wider spread at higher SVF.

The following highlights from the literature are evident:

- The most cases investigated are of the supply voltage frequency range of power frequency and below,
- The most investigated PD defect is air cavity and of thickness in the order of 1 mm,
- The investigated PD characteristics are PRPDP, PDRR, PDIV, and PD magnitude.

There are disagreements and inconsistencies on how PRPDP relates to the frequency of the supply voltage. Bodega et al. [13] and Morshuis et al. [15] concluded that the PRPDP is generally invariable with the change of supply voltage frequency. However, Cavallini and Montanari [11] reported that SVF increases the overall shape of the PRPDP and shifts towards the zero crossing of the voltage waveform. Forssen and Edin [20] also reported observing changes in PRPDP in response to variations in the SVF. However, they did not give further details on the correlations. On closer analysis of their article, their findings were opposite than those reported by Cavallini and Montanari [11]. Inconsistencies in the findings by various researchers on the relationship between SVF and PRPDP can be attributed to the statistical nature and deterministic memory effect in PD mechanisms.

PD repetition rate and PD amplitude are the other parameters that have been widely investigated for dependency on SVF variations. As with the PRPDP characteristic, there is generally a balance between agreement and inconsistencies with regard to findings by researchers on how PDRR and magnitude respond to changes in SVF.

Despite the agreements and shortcomings on the findings of PD activity's frequency dependency, there has been consensus on the identification of factors involved in influencing how supply voltage frequency affects PD activity. The factors are: statistical time lag, surface conductivity of the cavity, and the residual charge decay [22,33]. These factors influence PD mechanisms in complex, sometimes synergistic and in some cases in opposition. In that regard, PD models become useful in analyzing each PD characteristic's response to SVF as influenced by variations in each PD mechanism's parameter. The next section is a review of PD modeling techniques.

2.2. PD Models Overview

Generally, PD modeling can be classified into three categories, namely: the 3-capacitor (ABC), analytical models, and Finite Element Analysis or electric current and electrostatic model. Modeling has facilitated better understanding of PD mechanisms and complemented experimental measurement-based studies. In a recent contribution, Pan et al. [34] presented a useful state-of-the art review of PD models. In essence, each modeling technique has strengths and weaknesses depending on the context of its application.

The ABC PD model can be described as representing the PD specimen as an assemble of equivalent capacitors; the A, B, C capacitors. The PD event becomes the act of repetitive discharging and charging the capacitor that represents the cavity.

Danikas [35] critiqued the use of the classical ABC model as a tool for estimating PD magnitude. He identified the disadvantages of using the classical ABC model in that a cavity cannot be treated as pure capacitance as this can only be true if the cavity is bounded by metallic electrodes. In that regard, the Pedersen (induced-charge) model could be considered as a better option because it incorporates the geometry and positioning of the cavity in the insulation although it assumes a full volume discharge of the cavity. However, the Pedersen model has its own disadvantages such as the assumption of complete volume discharge which is open to question, and that the predictive power of the model starts deviating for larger cavities.

Achillides [36,37] critically compared and contrasted the commonly used PD models in response to criticisms of the ABC model. The author argued that the ABC model is capable of representing PDs based on the change of capacitance, and that the non-equipotential distribution on the surface walls is just a geometrical constraint that does not affect the main PD characteristics of interest [37]. There are possible mitigations on the equipotential and geometric constraints that include appropriate arrangement of equivalent capacitors.

Similarly, many authors have proven in various ways that the ABC PD model is generally a valid and powerful tool for analyzing PD phenomena [32,36,37].

Despite the advantages and disadvantages of each PD modeling technique, the PD models have generally been useful in confirming the common understanding of PD mechanisms theory. PD models can be used in investigating various aspects of PD such as dependency on frequency of the supply voltage. The ABC model is a strong candidate for such a study for the following reasons: (i) it requires less computing power than the other types of PD models, (ii) the various parameters in PD mechanisms can be discretely controlled, and (iii) the model can be modified to incorporate other aspects of PD mechanisms such as cavity surface conductivity and seed electron availability. In the next section, a more detailed literature review of the ABC PD model is presented.

2.3. The 3-Capacitor (ABC) PD Model Overview

Achillides [37] outlined the evolution account of the ABC PD model that was pioneered by Germant and Philippoff. The ABC model reduces the discharging cavity and surrounding dielectric medium to a set of equivalent capacitances. A PD event is equivalent to discharging the capacitor that represents the cavity. Whitehead in 1952 [32] incorporated a statistically controlled switch across the discharging capacitor in the model to more accurately represent the statistical nature of PD.

Boggs [38] used the ABC model to describe the occurrence of PD activity in solid dielectrics. Toader and Mariana [39] improved the model to meet their requirements of investigating and obtaining the apparent charge and PD energy. Christina et al. [40] improved the extended Whitehead model to study the influence of increasing applied voltage amplitude across different void sizes. These properties help on further understanding the efficacy of the ABC model in dealing with different parameters. Danikas et al. [41] compared the simulated and experimented results from polyethylene samples using artificial cylindrical voids. The PD model used for the simulated results is the ABC model. The simulated and experimental results compared well, thereby further proving the efficacy of the classical ABC model in PD activity analysis.

Paoletti and Golubev [3,42,43] presented a modified ABC model in contrast with the classical one. The insulation and cavity are each represented by a parallel combination of equivalent capacitors and resistors [44]. The cavity surface conductivity is represented by an equivalent resistor in parallel with the equivalent capacitor. The same approach is also used by Takahashi et al. [45]. They argued that the 3-capacitor model is too simple to be used in the modeling of PD phenomena. Hence, they investigated the behavior of the 3-capacitor model with dissipation since such effect cannot be ignored in real phenomena. The dissipation effect is modeled as resistance in parallel with the discharge gap. This modification is of interest in the present paper where the effect of the variations of cavity surface conductivity on PD characteristics' response to changes in SVF is investigated.

The ABC model is also used on investigating the interaction of PD in two closely coupled cavities by Agoris et al. [46]. The gas cavities and the dielectrics are modeled as lumped capacitances. The breakdown events are then modeled as voltage-controlled switches that are in parallel to the cavities. These modifications give ideas on how the ABC model can be modified to understand the interaction that multiple voids have on each other. Chia and Liew [47] implemented switching logic on the lumped capacitance model. The breakdown voltage in the respective multiple voids governs the switching logic of the lumped capacitance. Multiple capacitors can be strategically implemented to further identify and understand the precise nature of the PD activity within voids. The improvements are of importance to note if the present work is to be extended to cavity PD occurrence in closely coupled multiple voids.

Further work by Achillides et al. [48] improved the classical ABC model of a gas-cavity based on streamer concepts (such as inception and propagation) of the breakdown mechanism of gas by using a voltage-controlled triggering device in controlling an ideal switch. The switch is ON when the voltage in the cavity reaches the minimum level and

is OFF when the voltage across the cavity is below the calculated voltage level. The ON and OFF values are calculated depending on cavity properties which include geometry and location. The present paper adapted and extended the concept of voltage controlled switching.

In addition to the work by Achillides et al. [48], Gowda and Anandraj [5] modified the original basic ABC model by also implementing a circuit breaker switch that is controlled by a signal. Instead of using an ideal switch, they used a comparator switch that takes in the voltage across the cavity and compares it with the set breakdown voltage. If the voltage across the cavity exceeds the breakdown voltage, then the circuit breaker operates its ON and OFF states. In addition, a resistor is placed in parallel with the capacitor to represent the insulation resistance of the material. The concept of cavity voltage comparison with preset inception voltage, and the ON and OFF states are adapted in the present paper.

Chen et al. [49] present a capacitance equivalent circuit model for partial discharges occurring in transformer oil bubbles. The modified conditions include: (i) the manipulation of discharge time using controlled switches, (ii) representation of the role of space charge and residual voltage using controlled current switching and voltage sources, respectively, and (iii) a protective resistance, filter inductance, and detection impedance in series with each other added for better approximation of simulated results to the measured apparent PD magnitudes. The influence of residual voltage, role of space charge, and inception and extinction voltage can then be examined by adjusting the modified conditions and parameters. With residual charge effect being another frequency dependent variable of interest, these modifications could be adapted to a cavity in solid dielectric insulation to understand the role of residual charge.

Haghjoo et al. [32] successfully used the concept of the PD model but applied in the context of the air-filled cavities embedded in medium voltage power cable insulation. Variables such as the cavity air pressure and temperature and statistical time lag of the seed electrons were modeled analytically as mathematical expressions and incorporated into the model components such as those determining residual voltage in the cavity and the statistically controlled switch function. Van Jaarsveldt and Gouws [50] used the same concept and implemented in MATLAB® Simulink® to host the modified ABC PD model. The same approach is adopted in the present work but using parallel plate electrode geometry.

Negm et al. [8] analyzed both the dipole and the ABC model but ultimately employed the latter model. They developed a frequency-dependent PD model to investigate the influence of the statistical time lag and trap time constant of variable frequency of the applied voltage on charge distribution and PD magnitude. The model uses capacitors in parallel with resistors to represent permittivity and conductivity through, around, below and above a cavity. The work by Negm et al. [8] is of particular interest to the present work as it investigates frequency dependence of PD phenomena. However, their work mainly focused on the statistical time lag while, in the present work, the cavity surface conductivity will also be comparatively investigated.

Of interest is the numerical modeling review of PDs in dielectric-bounded cavities. Pan et al. [34] summarize the various ABC PD models in the literature. They present circuit structures, characteristics, and explanations for each of the capacitance models. The model is used to simulate situations of double cavities, residual space charge effects and insulation resistance, cavity and surface resistance, as well as the discharge channel resistance. The circuit structures presented give insights on the implementation and placement of components (resistors and capacitors) on the PD model used in the present paper.

Lastly, from the above background and review of PD modeling presented in the literature, the choice on the ABC PD model structure or modification best to implement depends on the requirements, specifications, and area of focus that the user wants to simulate [51]. Combining some of the aspects, modifications and circuit architectures reviewed in this section, the PD model in the present work is implemented in order to

study the supply voltage frequency-dependent PD mechanisms. The model drawn out from different variations and combinations as reviewed above is presented in the next section to represent the statistical time lag and the cavity surface conductivity.

3. Using the ABC PD Model to Study the Influence of Voltage Frequency on PD Characteristics

The ABC PD model equivalent electrical circuit and values used shown in Figure 1 and Table 2 below are implemented in MATLAB® Simulink®.

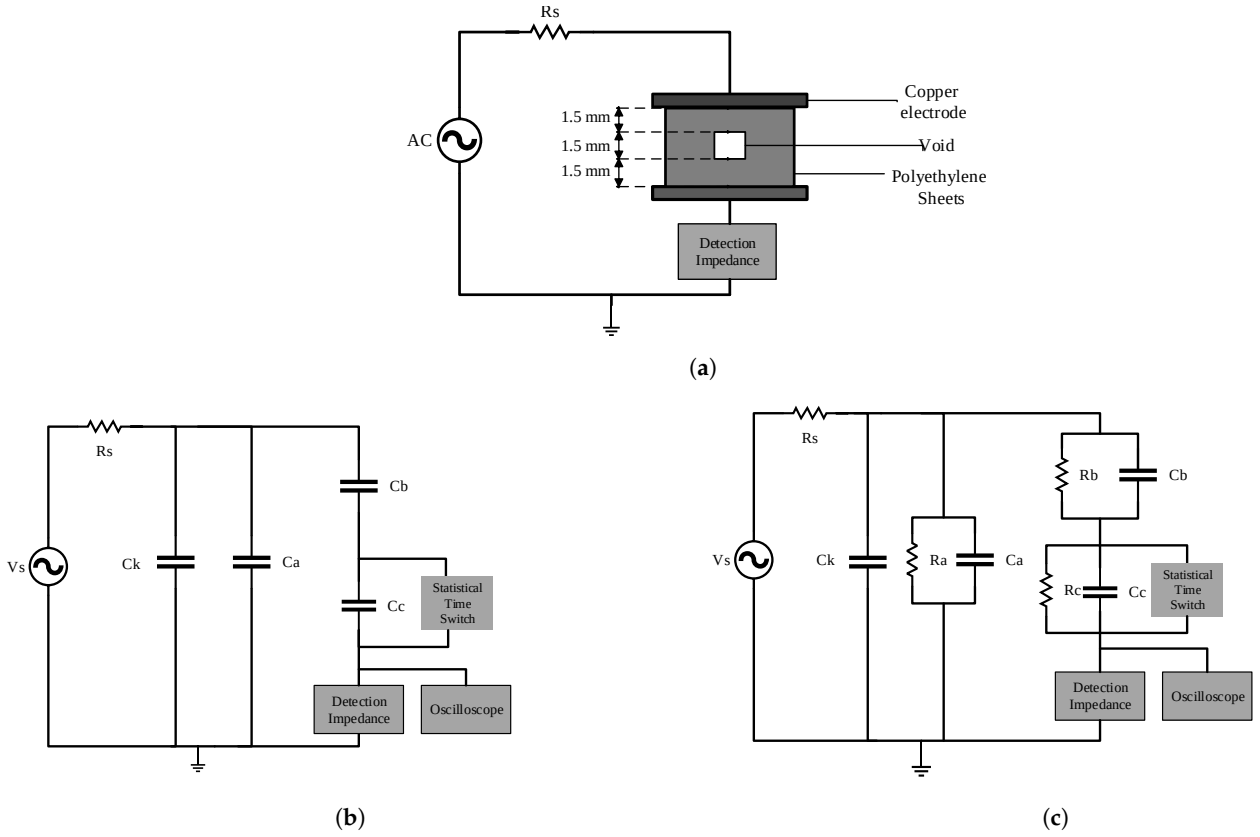


Figure 1. Equivalent circuit of the PD detection system with the ABC model implemented in MATLAB® Simulink®. (**a**) schematic of test specimen; (**b**) capacitors only model; (**c**) capacitors with resistors model.

Table 2. Parameter definition and values used for the ABC model simulated in MATLAB® Simulink®.

Parameter	Definition	Value
R_s	Supply source current limiting resistor	5.0×10^2 Ω
C_k	Coupling capacitor	1.0×10^{-9} F
R_a	Equivalent resistance of the healthy part of the dielectric	2.0×10^{15} Ω
C_a	Capacitance of the healthy part of the dielectric	1.5×10^{-10} F
R_b	Equivalent resistance of the dielectric in series below and above the cavity	3.0×10^{14} Ω
C_b	Capacitance of the dielectric in series below and above the cavity	1.0×10^{-12} F
R_c	Equivalent resistance of cavity surface	6.4×10^{12} Ω
C_c	Capacitance of the cavity	3.0×10^{-13} F
V_{so}	Cavity spark-over voltage	12 kV
V_{ext}	Cavity extinction voltage	10 kV

A partial discharge occurs when two conditions are met: (i) there is sufficient electrostatic potential energy (electric field strength) in the cavity that exceeds the cavity's breakdown strength and (ii) there is the availability of a starting 'free' electron so as to initiate a critical electron avalanche [52]. The inception electric field is dependent on the applied voltage amplitude amongst other factors. The voltage across the electrodes at

which the cavity breakdown strength is exceeded is the PD inception voltage (PDIV). The corresponding voltage across the cavity at which the cavity breaks down is the gap spark-over voltage (V_{so}). The voltage at which the discharge stops is PD extinction voltage (PDEV). The incorporation into a model of the above mentioned PD parameters (PD inception voltage, gap spark-over gap, starting electron availability, PD extinction voltage) is a key necessity of any PD modeling. Figure 2 presents the flowchart of the sequence and logical steps followed when executing a PD event in MATLAB® Simulink®.

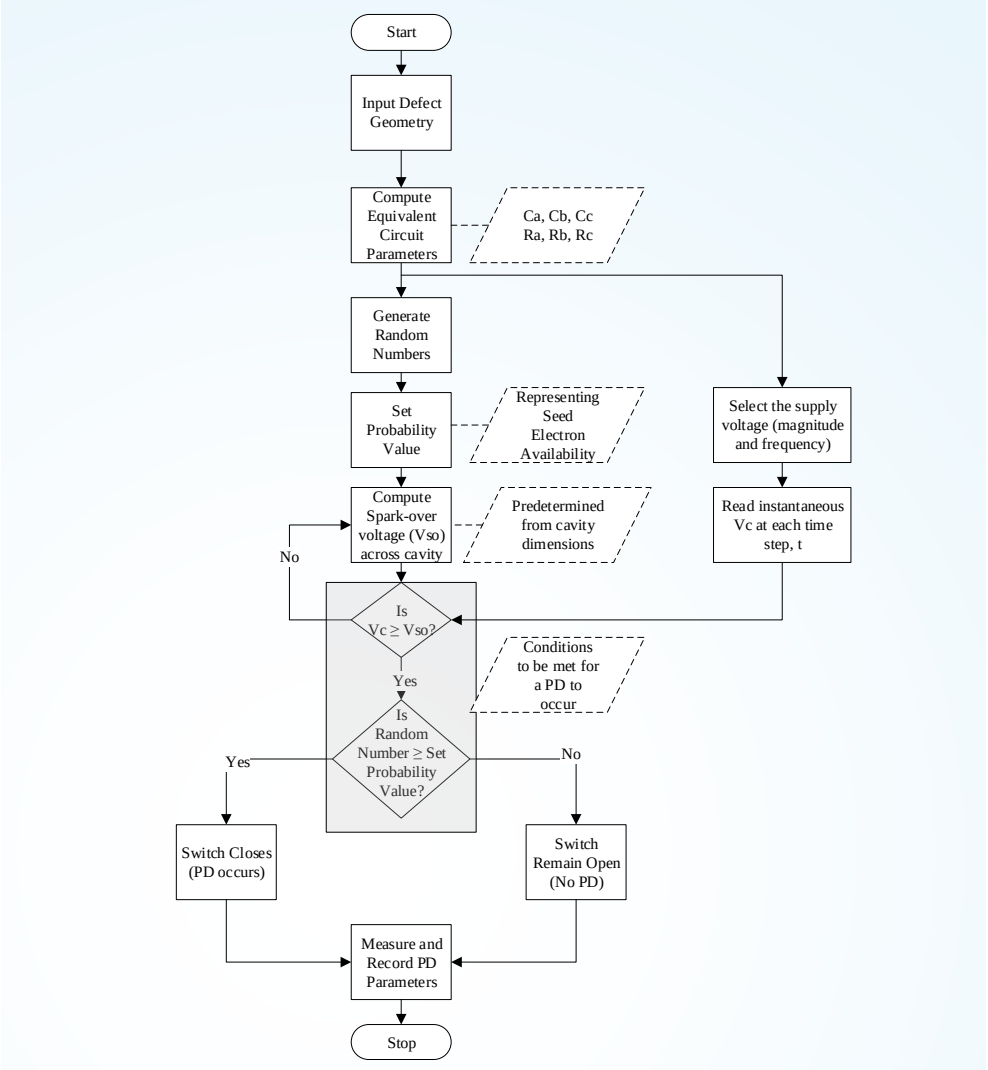


Figure 2. Flow diagram of the implemented PD model [53].

3.1. The Cavity Spark-Over Voltage

Callender and Lewin [54] highlighted the origins and limitations of the physical concepts used in PD phenomena modeling. The discussion was restricted to cavity PD occurrence in AC systems that is relevant in the present work. A critique of the applicability of PD modeling to the physical phenomena is provided. Of particular interest, in the context of the present work, is the PD inception electric field. The analytical expression representing the critical field intensity that initiates self-propagating electron avalanches in a PD event is given by Equation (1) [54]:

$$E_{cr} = Ap[1 + \frac{B}{(pL)^{\frac{1}{2}}}] \quad (1)$$

where E_{cr} (Vm^{-1}) is the initiating critical electric field, A and B are constants 24.2 $\mathrm{VPa}^{-1}\mathrm{m}^{-1}$ and 8.6 $\mathrm{Pa}^{\frac{1}{2}}\mathrm{m}^{\frac{1}{2}}$, respectively, p is the gas pressure in a cavity (Pa), and L is the cavity length (m) in the direction of the electric field.

The inception field equation was empirically determined from a system with bigger discharge gaps (in cm range) which differs from the PD system of smaller gaps (in mm range). The deviations that may arise on the gap spark-over voltage from extrapolation are not unexpected. Alternatively, the discharge gap spark-over voltage can be determined using the Paschen curve. The Paschen curve approach is adopted in this present work in setting up the gap spark-over voltage as it is specifically for discharge in smaller gaps. Assuming the standard conditions for temperature and pressure for a 1.5 mm cylindrical void, a breakdown voltage (V_b) of ≈8 kV is determined. In the simulations, however, a gap spark-over voltage of 12 kV (i.e., $Vso = 1.5V_b$) is used to cater for changes or deviations of cavity conditions from standard temperature and pressure ones. After setting the gap spark-over voltage, the other condition for PD to initiate is the availability of the seed electron that is presented in the next section.

Despite some disagreements elsewhere as highlighted in Section 2.1 in the literature, the factors causing PD activity to respond to the changes in the supply voltage frequency are generally agreed to be the statistical time lag, surface resistance of the cavity, and the residual charge decay [22,33]. In the present paper, the cavity PD parameters investigated are the statistical time lag, as well as the surface resistance of the cavity wall. The next sections explain how the two variables were implemented in the model.

3.2. Statistical Time Lag

The condition of the availability of a 'free/seed/initiatory' electron is implemented in the Simulink® model in two stages. Firstly, a probability value representing seed electron availability is set. Secondly, random numbers are generated to represent the stochastic behavior occurrence into the model. The set probability value in the first stage is then used as a condition to check against the random generated numbers in setting the seed electron availability. For instance, for randomly generated numbers between 0 and 1, setting probability values of 0.25, 0.5, and 1, respectively, represent a 25%, 50%, and 100% seed electron availability, respectively.

In order to investigate the effect of statistical time lag influence on supply voltage frequency dependence, all of the other parameters of the PD model are kept constant. The only adjusted parameter is the seed electron probability represented by the statistical time switch subsystem as shown in Figure 1. For a scarcity probability (25%) of the seed electron availability, the supply voltage frequency is swept from 1 Hz to 200 Hz, and the changes in the PD characteristics are noted. This simulates scarcity of the seed electron in situations of unvented and unaged cavity defects. The process is repeated for abundancy seed electron availability of 100%, signifying the ready presence of the 'starting' electron. For both cases of abundancy and scarcity of seed electron availability, the frequency of the supply voltage is varied while observing the PRPDP, PD pulse amplitude, and PDRR. Simulation results are compared and contrasted with reference to the physically measured results available in the literature.

3.3. Cavity Surface Resistance

The surface resistance of the cavity walls is another supply voltage frequency dependent mechanism factor investigated in this paper. The resistor, R_c, in parallel with the cavity capacitor as shown in Figure 1c represents the surface resistance of the cavity walls. It is assumed that the conductivity of the air in the cavity is negligible. In order to investigate how the PD process at each frequency of the supply voltage responds to variation of the cavity surface resistance (R_c), the statistical time lag and other PD model parameters are held constant. The cavity's surface resistance is then varied whilst observing the resultant PD characteristics at each supply frequency. The process is repeated as the supply voltage frequency is swept from 1 Hz to 200 Hz. The simulated results are then compared and

contrasted with the measured experimental results available in the literature. In addition, the simulation results of the capacitor only ABC model and the capacitors with resistors modified ABC model were compared as presented in the next section.

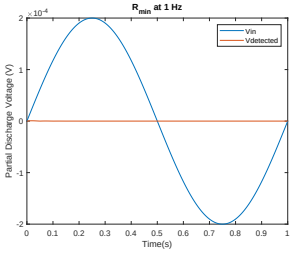
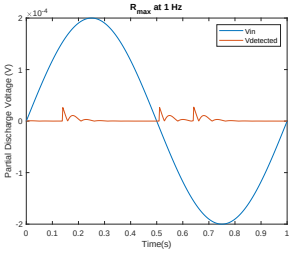
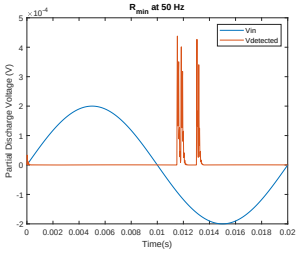
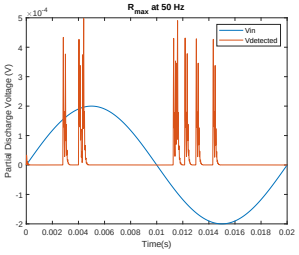
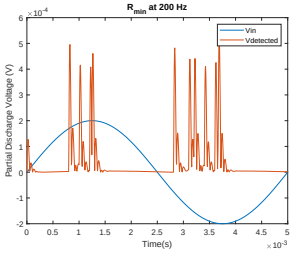
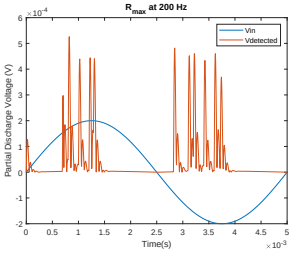
4. Results and Discussion

The outcomes of the simulations are presented in this section. The extent to which the statistical time lag, and cavity surface resistance influence SVF-dependent PD characteristics is presented.

4.1. The Extent to Which Cavity Surface Resistance Influences the PD Characteristics' Response to SVF Variations

In order to observe the effect of surface resistance on PD characteristics at different supply voltage frequencies, the cavity surface resistance, R_c, is varied from R_{min} to R_{max}. Typical values of R_{min} and R_{max} are obtained from the literature [8,55,56]. It is noted that the terminology of 'conductivity' is commonly used in the cited literature. However, for the purpose of the simulation in the present work, resistance is used. The seed electron probability is set to abundancy (100%) in all cases. The procedure is repeated for different frequencies. Results for SVF of 1 Hz, 50 Hz, and 200 Hz and PD characteristics are plotted and presented as shown in Table 3.

Table 3. Cavity surface resistance influence on PD characteristics at different frequencies. R_c values used: R_{min} is 6.0 $\times 10^9$ Ω and R_{max} is 6.0 $\times 10^{12}$ Ω as obtained from Hudon et al. [55] and Morshuis [56].

Frequency	Comments	R_{min}	R_{max}
1 Hz	No PD pulses are observed at the minimum selected surface resistance value, R_{min}. However, as the resistance R_c is varied to the maximum, R_{max} PD pulses become detectable.		
50 Hz	At R_{min}, there are no PD pulses in the positive half cycle but are observed in the negative half. As R_c is changed to R_{max}, there is an increase in PD pulses observed in both half cycles. The increase in surface resistance at 50 Hz has an effect on PD characteristics.		
200 Hz	There is a slight change on the observed PD patterns as the surface resistance, R_c is changed from R_{min} to R_{max}. Therefore, at 200 Hz (representing higher frequencies), surface resistance of the cavity has a minor influence.		

The general trend in Table 3 results is that the PRPDP and PDRR characteristics are more sensitive to variations in the cavity surface resistance at lower supply voltage frequencies than at higher supply voltage frequencies. A possible practical implication of this trend is that since cavity surface conductivity increases with PD defect ageing; a frequency sweep while monitoring the response of the PRPDP and PDRR can reveal whether the defect is aged or not. This behavior, however, is opposite that of the seed electron's statistical time lag.

The change of PDRR for different values of cavity surface resistance at different frequencies (1 Hz, 50 Hz, and 200 Hz) is shown in Figure 3. At 1 Hz (lower frequency), varying the cavity surface resistance has an effect on PDRR. The sensitivity of PDRR to changes of cavity surface resistance is highest at 50 Hz. The responsible mechanism would be a subject of future research.

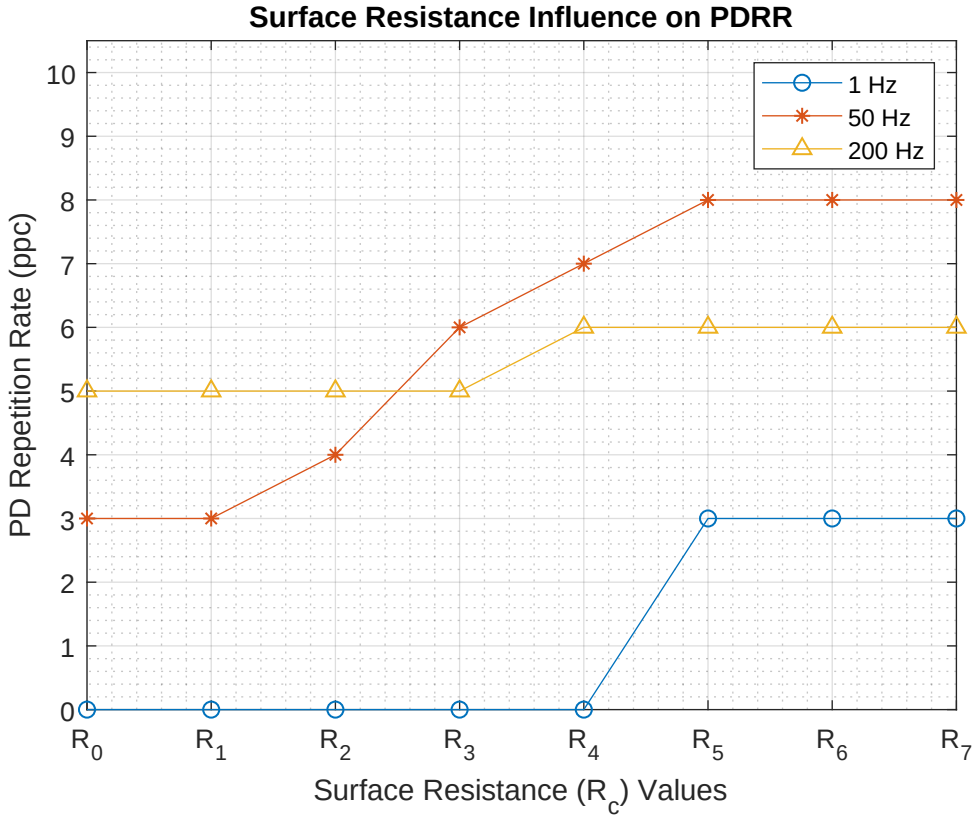
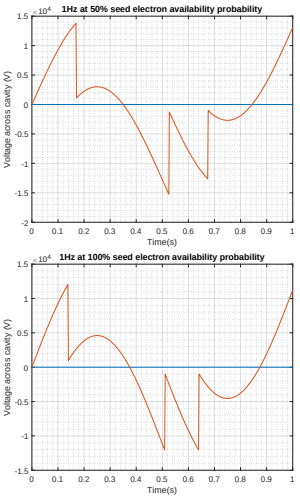
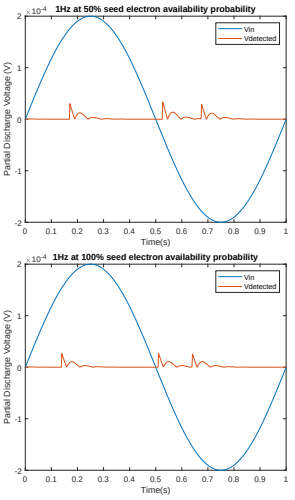
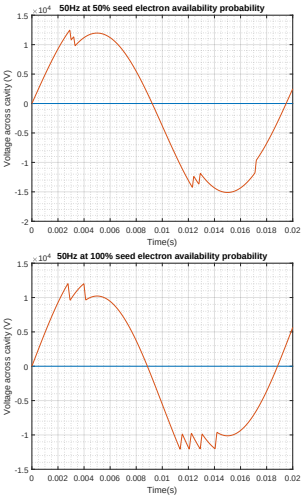
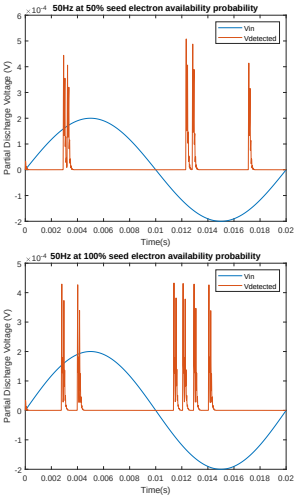
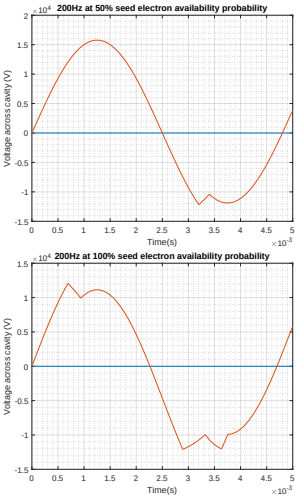
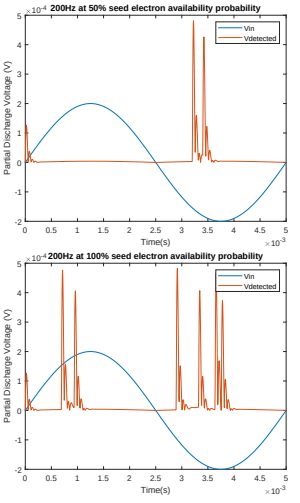


Figure 3. Cavity surface resistance influence on PDRR at different frequencies. Surface Resistance (R_c) values: $R_0 = 3.0 \times 10^9$ Ω, $R_1 = 6.0 \times 10^9$ Ω, $R_2 = 9.0 \times 10^9$ Ω, $R_3 = 3.0 \times 10^{10}$ Ω, $R_4 = 9.0 \times 10^{10}$ Ω, $R_5 = 6.0 \times 10^{12}$ Ω, $R_6 = 9.0 \times 10^{12}$ Ω, and $R_7 = 3.0 \times 10^{15}$ Ω [55,56].

4.2. The Extent to Which the Statistical Time Lag Influences the PD Characteristics' Response to SVF Variations

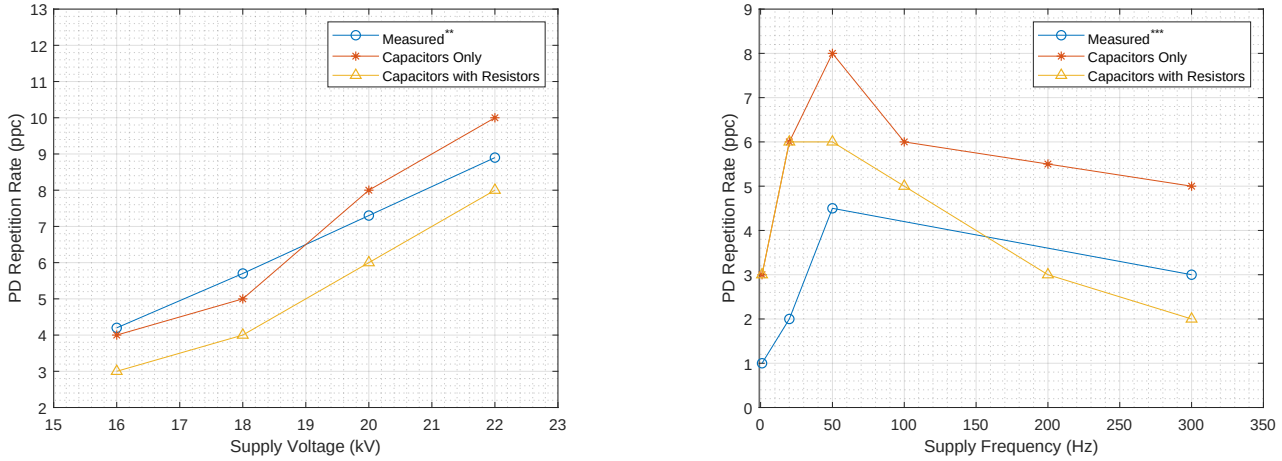
In order to observe the effect of the statistical time lag on PD characteristics as a function of supply voltage frequency, the seed electron probability is set to 25% and 100% representing scarcity and abundancy, respectively. The resultant PD phase-resolved patterns are plotted and presented for the frequencies: 1 Hz, 50 Hz, and 200 Hz as shown in Table 4. The trend is that, at lower frequencies, PD characteristics do not respond to variations in the statistical time lag. At higher frequencies, however, variations in the statistical time lag change the PRPDP and PDRR.

Table 4. Statistical time lag influence on PD characteristics at different frequencies.

Frequency	Comments	PD Pulse Superimposed on Sinusoidal Voltage Wave	PRPDP
1 Hz	It can be seen that the PDRR and PRPDP are not affected by changes in the statistical time lag at low frequency of 1 Hz.		
50 Hz	The PDRR slightly increases by 50% in the negative half cycle. The PRPDP has also changed; pulses get closer to each other and occur earlier in the cycle at abundancy probability compared to that at scarcity probability. PD pulse amplitude has increased as compared to that at 1 Hz. The increase is due to increased gap-overvoltage.		
200 Hz	The PRPDP and PDRR are affected by statistical time lag at 200 Hz. At scarcity seed electron availability, there are less pulses per cycle than at abundant probability. Notably, in the positive cycle, there is no PD occurring despite the voltage exceeding the spark over-voltage. At higher SVF and seed electron scarcity, the rate of change of the sinusoidal voltage can be high such that half a cycle is completed before the seed electron is available. However, at abundant seed electron, despite the fast rising supply voltage, PDs still occur.		

4.3. Comparison of Capacitor Only ABC and Modified ABC Model; Simulation Results versus Experimentally Measured Results Obtained from the Literature

This section is a comparison of the efficacy of the ABC model with and without resistance components. Simulations are done for the same situations using both models. The model that gives results closer to the practically obtained in the literature is regarded as being more accurate. The pulses per cycle as a function of the supply voltage amplitude and frequency are presented in Figure 4.



(**a**) (**b**)

Figure 4. Simulated results using capacitors only ABC model and capacitors with resistors model plotted together with measured data obtained from the literature (**a**) supply voltage amplitude (**: measured values as reported by Illias et al. [26]; NB: The last point at 22 kV has been extrapolated); (**b**) supply voltage frequency (***: measured values as reported by Cavallini et al. [11]).

The pulses per cycle increase as the applied voltage amplitude is increased as seen in Figure 4a. This is because increasing the applied voltage amplitude increases the electric field strength in the cavity. Increase in the electric field strength in the cavity increases the number of PD events per cycle of the sinusoidal voltage waveform.

Figure 4b shows the relationship between the PDRR and the supply voltage frequency. Simulated results of both models are compared to the measurements as obtained from the literature. In addition to the experimental measurements in literature, more points are added to the simulated results to fill in the gaps of frequencies between 50 Hz and 300 Hz. The trends are similar to those of the experimental measurements. PDRR increases as supply voltage frequency is increased from 1 Hz to 50 Hz. This trend has been reported by a notable number of researchers who have studied the frequency range from 0.01 Hz up to 50 Hz [19,20,23,25,26,57]. However, beyond 50 Hz, the PDRR decreases with an increase in SVF. This trend has been reported by some researchers who have studied frequency ranges that are above 50 Hz. However, researchers studying frequencies above 50 Hz have been relatively few. Some researchers have studied up to 100 Hz [21,22,32] and others have only taken two supply frequency points to draw out their conclusions. Extrapolations in Figure 4b therefore help in giving a more complete picture. Negm et al. [8] studied the frequencies in the range 50 Hz to 600 Hz. They noted that an increase in supply frequency decreases the number of pulses per cycle, which is in agreement with the simulation results in the present work.

The present work has investigated statistical time lag and surface conductivity with respect to how they affect the PD characteristics' dependence on variations of the SVF. The ABC model used that incorporated two of the frequency dependent mechanisms (statistical time lag and cavity surface conductivity) is more realistic to the practical occurrence of the PD phenomena. It is however notable that the residual charge deposited on the cavity surfaces after every PD event can also influence the PD characteristics' response to

variations in the supply voltage frequency [58]. Incorporation of the residual charge in the ABC model could therefore be an interesting future extension of the work presented in this paper.

5. Conclusions

In PD phenomena, it is necessary to understand how the various discharge parameters influence the manner in which PD characteristics respond to variations in the supply voltage frequency. In this paper, the PD mechanism parameters investigated are the probability of seed electron availability and cavity surface resistance. The analysis was done through simulations using the modified ABC PD model implemented in MATLAB® Simulink®. The findings are that the phase-resolved PD pattern and PD repetition rate characteristics are more sensitive to variations in the availability probability of the seed electron at higher frequencies of the supply voltage. At scarce seed electron availability, the pulse repetition rate is lower than that at abundant seed electron availability. The opposite trend is observed for the cavity surface resistance in the sense that at higher frequencies of the supply voltage, the variation of the cavity surface resistance from minimum to maximum possible values result in unnoticeable changes in both phase-resolved PD patterns and the PD repetition rate. At lower SVF, variations of the cavity surface resistance from minimum to maximum result in noticeable changes in PRPDP and PDRR. These findings confirm the complexity of PD mechanisms that partly explains why there have been inconsistencies in findings by various researchers on the relationship between PD characteristics and SVF variations. The paper also concludes that incorporating resistors in parallel with the capacitors in the ABC model makes it more realistic than the model made up of capacitors only.

Author Contributions: The authors have contributed to different parts of the paper preparation as follows: Conceptualization, T.V. and C.N.; methodology and software, T.V.; validation and analysis, T.V. and C.N.; writing—original draft preparation, T.V.; writing—review and editing, T.V. and C.N.; supervision, C.N. All authors have read and agreed to the published version of the manuscript.

Funding: This research received no external funding.

Conflicts of Interest: The authors declare no conflict of interest.

References

1. Montanari, G.C. Envisaging links between fundamental research in electrical insulation and electrical asset management. *IEEE Electr. Insul. Mag.* **2008**, *24*, 7–21. [CrossRef]
2. Heising, C. *IEEE Recommended Practice for the Design of Reliable Industrial and Commercial Power Systems (Gold Book)*; IEEE Std 493-1997 [IEEE Gold Book]; IEEE: Piscataway, PA, USA, 1998; pp. 1–464. [CrossRef]
3. Paolitti, G.; Golubev, A. Partial discharge theory and technologies related to traditional testing methods of large rotating apparatus. In Proceedings of the Conference Record of the 1999 IEEE Industry Applications Conference, Thirty-Forth IAS Annual Meeting (Cat. No.99CH36370), Phoenix, AZ, USA, 3–7 October 1999; Volume 2, pp. 967–981. [CrossRef]
4. McAllister, I.W. Electric field theory and the fallacy of void capacitance. *IEEE Trans. Electr. Insul.* **1991**, *26*, 458–459. [CrossRef]
5. Gowda, D. Modeling of partial discharge (PD) for solid insulation with void and building a hardware setup to measure partial discharge. In Proceedings of the 2016 Biennial International Conference on Power and Energy Systems: Towards Sustainable Energy (PESTSE), Bengaluru, India, 21–23 January 2016; pp. 1–7. [CrossRef]
6. Eigner, A.; Rethmeier, K. An overview on the current status of partial discharge measurements on AC high voltage cable accessories. *IEEE Electr. Insul. Mag.* **2016**, *32*, 48–55. [CrossRef]
7. Niemeyer, L. A generalized approach to partial discharge modeling. *IEEE Trans. Dielectr. Electr. Insul.* **1995**, *2*, 510–528. [CrossRef]
8. Negm, T.S.; Refaey, M.; Hossam-Eldin, A.A. Modeling and simulation of internal Partial Discharges in solid dielectrics under variable applied frequencies. In Proceedings of the 2016 Eighteenth International Middle East Power Systems Conference (MEPCON), Cairo, Egypt, 27–29 December 2016; pp. 639–644. [CrossRef]
9. Romano, P. Influence on PD parameters due to voltage conducted disturbances. *IEEE Trans. Dielectr. Electr. Insul.* **2004**, *11*, 160–165. [CrossRef]

10. Florkowski, M.; Florkowska, B.; Furgał, J.; Zydron, P. Impact of high voltage harmonics on interpretation of partial discharge patterns. *IEEE Trans. Dielectr. Electr. Insul.* **2013**, *20*, 2009–2016. [CrossRef]
11. Cavallini, A.; Montanari, G.C. Effect of supply voltage frequency on testing of insulation system. *IEEE Trans. Dielectr. Electr. Insul.* **2006**, *13*, 111–121. [CrossRef]
12. IEEE PES Transformers Committee. *IEEE Guide for Failure Investigation, Documentation, and Analysis for Power Transformers and Shunt Reactors*; IEEE Std C57.125-1991; IEEE: Piscataway, PA, USA, 1992; pp. 1–60.
13. Bodega, R.; Cavallini, A.; Morshuis, P.H.F.; Wester, F.J. The effect of voltage frequency on partial discharge activity. In Proceedings of the Annual Report Conference on Electrical Insulation and Dielectric Phenomena, Quintana Roo, Mexico, 20–24 October 2002; pp. 685–689. [CrossRef]
14. Bodega, R.; Morshuis, P.H.F.; Lazzaroni, M.; Wester, F.J. PD recurrence in cavities at different energizing methods. *IEEE Trans. Instrum. Meas.* **2004**, *53*, 251–258. [CrossRef]
15. Morshuis, P.H.F.; Bodega, R.; Lazzaroni, M.; Wester, F.J. Partial discharge detection using oscillating voltage at different frequencies. In Proceedings of the IMTC/2002, 19th IEEE Instrumentation and Measurement Technology Conference (IEEE Cat. No.00CH37276), Anchorage, AK, USA, 21–23 May 2002; Volume 1, pp. 431–435. [CrossRef]
16. Venge, T.; Nyamupangedengu, C. Influence of Variable Frequency of the Applied Voltage on Cavity Partial Discharge Parameters: A Critical Review. In Proceedings of the 2019 Southern African Universities Power Engineering Conference/Robotics and Mechatronics/Pattern Recognition Association of South Africa (SAUPEC/RobMech/PRASA), Bloemfontein, South Africa, 29–31 January 2019; pp. 582–587. [CrossRef]
17. Seri, P.; Naderiallaf, H.; Montanari, G.C. Modelling of supply voltage frequency effect on partial discharge repetition rate and charge amplitude from AC to DC at room temperature. *IEEE Trans. Dielectr. Electr. Insul.* **2020**, *27*, 764–772. [CrossRef]
18. Forssen, C.; Edin, H. Influence of cavity size and cavity location on partial discharge frequency dependence [polymer insulation]. In Proceedings of the 17th Annual Meeting of the IEEE Lasers and Electro-Optics Society, 2004, LEOS 2004, Rio Grande, PR, USA, 11 November 2004; pp. 438–441. [CrossRef]
19. Forssen, C.; Edin, H. Partial discharges in a cavity at variable applied frequency part 1: Measurements. *IEEE Trans. Dielectr. Electr. Insul.* **2008**, *15*, 1601–1609. [CrossRef]
20. Forssen, C.; Edin, H. Partial discharges in a cavity at variable applied frequency part 2: Measurements and modeling. *IEEE Trans. Dielectr. Electr. Insul.* **2008**, *15*, 1610–1616. [CrossRef]
21. Forssen, C.; Edin, H. Modeling partial discharges in a cavity at different applied frequencies. In Proceedings of the 2007 Annual Report—Conference on Electrical Insulation and Dielectric Phenomena, Vancouver, BC, Canada, 14–17 October 2007; pp. 132–135. [CrossRef]
22. Illias, H.A.; Chen, G.; Lewin, P.L. Modeling of Partial Discharges from a Spherical Cavity within a Dielectric Material under Variable Frequency Electric Fields. In Proceedings of the 2008 Annual Report Conference on Electrical Insulation and Dielectric Phenomena, Quebec, QC, Canada, 26–29 October 2008; IEEE: Piscataway, PA, USA, 2008; pp. 447–450. [CrossRef]
23. Illias, H.A.; Chen, G.; Lewin, P.L. Partial discharge modelling in a spherical cavity within a dielectric insulation material as a function of frequency. In Proceedings of the 2009 IEEE Electrical Insulation Conference, Montreal, QC, Canada, 31 May–3 June 2009; pp. 55–59. [CrossRef]
24. Illias, H.A.; Chen, G.; Lewin, P.L. Partial discharge measurements for spherical cavities within solid dielectric materials under different stress and cavity conditions. In Proceedings of the 2009 IEEE Conference on Electrical Insulation and Dielectric Phenomena, Virginia Beach, VA, USA, 18–21 October 2009; pp. 388–391. [CrossRef]
25. Illias, H.A.; Chen, G.; Lewin, P.L. Comparison of partial discharge measurement and simulation results for spherical cavities within solid dielectric materials as a function of frequency using Finite Element Analysis method. In Proceedings of the 2010 IEEE International Symposium on Electrical Insulation, San Diego, CA, USA, 6–9 June 2010; pp. 1–5. [CrossRef]
26. Illias, H.; Chen, G.; Lewin, P.L. Partial discharge behavior within a spherical cavity in a solid dielectric material as a function of frequency and amplitude of the applied voltage. *IEEE Trans. Dielectr. Electr. Insul.* **2011**, *18*, 432–443. [CrossRef]
27. Miller, R.; Black, I.A. Partial Discharge Measurements over the Frequency Range 0.1 Hz to 50 Hz. *IEEE Trans. Electr. Insul.* **1977**, *EI-12*, 224–233. [CrossRef]
28. Miller, R.; Black, I.A. Partial Discharge Energy Measurements on Electrical Machine Insulation When Energized at Frequencies between 0.1 Hz and Power Frequency. *IEEE Trans. Electr. Insul.* **1979**, *EI-14*, 127–135. [CrossRef]
29. Fynes-Clinton, D.; Nyamupangedengu, C. Partial discharge characterization of cross-linked polyethylene medium voltage power cable termination defects at very low frequency (0.1 Hz) and power frequency test voltages. *IEEE Electr. Insul. Mag.* **2016**, *32*, 15–23. [CrossRef]
30. Cavallini, A.; Ciani, R.; Conti, M.; Morshuis, P.F.H.; Montanari, G.C. Modeling memory phenomena for partial discharge processes in insulation cavities. In Proceedings of the 2003 Annual Report Conference on Electrical Insulation and Dielectric Phenomena, Albuquerque, NM, USA, 19–22 October 2003; pp. 723–727. [CrossRef]
31. Hauschild, W.; Cavallini, A.; Montanari, G.C. Effect of supply voltage frequency on testing of insulation system. *IEEE Trans. Dielectr. Electr. Insul.* **2006**, *13*, 1189–1191. [CrossRef]

32. Haghjoo, F.; Khanahmadloo, E.; Shahrtash, S.M. Comprehensive 3-capacitors model for partial discharge in power cables. *Compel. Int. J. Comput. Math. Electr. Electron. Eng.* **2012**, *31*, 346–368. [CrossRef]
33. Edin, H. Partial Discharges Studied with Variable Frequency of the Applied Voltage. Ph.D. Thesis, Kungl Tekniska Hogskolan (KTH), Stockholm, Sweden, 2001.
34. Pan, C.; Chen, G.; Tang, J.; Wu, K. Numerical modeling of partial discharges in a solid dielectric-bounded cavity: A review. *IEEE Trans. Dielectr. Electr. Insul.* **2019**, *26*, 981–1000. [CrossRef]
35. Danikas, M.G. The definitions used for partial discharge phenomena. *IEEE Trans. Electr. Insul.* **1993**, *28*, 1075–1081. [CrossRef]
36. Achillides, Z.; Danikas, M.G.; Kyriakides, E. Partial discharge modeling and induced charge concept: Comments and criticism of pedersen's model and associated measured transients. *IEEE Trans. Dielectr. Electr. Insul.* **2017**, *24*, 1118–1122. [CrossRef]
37. Achillides, Z.; Georghiou, G.E.; Kyriakides, E. Partial discharges and associated transients: The induced charge concept versus capacitive modeling. *IEEE Trans. Dielectr. Electr. Insul.* **2008**, *15*, 1507–1516. [CrossRef]
38. Boggs, S.A. Partial discharge. III. Cavity-induced PD in solid dielectrics. *IEEE Electr. Insul. Mag.* **1990**, *6*, 11–16. [CrossRef]
39. Toader, M.; Mariana, D. Electrical insulation study using partial discharge model. In Proceedings of the 2000 10th Mediterranean Electrotechnical Conference, Information Technology and Electrotechnology for the Mediterranean Countries, MeleCon 2000 (Cat. No.00CH37099), Lemesos, Cyprus, 29–31 May 2000; Volume 3, pp. 1060–1063. [CrossRef]
40. Christina, A.J.; Salam, M.A.; Rahman, Q.M.; Arifin, M.S.; Wen, F.; Ang, S.P.; Hasan, S. Partial discharge modeling with increasing applied voltages across different void sizes. In Proceedings of the 2017 4th International Conference on Advances in Electrical Engineering (ICAEE), Hong Kong, China, 27–29 October 2017; pp. 22–25. [CrossRef]
41. Kolev, N.P.; Danikas, M.G.; Gadjeva, E.D.; Gourov, N.R. Development of partial discharge model, simulation and measurement. In Proceedings of the 1999 Annual Report Conference on Electrical Insulation and Dielectric Phenomena (Cat. No.99CH36319), Austin, TX, USA, 17–20 October 1999; Volume 1, pp. 214–217. [CrossRef]
42. Paoletti, G.; Golubev, A. Partial discharge theory and applications to electrical systems. In Proceedings of the Conference Record of 1999 Annual Pulp and Paper Industry Technical Conference (Cat. No.99CH36338), Seattle, WA, USA, 21–25 June 1999; pp. 124–138. [CrossRef]
43. Paoletti, G.J.; Golubev, A. Partial discharge theory and technologies related to medium-voltage electrical equipment. *IEEE Trans. Ind. Appl.* **2001**, *37*, 90–103. [CrossRef]
44. Yue, K.; Chen, J.; Ruan, H.; Qian, C. Study on partial discharge model of solid insulator. In Proceedings of the 2016 IEEE International Conference on High Voltage Engineering and Application (ICHVE), Chengdu, China, 9–22 September 2016; pp. 1–4. [CrossRef]
45. Suzuki, H.; Aihara, K.; Takahashi, T.; Okamoto, T. Deterministic Partial Discharge Model with Dissipation. In Proceedings of the IEICE International Symposium on Nonlinear Theory and its Applications (NOLTA2004), Fukuoka, Japan, 29 November–3 December 2004; pp. 143–146. [CrossRef]
46. Agoris, D.P.; Hatziargyriou, N.D. Approach to partial discharge development in closely coupled cavities embedded in solid dielectrics by the lumped capacitance model. *IEE Proc.—Sci. Meas. Technol.* **1993**, *140*, 131–134. [CrossRef]
47. Chia, P.Y.; Liew, A.C. Novel approach to partial discharge signals modeling in dielectric insulation void using extension of lumped capacitance model. In Proceedings of the PowerCon 2000, 2000 International Conference on Power System Technology, Proceedings (Cat. No.00EX409), Perth, Australia, 4–7 December 2000; Volume 3, pp. 1207–1212. [CrossRef]
48. Achillides, Z.; Kyriakides, E.; Georghiou, G.E. Partial discharge modeling: An improved capacitive model and associated transients along medium voltage distribution cables. *IEEE Trans. Dielectr. Electr. Insul.* **2013**, *20*, 770–781. [CrossRef]
49. Chen, X.; Bi, M.; Jiang, T.; Wang, Y. An equivalent circuit model for partial discharge occuring in transformer oil bubbles. In Proceedings of the 2016 IEEE International Conference on High Voltage Engineering and Application (ICHVE), Chengdu, China, 9–22 September 2016; pp. 1–4. [CrossRef]
50. Van Jaarsveldt, H.; Gouws, R. Partial discharge simulations used for the design of a non-intrusive cable condition monitoring technique. *J. Energy Power Eng.* **2013**, *7*, 2193–2201.
51. Illias, H.A.; Chen, G.; Lewin, P.L. Comparison between three-capacitance, analytical-based and finite element analysis partial discharge models in condition monitoring. *IEEE Trans. Dielectr. Electr. Insul.* **2017**, *24*, 99–109. [CrossRef]
52. Stone, G.C. Partial discharge diagnostics and electrical equipment insulation condition assessment. *IEEE Trans. Dielectr. Electr. Insul.* **2005**, *12*, 891–904. [CrossRef]
53. Venge, T.; Nyamupangedengu, C. Influence of Supply Voltage Frequency on Cavity Partial Discharge Parameters: Simulation Results. In Proceedings of the 2020 International SAUPEC/RobMech/PRASA Conference, Cape Town, South Africa, 29–31 January 2020; pp. 1–6. [CrossRef]
54. Callender, G.; Lewin, P.L. Modeling partial discharge phenomena. *IEEE Electr. Insul. Mag.* **2020**, *36*, 29–36. [CrossRef]
55. Hudon, C.; Bartnikas, R.; Wertheimer, M.R. Spark-to-glow discharge transition due to increased surface conductivity on epoxy resin specimens. *IEEE Trans. Electr. Insul.* **1993**, *28*, 1–8. [CrossRef]
56. Morshuis, P.H.F. Degradation of solid dielectrics due to internal partial discharge: some thoughts on progress made and where to go now. *IEEE Trans. Dielectr. Electr. Insul.* **2005**, *12*, 905–913. [CrossRef]

57. Nguyen, H.V.P.; Phung, B.T.; Morsalin, S. Modelling partial discharges in an insulation material at very low frequency. In Proceedings of the 2017 International Conference on High Voltage Engineering and Power Systems (ICHVEPS), Bali, Indonesia, 2–5 October 2017; pp. 451–454. [CrossRef]
58. Patsch, R.; Berton, F. The role of space charges in PD-processes. In Proceedings of the Proceedings of 2001 International Symposium on Electrical Insulating Materials (ISEIM 2001), 2001 Asian Conference on Electrical Insulating Diagnosis (ACEID 2001), 33rd Symposium on Electrical and Ele, Himeji, Japan, 22 November 2001; pp. 21–24. [CrossRef]

Appendix D

AFRICON 2021 Conference Paper

This appendix contains a publication handed in to the AFRICON Tanzania Conference in 2021.

A Review of Test Voltages Used in Partial Discharge Measurements

Tapiwa Venge
School of Electrical and Information Engineering
University of the Witwatersrand, Johannesburg
Johannesburg, South Africa
tapiwa.venge@students.wits.ac.za

Cuthbert Nyamupangedengu
School of Electrical and Information Engineering
University of the Witwatersrand, Johannesburg
Johannesburg, South Africa
cuthbert.nyamupangedengu@wits.ac.za

***Abstract*—This paper presents a literature review on the variety of test voltages used in partial discharge (PD) measurements. The relationship between electrical equipment, PD measurement and test voltage has been addressed. Conventional (based on the IEC60270 standard) and unconventional method are the main methods of electrical PD detection and measurement. These methods can be done under on-line and/or off-line conditions with each method having its own advantages and disadvantages. Despite the condition or method of detection, the test voltages presented, among others, are impulse, direct-current (DC), harmonics, damped alternating current (DAC), power frequency voltage and very low frequency (VLF). For each diagnostic test, the most suitable test voltage of choice is selected based on the specifications and requirements of the device under test. However, a single measuring technique might not be sufficient to completely analyze and assess the health status of the insulation. Therefore, the use of multiple techniques may be recommended in order to create a more comprehensive picture and yield better results.**

***Index Terms*—DC, HV equipment, insulation, partial discharges, PD measurement, power frequency, test voltage, VLF**

I. Introduction

High voltage (HV) power equipment and the components are important parts of electrical power systems i.e generation, distribution, transmission systems. Such equipment includes transformers, generators and motors, switchgear, solid insulated cables and castings [1]–[3]. A major part of HV equipment is electrical insulation which is often regarded as the weakest link in the whole network [4]. Therefore, studying and understanding how to effectively assess electrical insulation (EI) becomes paramount. The presence of partial discharges (PD) is one of the main indicators used to assess electrical insulation system quality. Hence, understanding PD phenomena enables corrective measures to be planned and implemented prior to further insulation degradation which in turn leads to saving costs by averting the risk of equipment failure [5]. Figure 1 presents the context of this paper which is the relationship between electrical equipment, PD measurements and test voltages; with the methods used in electrical PD measurements presented in the next section.

II. PD Measurement Methods

PD detection and measurement in HV equipment is performed using conventional and/or unconventional methods. In addition, PD tests and monitoring on these methods can be done 'off-line' or 'on-line'. Off-line PD testing is performed when the equipment under test is taken out of operational conditions. On-line PD testing is performed while the equipment under test is in operation. The advantages, disadvantages and relationships between conventional, unconventional, online and offline methods of PD testing are explored in this section.

The conventional, also known as classical, method of PD detection and measurement is mainly based on the IEC60270 standard [6]. The standard is specifically targeted at measuring partial discharges for alternating current (AC) voltages of up to 400 Hz and/or direct current (DC) voltages. Important information on PD activity is obtained through interpretation of a wide range of PD parameters such as PD pulse, repetition rate, inception and extinction voltage as well as PD phase distributions. Conventional methods are widely used in research and development, design and maintenance tests in universities, testing centers, power utilities and in the manufacturing industry [7]. Under off-line PD testing conditions, the classical method's use of different test voltages is one of its advantages. PD tests can be done under elevated electrical stresses and over-voltage conditions for improved PD signal sensitivity.

Unconventional methods of PD measurement is also known as the high frequency (HF) or ultra-high frequency (UHF) techniques. The PDs are detected using ultra-wideband techniques as well as non-electrical methods. One significant advantage over the conventional counterpart is that it is more suitable for online PD testing. However, PDs can be diminished and absent at the instance of observation which may result in the insulation being falsely deemed healthy. The consequence of this is that equipment's failure may occur prematurely leading to unscheduled interruptions.

On-line and off-line conditions of PD testing can be used in conventional and/or unconventional methods. The advantages and disadvantages of on-line and off-line conditions of PD testing are summarised in Table I.

The implementation of online PD testing is difficult under classical methods. Hence, off-line PD tests are mainly associated with the conventional way of PD measurement and the on-line tests with unconventional methods. The improved capabilities in continuous data logging and monitoring of

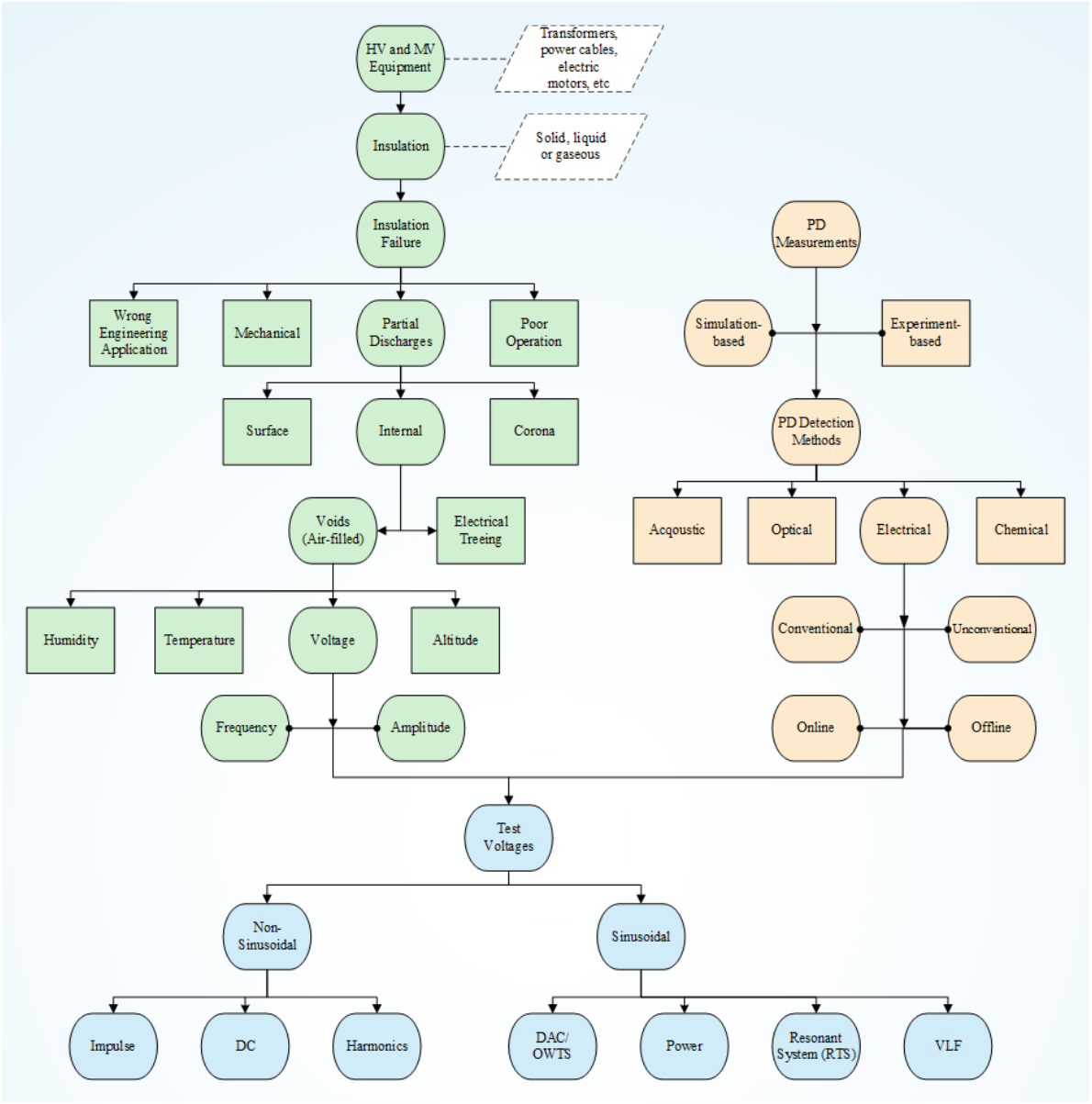


Fig. 1. Setting up the scene: Context of the present work

equipment has led to the growing interest in on-line condition of PD measurements. It should be noted that a single technique might not be sufficient to completely analyze and assess the condition of insulation. As such, the use of multiple techniques may be recommended in order to create a complete picture and yield better results.

III. Test Voltages

Test voltage or supply voltage is defined as the high voltage that is experienced on an object under test which causes partial discharges [8]. If the insulation media has the presence of impurities or air-filled cavities, it is the voltage that results in the occurrence of partial discharges. Therefore, any voltage present and responsible for PD activity in the insulation medium may be referred to as test voltage. Test voltage can be experienced intentionally and/or unintentionally depending on the operational or testing conditions of HV equipment.

Intentional test voltage experiences are those done in laboratory tests, design tests and factory acceptance tests. Under these conditions, a test voltage is intentionally applied across the insulation or object under test to check for the presence of partial discharges in the respective objects. Operational pure sinusoidal (power frequency: 50/60 Hz) test voltage may be considered as intentional test voltage. Unintentional test voltage experiences are those that are undesired. For instance, the voltages across the insulation that are experienced due to harmonics, lightning voltages, switching transients and other over-voltages. Intentional or not, these test voltages have an

TABLE I
ADVANTAGES AND DISADVANTAGES OF ON-LINE AND OFF-LINE PD TESTING

On-line PD Testing		**Off-line PD Testing**	
Advantages	***Disadvantages***	***Advantages***	***Disadvantages***
There is no downtime i.e equipment under test does not need to be switched off for it to be tested	Advanced earthing measures are required for safety on personnel	It is a proven and commonly used technology (uses the IEC60270 standard [6])	There is downtime i.e equipment under test has to be isolated from the system for it to be tested
Equipment under test is live or loaded when tested which may be useful in providing all information present during failure/PD activity	Data interpretation can prove to be difficult due to the vulnerability of this method to external interference/noise in the system	Measurement equipment or devices can be easily calibrated for better results and interpretation	Equipment under test is not live/ loaded during testing which may omit relevant information present during failure/PD activity
This method can be considered as economical due to the absence of downtime during PD testing	It is difficult to target specific equipment in the system (e.g transformer only) to be tested	Specific equipment can be easily targeted and selected for testing	This method can be costly due to downtime and outage costs when equipment is out of operation
Equipment is easily monitored through continuous data logging	Diminished PD magnitudes at instance of observation is illusive	Different customized test voltages (e.g DAC, VLF) can be used	Equipment to be tested has to be transported to testing facilities
Exact operational environmental conditions are easily monitored and are available for interpretation and analysis of results		This method has limited or no noise/external interference which isolates the PD signal for better interpretation/analysis of results	

impact on partial discharge activity hence it is important to understand their importance, relationship and effect on PD activity for better detection and classification of the phenomenon. The relationship between respective test voltages and PD activity is discussed in more detail next.

IV. NON-SINUSOIDAL TEST VOLTAGES

A. Harmonics

Harmonics are non-power frequency components riding on the operational power frequencies. The prevalence addition of grid-tied inverter-based renewable energy onto the national grids has enhanced the presence of harmonics. The increased use of modern power electronic gadgets also promotes 'noise' disturbances (which can be classified as harmonics) in communication and HV equipment [9]. The challenges associated with the presence of harmonics are common in all PD measurements and still need to be understood. Harmonics and other noise disturbance characteristics produce additional adverse effects on dielectric stress that are non-negligible [10]. Therefore, research on understanding harmonics occurrence and their control in electrical power systems as well as their effect on PD activity has been a sustained area of research. Florkowski [8] has reported on the influence of harmonics on PD activity as well as PD pattern interpretation. Experimental results concluded that disturbances caused by harmonics have a significant influence on PD occurrence, affecting parameters such as PD intensity and maximum charge. Understanding the influence that harmonics have on PD activity is therefore important in properly assessing PD signatures in avoiding misinterpretations and assessment of PD severity [11].

B. Impulse Voltages (Lightning and Switching)

Lightning strikes are one of the main contributors of high voltage impulses in electric power systems [12]. Another contributor is switching transient over-voltages which are a result of the increased use of power electronics gadgets that make use of pulse width modulation (PWM) characteristics. In addition, higher switching-on start-up currents of devices like induction motors can also present impulse-like signatures to equipment insulation. Impulse and switching over-voltages can have adverse consequences on PD activity, and consequently electrical insulation health. Therefore, the study of impulse voltage's effect on partial discharges is an area of research interest. Sun et al [13] experimentally investigated the influence of lightning impulse on a needle-plane configuration PD source in air. They observed that PD occurrence under impulse and AC voltages are similar. Kiiza et al [12] investigated the influence of HV impulses on PD activity in an artificial cavity embedded in oil-impregnated paper insulation. Their results concluded that HV impulses have an adverse impact PD activity occurrence as they can speed up the PD-induced insulation degradation process. Investigations of PD activity in mineral oil under impulse voltage conditions have been conducted [14]. Other studies have been done on the combined effect of HV impulse stress superimposed on AC voltages in order to simulate conditions where a lightning strike occurs on an operating transmission line or HV equipment [15], [16]. In laboratory and factory acceptance tests, to simulate lightning conditions, voltage and current impulse voltages are applied on equipment under test. The most commonly used impulse voltage under these tests is the 1.2/50 μs standard lightning voltage waveform.

C. Direct-Current (DC) Voltage

Direct-current (DC) voltage has been an alternative technology to AC technology in HV power transmission. The main advantage of high voltage DC (HVDC) is the better viability in power transmission over very long distances compared to high voltage AC (HVAC). This is because HVDC power transmission has less corona, minimal radio interference, dielectric and power losses due to the absence of the reactive component which in turn removes the need to compensate power system stability as in HVAC [17], [18]. In the South African context, an example of such a scheme is the Cahora–Bassa HVDC line which transmit electricity between Mozambique (Songo Station) and South Africa (Apollo Station) over a distance of 1 420 km. Other applications of HVDC include bulk power transmission of offshore wind parks and oil platforms, long overhead and sea cables as well as linking renewable energy sources such as hydro, geothermal, solar and wind farms to each other and/or the national grid [18], [19]. Geo-politically, HVDC transmission can be strategically used to transmit power across countries with or without political connections so as to avoid regional power competition. The study of PD activity under DC voltage has therefore been an area of ongoing research.

Partial discharges in HVDC systems are not the main contributing factor to insulation degradation as compared to HVAC voltage systems. This is because PD inception at DC voltage can be three times higher than the one required at AC [18], [20]. However, presence of partial discharges is still a precursor to insulation failure. Major problems in identifying PD activity under DC voltage stress has been the difficulty of distinguishing PD signals from 'noise' and identifying defect types mainly because of the absence of the voltage waveform's phase information [21], [22]. In addressing these difficulties, experimental work and strategies for noise rejection and identification of defect types have been studied [21], [23]. Other research studies have also been done on PD activity under AC and DC voltage combinations [23]–[25]. This approach uses PD characteristics under AC voltage as a benchmark test to check if a sample will experience PD activity. In addition, combined AC-DC voltage is the recommended test voltage for testing converter transformers' valve winding insulation [24].

V. Sinusoidal Test Voltages

Sinusoidal test voltages have the frequency attribute in common. Most HV equipment operate at power frequency (50/60 Hz) however they may be tested at different voltage frequencies for various reasons. The same principle applies for PD measurements; whereby partial discharges are measured at power frequency for online and some offline (laboratory) test conditions. In most offline tests applied voltage amplitudes similar to those that occur during normal operation are used to initiate PD activity in test objects. Equation 1 [26] shows that the power required by the supply voltage source to energize the electrical insulation is determined by the test voltage frequency f, test voltage magnitude U, and capacitance, C of the device under test.

$$P = 2\pi f C U^2 \tag{1}$$

PD testing in highly capacitive HV equipment at operational frequency (50/60 Hz) has presented limitations on the economical and realistic practicality of energizing sources [27]. Hence, the concept of using strategically varied supply frequencies has been adopted to mitigate this limitation. The selection of very low frequencies for highly capacitive test objects such as power cables is a commonly used approach in order to minimize the power rating, size, weight of the test equipment. For instance, with reference to Equation 1, using a power source frequency of 0.1 Hz rather than 50 Hz can reduce the testing equipment power demand by a factor of 500 [28]. The concept of using variable supply frequencies has also been used on testing highly inductive equipment. Higher frequencies (150-400 Hz) have been adopted in testing inductive equipment such as power transformers and reactors in order to avoid the transformer's magnetic core saturation [29], [30].

HV equipment operational frequency, normally known as the power frequency (50/60 Hz) can be often different from the testing frequency for reasons outlined above. Therefore, PD activity and parameters may differ due to the use of different operating and testing frequencies. However, despite the differences that might occur, these supply frequencies have to be used. The most commonly used test voltages are the operational/power frequency, damped AC (DAC) or oscillating wave test set (OWTS), very low frequency (VLF) and the resonant test system (RTS) techniques. How partial discharges behave under these different test voltage frequencies needs to be fully known to aid accurate comparative analysis of measurement results. The knowledge in that regard is however still immature. The next sections discuss the common types of PD test voltage frequency techniques.

A. Operational or Power Frequency (50/60 Hz)

The operational and/or power frequency (50/60 Hz) is the most common used operational frequency. Almost all HV equipment operate at this supply frequency. It is also the most commonly used test and supply frequency in laboratory tests during design and diagnostic tests as it brings some of the equipment's 'operating conditions' into the laboratory environment. The main reason for using this technique in PD measurement and testing is that PD effects and occurrence is directly comparable with how they would have been during normal in-service operation [31]. This technique presents a disadvantage especially for off-line testing of long power cables as it demands more power from the testing equipment. However, shorter cables and cable accessories can be tested without having the need for higher power from the testing equipment. Most of the knowledge on PD has been generated using power frequency voltages. However, due to the increasing use of non-power frequency test voltages, as presented in the next sections, the interest to understand PD behavior under non-power frequency test voltages has increased.

B. Oscillating Wave Test Set (OWTS/DAC)

Oscillating Wave Test Set (OWTS), also known as Damped AC (DAC) is an alternative technique of measuring partial discharges of highly capacitive test objects at frequencies other than the power frequency. An oscillating wave excitation voltage is achieved by charging the capacitive object (power cable) with a DC voltage and then discharging through an inductor. The DAC method offers temporary excitation to the test objects because it is short-lived i.e only last for milliseconds which can be considered as both an advantage and disadvantage [31]. It has been considered a lesser destructive method compared to the VLF counterpart [26]. Consequently, DAC has been the more preferred testing technique for non-destructive PD detection and diagnosis. Another advantage of using OWTS is that it provides excitation similar to that at operational frequency and therefore PD measurements are comparable to those at 50/60 Hz. In addition, it requires less power in comparison to that required at power frequency and is convenient to transport for onsite PD measurements [32]. Morshuis et al [33] investigated the use of OWTS/DAC to stress and detect PD activity of a service aged power cable. They found their results comparable to those obtained at power frequency, However, for frequencies above 200 Hz, PD amplitudes were slightly lower as compared to those observed at power frequency. The conclusion to this slight difference was the abundant availability of seed electrons after a PD event. Due to some shortfalls in the OWTS/DAC technique of PD detection, other non-power frequency techniques such as the very low frequency (VLF) have been developed.

C. Very Low Frequency (VLF)

Very Low Frequency (VLF) test voltage method uses supply frequency range between 0.01 and 1 Hz, with the most commonly used frequency being 0.1 Hz [34]. The two mainly used waveforms are the cosine–rectangular and the sinusoidal waveforms. VLF technique was adopted to solve the problem of the lack of polarity of DC voltage testing method as well as minimizing the size of HV supply source in comparison with the one required at 50 Hz. By using a power source frequency of 0.1 Hz rather than 50 Hz the testing equipment power demand can be reduced by a factor of 500 [28], [31]. Hence, it is the most preferred method of measuring PD activity in power cables especially at distribution level. The technology has also been used for PD measurements on generator stator bars, on-site extruded cable testing as well as oil-paper insulation MV cable testing [28]. Other advantages of using VLF include the ability to test longer cables, convenient transportation and installation of the testing equipment. One of the major disadvantages of using VLF is that, in most cases, test objects such as power cables must be taken out of operation or service when they have to be tested offline. Hence, it is mainly used in diagnostic and quality acceptance tests that are done offline in laboratory and factory facilities. Research shows that VLF PD measurements can be slightly different from those that are observed at 50 Hz [35], [36].

D. Resonant Test System (RTS)

Resonant Test System (RTS) technique uses supply frequency range between 20 and 300 Hz, although it is capable of measuring up to 400 Hz which falls under the range of the IEC60270 standard's allowable supply frequency [37]. This method is capable of on-site diagnosis of long power cables using higher frequencies. To further understand the parameters involved when dealing with RTS, Equation 2 is used.

$$At\ Resonance = \begin{cases} X_L = X_C \\ j\omega L = \frac{1}{j\omega C} \\ f = \frac{1}{2\pi\sqrt{LC}} \quad \textit{(resonant frequency)} \end{cases} \tag{2}$$

where X_L and X_C are inductance and capacitance impedance, respectively. f is the resonant frequency, L is the resonant test set's inductance and C is the test object capacitance. For given C and L, the frequency that gives resonance is the one that becomes the frequency of the test voltage. RTS systems can be implemented by making use of variable inductance and/or variable frequency [38], [39]. Inductance-tuned resonant system allows the usage of a fixed frequency and variable inductance to achieve resonance. The main advantage of this option with regard to PD measurement includes the flexibility that tests are done in laboratories using the grid national frequency (50/60 Hz) since no complex varied frequency is required from the test equipment [32]. Frequency-tuned resonant system uses the option of fixed inductance and variable frequency to achieve resonance. The main advantage of this option is the flexibility to test different types and lengths of cables [31]. In addition, RTS technique uses less power as the one required at power frequency and PD measurements are comparable to those at 50/60 Hz. However, RTS test equipment is heavy and requires large vehicles for transportation. This can present a limitation if testing has to be done in a constrained environments. RTS test techniques are therefore often more economically viable for use in transmission networks. The fact that RTS can test partial discharges at non-power frequency further underlines the need to understand the influence of frequency on PD mechanisms.

VI. Conclusion

A review of different types of test voltages and electrical PD measurement methods has been presented in this paper. The advantages, disadvantages and limitations of each PD measuring technique has been presented. Conventional methods are widely used in research and development, design and maintenance tests in universities, testing centers, power utilities and in the manufacturing industry. Under off-line PD testing conditions, the classical method's use of different test voltages is one of its advantages. However, unconventional methods have a significant advantage over the conventional counterpart of being more suitable for online PD testing which presents a continuous data logging and monitoring of equipment. All methods and techniques have their advantages and limitations, hence it is recommended that multiple techniques be used to create a complete picture and yield better results.

REFERENCES

[1] G. C. Stone, "Partial discharge diagnostics and electrical equipment insulation condition assessment," *IEEE Transactions on Dielectrics and Electrical Insulation*, vol. 12, no. 5, pp. 891–904, Oct 2005.

[2] G. J. Paoletti and A. Golubev, "Partial discharge theory and technologies related to medium-voltage electrical equipment," *IEEE Transactions on Industry Applications*, vol. 37, no. 1, pp. 90–103, Jan 2001.

[3] S. A. Boggs, "Partial discharge: overview and signal generation," *IEEE Electrical Insulation Magazine*, vol. 6, no. 4, pp. 33–39, July 1990.

[4] G. C. Montanari, "Envisaging links between fundamental research in electrical insulation and electrical asset management," *IEEE Electrical Insulation Magazine*, vol. 24, no. 6, pp. 7–21, 2008.

[5] L. Niemeyer, "A generalized approach to partial discharge modeling," *IEEE Transactions on Dielectrics and Electrical Insulation*, vol. 2, no. 4, pp. 510–528, Aug 1995.

[6] "High-voltage test techniques - partial discharge measurements," *SANS 60270:2000 (IEC 60270:2000)*, pp. 1–53, 2007.

[7] C. Nyamupangedengu, "Pd-type-dependent spectral bandwidth in solid polymer dielectrics," Ph.D. dissertation, University of the Witwatersrand Johannesburg, Johannesburg (South africa), 2011.

[8] M. Florkowski, "Influence of high voltage harmonics on partial discharge patterns," in *Proceedings of 5th International Conference on Properties and Applications of Dielectric Materials*, vol. 1, May 1997, pp. 303–306 vol.1.

[9] R. Candela, I. Romano, and P. Romano, "Influence on pd parameters due to distorted voltage," in *2003 Annual Report Conference on Electrical Insulation and Dielectric Phenomena*, Oct 2003, pp. 593–596.

[10] P. Romano, "Influence on pd parameters due to voltage conducted disturbances," *IEEE Transactions on Dielectrics and Electrical Insulation*, vol. 11, no. 1, pp. 160–165, Feb 2004.

[11] M. Florkowski, B. Florkowska, J. Furga, and P. Zydron, "Impact of high voltage harmonics on interpretation of partial discharge patterns," *IEEE Transactions on Dielectrics and Electrical Insulation*, vol. 20, no. 6, pp. 2009–2016, 2013.

[12] R. C. Kiiza, R. Nikjoo, M. G. Niasar, X. Wang, and H. Edin, "Effect of high voltage impulses on partial discharge activity in a cavity embedded in paper insulation," in *2012 Annual Report Conference on Electrical Insulation and Dielectric Phenomena*, 2012, pp. 133–136.

[13] Z. Sun, X. Zhao, J. Li, and Y. Li, "Experiment investigation of partial discharges under impulse voltage," in *2009 IEEE 9th International Conference on the Properties and Applications of Dielectric Materials*, 2009, pp. 525–529.

[14] Suwarno and Aulia, "Effect of lightning impulse voltage to the pd activity and breakdown voltage of liquid insulation," in *The 2nd IEEE Conference on Power Engineering and Renewable Energy (ICPERE) 2014*, 2014, pp. 171–174.

[15] R. J. Densley, "Partial discharges in electrical insulation under combined alternating and impulse stresses," *IEEE Transactions on Electrical Insulation*, vol. EI-5, no. 4, pp. 96–103, 1970.

[16] J. Wu, P. V. M. van Nes, A. Rodrigo Mor, and J. J. Smit, "Partial discharges in xlpe insulated cable under superimposed transient voltages," in *2019 IEEE Electrical Insulation Conference (EIC)*, 2019, pp. 221–225.

[17] M. R. Rahimi, R. Javadinezhad, and M. Vakilian, "Dc partial discharge characteristics for corona, surface and void discharges," in *2015 IEEE 11th International Conference on the Properties and Applications of Dielectric Materials (ICPADM)*, 2015, pp. 260–263.

[18] M. H. Okba, M. H. Saied, M. Z. Mostafa, and T. M. Abdel- Moneim, "High voltage direct current transmission - a review, part i," in *2012 IEEE Energytech*, 2012, pp. 1–7.

[19] P. K. Olsen, F. Mauseth, and E. Ildstad, "The effect of dc superimposed ac voltage on partial discharges in dielectric bounded cavities," in *2014 ICHVE International Conference on High Voltage Engineering and Application*, 2014, pp. 1–4.

[20] E. A. Morris and W. H. Siew, "Partial discharge activity in polymeric cable insulation under high voltage ac and dc," in *2017 52nd International Universities Power Engineering Conference (UPEC)*, 2017, pp. 1–4.

[21] H. Niu, A. Cavallini, G. C. Montanari, and Y. Zhang, "Noise rejection strategy and experimental research on partial discharge at dc voltage," in *2009 IEEE 9th International Conference on the Properties and Applications of Dielectric Materials*, 2009, pp. 489–492.

[22] R. Guo, K. Wang, Z. Xu, J. Li, J. Sun, and H. Cheng, "Partial discharge characteristics and classification in oil-paper insulation under dc voltage," in *2016 IEEE International Conference on High Voltage Engineering and Application (ICHVE)*, 2016, pp. 1–4.

[23] E. Corr and W. H. Siew, "Analyses of partial discharges in dielectric samples under dc excitation," in *2015 50th International Universities Power Engineering Conference (UPEC)*, 2015, pp. 1–6.

[24] S. Li, W. Si, and Q. Li, "Partition and recognition of partial discharge development stages in oil-pressboard insulation with needle-plate electrodes under combined ac-dc voltage stress," *IEEE Transactions on Dielectrics and Electrical Insulation*, vol. 24, no. 3, pp. 1781–1793, 2017.

[25] S. Li, Q. Li, W. Si, J. Yao, Y. Shi, and T. Zhang, "Partial discharge characteristics in pre-breakdown processes of oil-pressboard insulation with needle-plate defect under ac-dc combined voltage," in *2018 IEEE Electrical Insulation Conference (EIC)*, 2018, pp. 18–21.

[26] M. G. Niasar, X. Wang, and R. C. Kiiza, "Review of partial discharge activity considering very-low frequency and damped applied voltage," *Energies*, vol. 14, no. 440, 2021.

[27] R. Bodega, A. Cavallini, P. H. F. Morshuis, and F. J. Wester, "The effect of voltage frequency on partial discharge activity," in *Annual Report Conference on Electrical Insulation and Dielectric Phenomena*, 2002, pp. 685–689.

[28] B. Florkowska, P. Zydron, and M. Florkowski, "Analysis of pd phase-resolved images at low frequency of testing voltage," in *Conference Record of the 2004 IEEE International Symposium on Electrical Insulation*, 2004, pp. 143–146.

[29] "Ieee guide for failure investigation, documentation, analysis, and reporting for power transformers and shunt reactors," *IEEE Std C57.125-2015 (Revision of IEEE Std C57.125-1991)*, pp. 1–84, 2015.

[30] A. Cavallini and G. C. Montanari, "Effect of supply voltage frequency on testing of insulation system," *IEEE Transactions on Dielectrics and Electrical Insulation*, vol. 13, no. 1, pp. 111–121, Feb 2006.

[31] A. Eigner and K. Rethmeier, "An overview on the current status of partial discharge measurements on ac high voltage cable accessories," *IEEE Electrical Insulation Magazine*, vol. 32, no. 2, pp. 48–55, March 2016.

[32] L. W. van Veen, "Comparison of measurement methods for partial discharge measurement in power cables," Ph.D. dissertation, Delft University of Technology, Netherlands, 2014.

[33] P. H. F. Morshuis, R. Bodega, M. Lazzaroni, and F. J. Wester, "Partial discharge detection using oscillating voltage at different frequencies," in *IMTC/2002. Proceedings of the 19th IEEE Instrumentation and Measurement Technology Conference (IEEE Cat. No.00CH37276)*, vol. 1, 2002, pp. 431–435 vol.1.

[34] "Ieee guide for field testing of shielded power cable systems using very low frequency (vlf)(less than 1 hz)," *IEEE Std 400.2-2013*, pp. 1–60, 2013.

[35] D. Fynes-Clinton and C. Nyamupangedengu, "Partial discharge characterization of cross-linked polyethylene medium voltage power cable termination defects at very low frequency (0.1 hz) and power frequency test voltages," *IEEE Electrical Insulation Magazine*, vol. 32, no. 4, pp. 15–23, July 2016.

[36] R. Miller and I. A. Black, "Partial discharge measurements over the frequency range 0.1 hz to 50 hz," *IEEE Transactions on Electrical Insulation*, vol. EI-12, no. 3, pp. 224–233, June 1977.

[37] E. Gockenbach and W. Hauschild, "The selection of the frequency range for high-voltage on-site testing of extruded insulation cable systems," *IEEE Electrical Insulation Magazine*, vol. 16, no. 6, pp. 11–16, 2000.

[38] P. Coors and S. Schierig, "Hv ac testing of super-long cables," in *Conference Record of the 2008 IEEE International Symposium on Electrical Insulation*, 2008, pp. 636–640.

[39] W. Schufft, P. Coors, W. Hauschild, and J. Spiegelberg, "Frequency-tuned resonant test systems for on-site testing and diagnostics of extruded cables," in *1999 Eleventh International Symposium on High Voltage Engineering*, vol. 5, 1999, pp. 335–339 vol.5.